

SWANSEA UNIVERSITY



Swansea University
Prifysgol Abertawe

DOCTORAL THESIS

Dualities in quantum field theory from string theory

by:
Mohammad Reza Akhond

*A thesis submitted in fulfillment of the requirements
for the Doctor of Philosophy*

of the

Department of Physics,
Faculty of Science and Engineering,
Swansea University

June 14, 2022

Declaration of Authorship

I, Mohammad Akhond, declare that this thesis titled, “Dualities in quantum field theory from string theory” and the work presented in it are my own. I confirm that:

- This work has not previously been accepted in substance for any degree and is not being concurrently submitted in candidature for any degree.
- This thesis is the result of my own investigations, except where otherwise stated. Other sources are acknowledged by footnotes giving explicit references. A bibliography is appended.
- I hereby give consent for my thesis, if accepted, to be available for photocopying and for inter-library loan, and for the title and summary to be made available to outside organisations.
- The University’s ethical procedures have been followed and, where appropriate, that ethical approval has been granted.

Signed: M. Akhond

Date: 14/06/2022

Acknowledgements

I would like to thank my advisor, Adi Armoni, for his continued support, guidance, and friendship throughout my PhD studies. Thank you for giving me the freedom to explore my own interests, and for your laid back and informal style, which is a refreshing contrast to the anxiety that comes free with a PhD.

When non-physicists ask what I do, I tell them that I talk to my friends and write down what we discussed. I am most grateful to my collaborators, for making my life simple and fun, and for showing me how to be a better researcher by example. Guillermo Arias-Tamargo, for your calm and patient approach, and your organizational skills. Federico Carta, for your energy, dedication, and enthusiasm for our subject. Siddharth Dwivedi, for being a Mathematica monk, doing many detailed calculations. Hirotaka Hayashi, for having the lowest ratio of words spoken in a meeting, to results produced by the next. Sung-Soo Kim, for using your connections to convert our semi-recreational project, into a long-lasting and fruitful collaboration. Andrea Legramandi, for resolving puzzles quicker than I can find or appreciate them. Alessandro Mininno, for taking leadership when necessary. Carlos Nunez, for your infinite source of curiosity, which transcends superficial boundaries between different subfields and disciplines. Lucas Schepers, for your diverse and creative ways to gain insight into problems. Stefano Speziali, for continuously questioning our results. Shigeki Sugimoto, for questioning all assumptions, and for your enormous patience with physics and with your collaborator. Futoshi Yagi, for being a wizard with brane webs, and for our physics discussions which always leave me energized.

I would be remiss not to thank Prem Kumar and Dan Thompson for making our group more vibrant.

Far too many people need to be credited for my social life in Swansea, the following are a select few. Pedro, Sybille, Fernando, Stan, Robin, Alex, Christina, and Roberta, for introducing me to climbing. Lucas, for being a classical music nerd. Laura, Kostas and Freya for our mutual appreciation of herbs and other substances. Dawid and Sergio, for great food and greater laughs. John and Astrid, for our cold water dip and bonfire. Karol for awesome vegan recipes and Ricardo for Chilean wisdom. Marika for Carbonara. Everybody in room 606 of the Vivian tower that I shared my office, and many drinks and dinners with: Giacomo, Natalia, Luke, Lewis, Neil, David, Shaun, Will and Ali.

I would not be where I am today, without my family. I'm indebted to my parents, Elham and Saeed, for sacrificing their social and professional lives, in search of a better future for me and my sister. And to my sister, Saina, for sparking my interest in science from an early age, and for being my role model. I can never repay you for all of your love and support.

Contents

| | | |
|----------|--|-----------|
| 1 | Phases of QCD₃ from type 0 strings and Seiberg duality | 5 |
| 1.1 | Overview of type 0B | 7 |
| 1.1.1 | A pseudo-moduli space | 10 |
| 1.1.2 | Hanany-Witten setup | 11 |
| 1.2 | 3d dualities from non-supersymmetric brane configurations | 13 |
| 1.2.1 | Level-rank duality | 13 |
| 1.2.2 | Including flavours | 15 |
| | Electric theory | 15 |
| | Magnetic theory | 17 |
| 1.3 | Phase diagram | 19 |
| 1.3.1 | Region I: Bosonization | 19 |
| 1.3.2 | Symmetry breaking | 21 |
| | Region II' | 21 |
| | Region II | 22 |
| 1.4 | Comments about QED ₃ | 22 |
| 1.4.1 | QED ₃ with vanishing CS-term | 23 |
| 2 | Magnetic quivers for 5d SCFTs | 24 |
| 2.1 | Tools from the plethystic programme | 26 |
| 2.1.1 | What is a Hilbert series? | 26 |
| 2.1.2 | Coulomb branches | 27 |
| | Coulomb branch Hilbert series for non-simply laced quivers | 28 |
| 2.1.3 | Higgs branches | 30 |
| 2.1.4 | Highest weight generating functions | 30 |
| 2.2 | Factorised 3d $\mathcal{N} = 4$ orthosymplectic quivers | 31 |
| 2.2.1 | The $E_1 \times E_1$ sequence | 32 |
| 2.2.2 | The $E_1 \times E_3$ sequence | 36 |
| 2.2.3 | The $E_3 \times E_3$ sequence | 39 |
| 2.2.4 | The $E'_3 \times E'_3$ sequence | 41 |
| 2.2.5 | The $E'_3 \times E_4$ sequence | 44 |

| | | |
|----------|--|-----------|
| 2.2.6 | The $E_4 \times E_4$ sequence | 45 |
| 2.2.7 | The $E_5 \times E_5$ sequence | 47 |
| 2.2.8 | The $E'_5 \times E'_5$ sequence | 49 |
| 2.2.9 | The $E_{5'} \times E_6$ sequence | 51 |
| 2.2.10 | The $E_6 \times E_6$ sequence | 53 |
| 2.2.11 | The $E_7 \times E_7$ sequence | 55 |
| 2.2.12 | An outlier: the $E_8 \times E_8$ theory | 58 |
| 2.3 | Magnetic quivers from brane webs with $O7^+$ -planes | 59 |
| 2.3.1 | Pure $SO(N)$ theory | 59 |
| 2.3.2 | $SO(N)$ with $N_v \leq N - 5$ | 61 |
| | $N = 2r$ | 64 |
| 2.3.3 | $SO(N)$ with $N_v = N - 4$ flavours | 67 |
| | $N=4$ | 68 |
| | $N=5$ | 68 |
| | $N=6$ | 69 |
| 2.3.4 | $SO(N)$ with $N_v = N - 3$ | 70 |
| | $N = 4$ | 72 |
| 3 | Electrostatic description of 3d SCFTs | 74 |
| 3.1 | Geometry | 75 |
| 3.1.1 | Study of the partial differential equation | 77 |
| 3.1.2 | Asymptotic behaviour | 78 |
| 3.2 | Charges and other important quantities | 79 |
| 3.2.1 | Hanany–Witten set-up and linking numbers | 81 |
| 3.2.2 | Holographic central charge | 83 |
| | Generic balanced quiver | 84 |
| 3.3 | Some examples | 85 |
| 3.3.1 | Generic triangular rank function | 85 |
| 3.3.2 | Generic trapezoidal rank function | 87 |
| 3.4 | Mirror Symmetry | 90 |
| 3.4.1 | Geometry and Mirror Symmetry | 94 |
| 3.4.2 | A purely geometric formulation of mirror symmetry | 96 |
| 3.4.3 | The scaling for generic rank functions | 96 |
| 3.5 | Summary | 98 |

Introduction

Quantum field theory (QFT), is a powerful framework to study diverse phenomena in physics. The range of topics includes the interactions of elementary particles, the continuum limit of condensed matter systems defined on a lattice, models of the expanding universe, as well as quantum gravity. Despite its enormous breadth of applications, it is still quite poorly understood. From a pragmatic point of view, a generic QFT is well understood in the perturbative regime, where one has a small expansion parameter or coupling constant. That we have a satisfactory understanding of QFTs in the weakly coupled regime, is highlighted by the fact that we have a single formalism, namely feynman diagrams, that can be applied to *any* weakly coupled theory. Conversely, there is no universal framework to understand non-perturbative and strong coupling phenomena. Instead, we have a distinct set of tools, which apply to distinct sets of very special theories, such as those with supersymmetry or topological theories. From this perspective, to understand the strong coupling dynamics of a QFT, is to develop a unique formalism that can be applied to solve a generic strongly coupled QFT. The reader should be warned that this thesis will not achieve such an ambitious goal. However, it is good to keep this general philosophy in mind, as a broader motivation for some of the work presented. We will provide, instead, a collection of data points for particular sectors of strongly coupled QFTs that are under analytic control. One can hope that some day, these data points can provide the foundations for a more systematic and universal approach. From a more formal viewpoint, quantum field theory, as of yet, has no rigorous mathematical basis. This is particularly bothersome, given the deep interconnections between ideas in modern mathematics and those of QFT [1]. The goal of this thesis is to introduce its reader to a few notable examples, where the former issue can be overcome. The unifying theme of all these examples is their relation to brane dynamics in string theory [2]. We will make extensive use of the string theory embedding of the QFTs under consideration, in order to illuminate their strong coupling dynamics.

A useful gadget in our endeavour, is the notion of duality, broadly defined as an equivalence between two naively inequivalent quantum field theories. The simplest example is electric-magnetic duality; Maxwell's theory in $3 \leq d \leq 5$ spacetime dimensions is dual to a theory of free $(d - 3)$ -form fields, where the equations of motion and Bianchi identity are

mapped to one another under this duality. More interesting are dualities between interacting theories, where two different QFTs flow to the same conformal manifold. Indeed, the two QFTs in question may even start life in different spacetime dimensions. One concrete example of field theory dualities, which will show up repeatedly in this thesis, is 3d mirror symmetry[3]. We will review salient features of this intriguing duality symmetry in section 3.4. It is worth remarking, that string theory is deeply aware of field theory dualities. Indeed, mirror symmetry is a consequence of S-duality of type IIB string theory[4]. Perhaps the most remarkable instance of duality, is that of the AdS/CFT correspondence [5], which posits an equivalence between string theory on anti de Sitter space, times a compact manifold M , and a conformal field theory living on its boundary[5]. The relevance of duality in understanding non-perturbative phenomena, is rooted in the fact that often dualities map the strong coupling dynamics of one theory to the weak coupling dynamics of the dual theory. This is indeed true of both mirror symmetry and the AdS/CFT correspondence.

One of the unifying themes of this thesis, is brane dynamics in string theory, and their interplay with gauge theories. In particular, throughout this work, we will use the string embeddings of various QFTs, to illuminate their strong coupling dynamics. The examples provided here are very rare, in that they lie at the intersection of theories, that are highly non-trivial interacting theories, yet we have them under good analytic control. In particular, in chapter 1 we consider a non-supersymmetric Hanany-Witten-like setup in type-0 string theory that flows to three-dimensional Quantum Chromodynamics (QCD₃) at low energies. The recent developments in understanding the quantum phases of QCD₃ [6], together with some intuitive knowledge of the supersymmetric cousins of this brane setup allow us to identify the string theory origin of the various phases of QCD₃. The stringy interpretation geometrises many aspects of the QFT.

One of the most remarkable predictions of string theory is the existence of UV complete quantum field theories in 5 (and 6) spacetime dimensions. Their mere existence, forces us to expand our view of quantum field theories, as these fixed points cannot be reached by traditional means of perturbing around free field Lagrangians. Yet, by now, there is overwhelming evidence to support their existence, mostly due to stringy constructions starting with the seminal papers [7–10]. Broadly speaking, there are three independent, yet complementary points of view for studying these SCFTs, namely their embedding into type IIB brane webs [11–30], geometric engineering [8, 31–39] and holography [40–46].

Many 5d SCFTs, admit supersymmetry preserving mass deformations, which trigger an RG flow, whose low energy dynamics is effectively captured by an $\mathcal{N} = 1$ gauge theory. Such deformations, preserve the $SU(2)_R$ symmetry, while breaking the flavour symmetry. An important dynamical question is therefore to determine the full global symmetry of the parent SCFT of a given 5d gauge theory. 5d SCFTs and gauge theories, can possess a Higgs branch

of their moduli space of vacua, which in the gauge theory regime can be constructed as the hyperKähler quotient [47, 48]. In the SCFT limit, the hyperKähler quotient, is no longer accessible, due to the lack of a Lagrangian description, making the study of the Higgs branch in this limit more challenging. There are, by now, a plethora of techniques to determine the enhanced global symmetry of the SCFT parent of a given 5d gauge theory, such as 7-brane analysis [49–51], superconformal indices [52], as well as geometric approaches [53]. One particularly elegant approach to determine the SCFT flavour symmetries as well as the Higgs branch of the SCFT, pioneered in [54], is to consider their magnetic quivers. The magnetic quiver (MQ), of a given 5d theory, is a 3d $\mathcal{N} = 4$ quiver gauge theory, whose Coulomb branch is isomorphic to the Higgs branch of the 5d theory in question. In many cases, though not always, one can show that the magnetic quiver of a given 5d theory, is the 3d mirror of its torus compactification. This leads to an interesting interplay between 5d $\mathcal{N} = 1$ theories and 3d $\mathcal{N} = 4$ theories, and has prompted many recent studies [54–70].

We present two separate studies of magnetic quivers for 5d SCFTs in chapter 2. The difficulty in analysing 5d SCFTs, is partially due to their inherently strongly coupled nature, and hence the absence of a Lagrangian description. The magnetic quiver perspective, elegantly overcomes this difficulty by encoding the Higgs branch spectrum of a given 5d SCFT, in the Coulomb branch of its magnetic quiver. On the other hand, knowledge of 5d physics can lead to non-trivial predictions for 3d physics, as exemplified by the plethora of examples of factorised orthosymplectic quivers in chapter 2.2. Other surprising results from the perspective of 3d gauge theories is the equality of moduli spaces of orthosymplectic magnetic quivers with unitary non-simply-laced magnetic quivers.

We now provide a breakdown of the content of the main chapters in this thesis. In chapter 1 we discuss brane configurations similar to those constructed by Hanany and Witten [4] in type IIB, but we work in type 0 string theory. The latter is a non-supersymmetric cousin of type IIB. The Hanany-Witten-like set-up we consider allows us to construct a UV-completion of three-dimensional Quantum Chromodynamics (QCD₃). We then use the brane configuration and standard brane moves [71], to construct a Giveon-Kutasov [72] dual of this theory. Using the original brane system and its dual, we recover all the recently proposed quantum phases of QCD₃ [6]. The contents of this chapter were published in [73]. Chapter 2 contains two closely related but independent studies. In section 2.2, we provide sequences of 3d $\mathcal{N} = 4$ quiver gauge theories whose moduli space of vacua factorises into two decoupled sectors. This is highly suggestive, that the infra-red fixed points of these theories are the direct sum of two decoupled SCFTs. The main evidence to support these claims are Hilbert series computations of both the Higgs and Coulomb branches of the moduli space. In light of keeping the physical results front and centre, we have omitted many technical details of the computations. The interested reader can consult the paper [56], where this work was published, for

a more thorough technical treatment. Similarly, many of the results summarised in section 2.2, rest on brane web techniques developed by the author in [55]. The exclusion of these techniques from this thesis is rooted in their technical nature, as well as the author's desire for brevity. Section 2.3 is dedicated to the study of brane webs with $O7^+$ -planes. We focus on the Higgs branch of the SCFT parents of 5d $\mathcal{N} = 1$ $SO(N)$ gauge theory with hypermultiplets on the vector representation of the gauge group. We provide a prescription to read off the magnetic quivers for these theories directly from their brane webs. We then compute the Coulomb branch Hilbert series for the magnetic quivers in order to verify them. The results of this chapter were published in [57]. Chapter 3 is dedicated to the holographic duals of the infra-red fixed points of 3d $\mathcal{N} = 4$ linear quiver gauge theories. The results of this study were published in [74]. As with the other chapters, many technicalities are omitted, and the interested reader is directed to reference [74].

Chapter 1

Phases of QCD_3 from type 0 strings and Seiberg duality

String theory has long been a source of insight for investigations in strong coupling dynamics of quantum field theory. In particular, dualities in field theories often follow from properties of the corresponding brane configuration in string theory. Having independent evidence from field theory and string theory is a step in verifying dualities. Most of the effort so far has been largely focused on supersymmetric theories in various dimensions, owing to the fact that non-perturbative phenomena in both string theory and field theory are better understood in that setting.

One may naturally ponder the ubiquity of dualities in generic QFTs, and their relationship to string theory. Indeed, recent years have seen progress made on the field theory front for non-supersymmetric gauge theories in three dimensions. There has been significant progress in the understanding of the phase diagram of QCD_3 with a Chern-Simons term.

Consider a $U(N_c)$ theory with N_f massless Dirac fermions and a level K Chern-Simons term. It was argued [75–78] (see also [79, 80]) that for $N_f/2 \leq K$ the theory admits a dual description in terms of a gauge theory coupled to scalars as follows

$$U(N_c)_{K, K \pm N_c} \oplus N_f \text{ fermions} \longleftrightarrow U\left(K + \frac{N_f}{2}\right)_{-N_c, -N_c \mp (K + N_f/2)} \oplus N_f \text{ scalars} . \quad (1.0.1)$$

However, one may wonder whether something changes for $N_f/2 > K$. In the case of $SU(N_c)$ gauge symmetry, it was conjectured in [6] that when $N^* > N_f/2 > K$, for some

unknown value N_f ¹ the theory admits a flavour symmetry breaking phase where

$$\text{U}(N_f) \rightarrow \text{U}(N_f/2 - K) \times \text{U}(N_f/2 + K). \quad (1.0.2)$$

A similar picture was developed in [6] also for $\text{SO}(N)$ and $\text{Sp}(N)$ gauge theories. For $N_f \geq N^*$ the theory is expected to flow to a CFT².

Following [83] which concerned the symplectic gauge group, we propose that the infrared phase diagram of $\text{U}(N_c)$ QCD_3 can be understood in terms of a non-SUSY Seiberg duality. Our proposal involves a modification of the UV theory, i.e. we start with a UV theory, which we refer to as the *electric* theory, whose Lagrangian is more complicated than QCD_3 . This theory flows in the IR to QCD_3 . The electric theory also admits a Seiberg dual description, which we refer to as the *magnetic* theory. The various IR phases of the electric theory (and so of QCD_3) can then be identified with the phases of the magnetic dual. In particular both the bosonized phase and the symmetry breaking phase, which will be our main focus, can be understood in terms of the condensation of a scalar field, namely the dual "squark", in the magnetic theory.

Our proposal of Seiberg duality is motivated by string theory³. In order to realise $\text{U}(N_c)$ QCD_3 we embed the gauge theory in a Hanany-Witten brane configuration of type 0B string theory. The brane configuration consists of N_c D3 branes suspended between an NS5 branes and a $(1, k)$ fivebrane. In addition, there exists N_f flavour branes and an $O'3$ orientifold plane. It is similar to the corresponding supersymmetric brane configuration of Gaiotto and Witten in type IIB [72].

By swapping the fivebranes we obtain the brane configuration that realises the magnetic Seiberg dual. The relation between field theory and string theory phenomena teaches us about non-supersymmetric brane dynamics. The aforementioned squark condensation translate into a reconnection of colour and flavour branes.

Our Seiberg duality proposal passes several non-trivial checks: as in the symplectic case [83] it satisfies global anomaly matching and RG flows after mass deformations. It is also supported by planar equivalence [88, 89]: when N_c, N_f, k are taken to infinity the electric theory becomes equivalent to a supersymmetric theory and the magnetic theory becomes equivalent to a supersymmetric theory. The electric and magnetic theories form an $\mathcal{N} = 2$

¹That there should be an upper bound on the number of flavours, for which a symmetry breaking phase appears is supported by large N_f studies of QCD_3 [81], which suggest a second order phase transition at leading order.

²In the 't Hooft limit, when $N_c \rightarrow \infty$ and K, N_f are kept fixed, the theory exhibits rich vacua [82]. The discussion of this limit is beyond the scope of this paper.

³Other approaches to obtain 3d duality with relation to string theory are given in [84, 85], while the possibility of relating these dualities to supersymmetric dualities were explored in [86, 87]

supersymmetric Giveon-Kutasov dual pair. Therefore, there exists a limit in which our non-supersymmetric dual pair becomes a known supersymmetric dual pair.

Another method of obtaining Seiberg duality in string theory is by using non-critical strings [90]. The method relies on the embedding of SQCD in non-critical string theory, pioneered in [91]. Instead of swapping the fivebranes, the duality is obtained by replacing the sign of the coefficient in front of the Liouville term in the string worldsheet action, $\mu \rightarrow -\mu$. The advantage of using this method is that the non-critical type 0 string does not contain a closed string tachyon in the bulk [92, 93]. The field theory that lives on the branes is the same in both the critical and the non-critical approaches.

In the following we will always denote the bare CS level by k , with $k \geq 0$. In addition, we define the frequently occurring combination

$$\kappa \equiv k - N_c + 2, \quad K \equiv \kappa - \frac{N_f}{2} \quad (1.0.3)$$

The rest of this chapter is organised as follows: in section 2 we review the essential properties of type 0B string theory and its brane configurations. In section 3 we consider a certain brane configuration and propose a Seiberg duality. In section 4 we show how the phase diagram of the electric theory manifest itself in the magnetic and in section 5 we focus on QED₃. Section 6 is devoted to conclusions.

1.1 Overview of type 0B

In this section we review aspects of D3 branes and O'3 planes in type 0 string theory. For the relevant background we refer the reader to [94].

Type 0B string theory can be obtained by a \mathbb{Z}_2 orbifold of type IIB, with the \mathbb{Z}_2 action generated by $(-1)^{F_s}$, the mod 2 spacetime fermion number operator. The untwisted sector is therefore identical to the bosonic sector of the parent type IIB theory. The twisted sector is composed of a tachyon in the NS-NS sector as well as a new full set of R-R fields. The tachyon will eventually be projected out by the orientifold action. The doubled set of R-R fields lead in effect to a doubling of the D-brane spectrum. In particular there are now two types of threebranes which we denote by D3 and D3' respectively.

The worldvolume theory on a stack of n D3 and m D3' branes was worked out in [95, 96]. It is a $U(n) \times U(m)$ gauge theory with 3 complex scalars in the adjoint representation, and a pair of bifundamental Weyl fermions.

In order to project out the closed string tachyon we make use of the $\Omega(-1)^{f_R}$ projection [97, 98]. Here, Ω is worldsheet parity and $(-1)^{f_R}$ is the operator that counts the number of right moving worldsheet fermions mod 2. Combining this with reflection in 6 spatial

directions I_6 we get an $O'3^\pm$ orientifold, the (3+1) dimensional fixed hyperplane with respect to the $\Omega(-1)^{f_R} I_6$ action. The existence of two types of orientifold planes follows from the fact that the NS-NS two form can have a non-trivial Wilson surface $\exp(i \int B)$ and the signs are chosen to reflect the R-R charge of the orientifold plane. Note that unlike the O3-planes of type IIB we do not have the additional possibilities associated with the R-R discrete torsion. Under the action of Ω , D3 turns into D3', thus requiring an equal number of each type of brane. In fact Ω projects out half of the doubled set of R-R fields in the closed string sector.

We are interested in stacks of N D3 branes (together with their image N D3's) on top of $O'3^\pm$, with the worldvolume directions of D3 and D3' parallel to that of the $O'3^\pm$ -plane (see table 1.2). The worldvolume theory of such a configuration was worked out in [96]. In both cases one has a $U(N)$ gauge field and 6 adjoint scalars parameterising the directions transverse to the worldvolume. There are also a pair of Weyl fermions which transform in the 2-index symmetric or antisymmetric representation of $U(N)$ in the configuration with $O'3^+$ and $O'3^-$ respectively. We will denote these theories by \mathcal{Y}^+ (\square), \mathcal{Y}^- (\boxplus) respectively, highlighting the orientifold type on which they live as well as the representation of the worldvolume fermions (the two features relevant for our purposes). We summarise this in table 1.1. The Lagrangian for these theories can be obtained by subjecting the component fields of $\mathcal{N} = 4$ SYM, collectively denoted by φ , to the constraints

$$J\varphi J^T = (-1)^F \varphi, \quad (1.1.1)$$

where $(-1)^F$ is the mod 2 fermion number operator and J is the symplectic form

$$J = \begin{pmatrix} 0 & \mathbb{1}_N \\ -\mathbb{1}_N & 0 \end{pmatrix}. \quad (1.1.2)$$

The choice of gauge group for the $\mathcal{N} = 4$ theory descends to the choice of fermion representation (figure 1.1); starting from the *parent* theory with $SO(2N)$ gauge group one lands on \mathcal{Y}^- (\boxplus), and the supersymmetric $Sp(N)$ theory leads to \mathcal{Y}^+ (\square) [99].

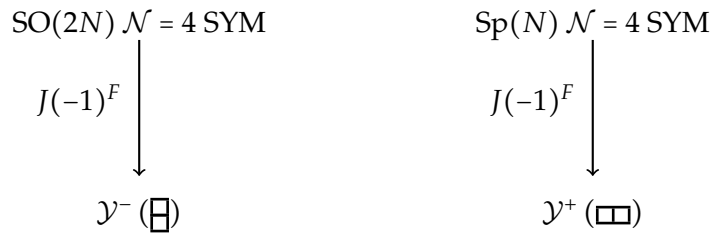


Figure 1.1. The “orientifold” daughters of $\mathcal{N} = 4$ SYM.

The Möbius amplitude for a single D3 and its image D3' separated by a distance $2|X_\pm|$

Table 1.1. The field content of the world volume theory of N D3 branes on top of an $O'3^\pm$ plane.

| $\mathcal{Y}^- (\boxminus)$ | U(N) | SO(6) | $\mathcal{Y}^+ (\boxplus)$ | U(N) | SO(6) |
|-----------------------------|------------------------------------|------------------------------------|----------------------------|----------------------------------|------------------------------------|
| B_μ^- | Adj | \cdot | B_μ^+ | Adj | \cdot |
| X_- | Adj | $\mathbf{6}_v$ | X_+ | Adj | $\mathbf{6}_v$ |
| ζ_- | $\boxminus \oplus \bar{\boxminus}$ | $\mathbf{4}_s \oplus \mathbf{4}_c$ | ζ_+ | $\boxplus \oplus \bar{\boxplus}$ | $\mathbf{4}_s \oplus \mathbf{4}_c$ |

across the $O'3^\pm$ is [96]

$$\mathcal{A}_{\mathcal{M}} = \pm \frac{V_4}{(8\pi^2\alpha')^2} \int_0^\infty dt \frac{f_2^8(iq)}{2t^3 f_1^8(iq)} \exp\left(\frac{-2tX_\pm^2}{\pi\alpha'}\right), \quad (1.1.3)$$

where $q = e^{-\pi t}$ and the $f_i(q)$ are defined as in [100]. We would like to extract the charge of the orientifold plane as well as the brane-orientifold potential. We note that the integrand in (1.1.3) is, up to a sign, identical to the case analysed in [101]. We will state the relevant results in the following. For large separation X_\pm , the leading order term as $t \rightarrow 0$ is given by

$$\mathcal{A}_{\mathcal{M}} \sim \pm \pi V_4 G_6(X_\pm^2), \quad (1.1.4)$$

where $G_6(X_\pm^2) = (4\pi^3)^{-1}|X_\pm|^{-4}\Gamma(2)$ is the 6d scalar propagator. We see that the long range potential between the branes and $O'3^-$ ($O'3^+$) is attractive (repulsive). For small X_\pm , (1.1.4) is no longer a valid approximation, instead one can expand the exponential in (1.1.3) around $X_\pm = 0$

$$\mathcal{A}_{\mathcal{M}} = \pm [\Lambda - MX_\pm^2 + \mathcal{O}(X_\pm^4)], \quad (1.1.5)$$

where the coefficients Λ , M are both positive, with the explicit form given in [101]. From this, it follows that there is a short range attractive (repulsive) force between the branes and $O'3^-$ ($O'3^+$) plane. The nature of the interaction at short and long distances from the orientifold is similar. Therefore, the theory with fermions in the antisymmetric (symmetric) representation is perturbatively stable (unstable). Note that instabilities of non-perturbative nature may still arise, but are less straightforward to detect in string theory. Instead, we may rely on the field theory analysis and try to revert some lessons back to the brane setup (as in section 1.3.2).

Notice that the (in)stability of the brane configuration translates in the worldvolume field theory to statements about the vev of the scalars X_\pm . This is obvious from the second term in (1.1.5), where the sign of the mass term for the scalars is positive (negative) for the theory with anti-symmetric (symmetric) fermions. In the Field theory, this is encoded in the 1-loop Coleman-Weinberg potential, which gets unequal contributions from the bosons and

fermions in each theory.

As observed in [102], the threebranes in type 0 carry the following charge and tension

$$Q_{D3} = \sqrt{\pi}, \quad T_{D3} = \frac{\sqrt{\pi}}{\sqrt{2}\kappa_0}. \quad (1.1.6)$$

It is then a matter of comparing (1.1.4) with $4V_4 G_6(X_{\pm}^2) T_{O'3^{\pm}} T_{D3} \kappa_0^2$ to see that the orientifold charge and tension are

$$Q_{O'3^{\pm}} = \pm \frac{Q_{D3}}{2}, \quad T_{O'3^{\pm}} = \pm \frac{T_{D3}}{2}. \quad (1.1.7)$$

This is clearly different from the situation in type II theories where an $O p^{\pm}$ plane carries $\pm 2^{p-5}$ units of $D p$ brane charge. The charges (1.1.7) of the $O'3^{\pm}$ relative to the D3 will be crucial in constructing seiberg dual pairs in the next section.

1.1.1 A pseudo-moduli space

The discussion in the previous section shows that the \mathcal{Y}^+ (\square) theory is unstable, namely the D3s are repelled away from the orientifold. But the analysis tells us nothing about where the stable vacuum of the theory lies. In a non-SUSY setup, the scalar vevs, or correspondingly the coordinates of the branes are not to be viewed as moduli but are rather dictated by the dynamics of the theory. Generically one expects a scalar potential $V(X_+)$ to be induced via loop corrections. It is however useful to have a completely kinematical discussion of the possible *pseudo-moduli* of the brane system before imposing the dynamical constraints. We will examine the situation both in string theory and field theory.

Using the $U(N)$ matrices, the most generic vev for the scalars X_+ takes the diagonal form

$$\langle X_+ \rangle = \text{diag}(a_1, a_2, \dots, a_N); \quad a_i \in \mathbb{R}. \quad (1.1.8)$$

From a field theoretic point of view, depending on the specific values of the eigenvalues a_i we encounter 3 possibilities:

- (i) The a_i are all distinct. In this case the gauge group is broken to its $U(1)^N$ maximal torus and the worldvolume fermions all become massive. There are also adjoint (charge 0) scalars for each $U(1)$ factor in $U(1)^N$
- (ii) When n of the N eigenvalues become exactly degenerate there is an enhanced $U(n)$ symmetry. The breaking pattern in this case takes the form

$$U(N) \rightarrow U(n) \times U(1)^{N-n}. \quad (1.1.9)$$

All worldvolume fermions are massive but there are scalars in the adjoint of the unbroken gauge group. A special case of this type is when all the eigenvalues coincide and the entire gauge symmetry is unbroken.

- (iii) There is a more exotic possibility. Consider the situation where n eigenvalues take the opposite sign of an exactly degenerate set of m eigenvalues, i.e.

$$\langle X_+ \rangle = \text{diag} \left(\overbrace{v, \dots, v}^n, \overbrace{-v, \dots, -v}^m, a_1, \dots, a_{N-(n+m)} \right). \quad (1.1.10)$$

The unbroken gauge symmetry is now $U(n) \times U(m) \times U(1)^{N-(n+m)}$. As in the cases (i), (ii) above there are scalars transforming in the adjoint of the unbroken gauge symmetry. Unlike those cases, there are now also massless fermions thanks to the cancellation between the positive and negative eigenvalues of equal magnitude. These fermions transform in the bi-fundamental of the non-abelian $U(n) \times U(m)$ factor of the unbroken gauge group.

From the string theory perspective, case (i) corresponds to a configuration where all branes are at distinct points away from the orientifold, that is, none of the D3s coincide. Case (ii) corresponds to n D3 branes coinciding in the bulk (away from the orientifold). Case (iii) is more interesting. Suppose that $v > 0$, then in the brane picture v denotes the coordinates of n D3 branes in the transverse space. On the other hand giving negative vevs to m of the scalars corresponds to separating m D3s from the orientifold in the negative direction. But only the quotient space, i.e. the positive direction is physical. When we send m D3s to a negative point in the transverse space, their image D3's are given positive coordinates and appear in the physical space. So we see that case (iii) corresponds to n D3s and m D3's coinciding at coordinate v in the bulk. The worldvolume theory of this configuration beautifully matches what one would expect from field theory discussed in (iii).

1.1.2 Hanany-Witten setup

We are interested in Hanany-Witten setups to study 3d theories, which requires the introduction of NS5 branes. Our construction is the non-SUSY analogue of the 3d $\mathcal{N} = 2$ setup in type IIB (see e.g. [2]). In particular, we have NS5 branes which are non-parallel in two of their spatial coordinates as in table 1.2, we distinguish them by referring to one as an NS5'. The orientifold charge is switched from $O'3^+$ to $O'3^-$ and vice versa on either side of an NS5 or NS5' which intersects the orientifold. We will only consider configurations where the orientifold is asymptotically $O'3^+$ and label only the asymptotic charge of the orientifold plane in our diagrams (see figure 1.2).

Table 1.2. The various extended objects and their orientation in $\mathbb{R}^{1,9}$. All objects extend along the shared $x^{0,1,2}$ directions as well as those indicated below.

| | | | |
|----------|---|---|-------|
| NS5 | 3 | 4 | 5 |
| NS5' | 3 | | 8 9 |
| D3 | | | 6 |
| O'3 | | | 6 |
| D5 | | | 7 8 9 |
| $(1, k)$ | $\begin{bmatrix} 3 \\ 7 \end{bmatrix}_\theta$ | | 8 9 |

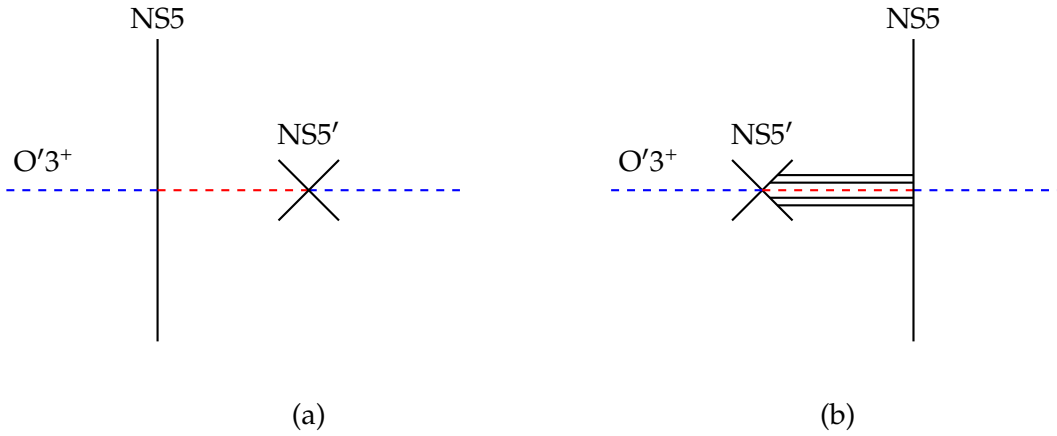


Figure 1.2. The Hanany-Witten effect. In passing from the configuration (a) to (b) a pair of D3s are created between the non-parallel NS5s.

Seiberg duality has a standard string theory derivation [71] which follows from a rearrangement of non-parallel NS5 branes in the Hanany-Witten setup. In constructions without an orientifold, it is possible to achieve this rearrangement without the need for the NS5 branes to intersect. This is done by using the freedom to separate them in a direction mutually transverse to the NS5 and NS5'. In the presence of an orientifold, the NS5s are bound to the orientifold plane and this is no longer possible. The NS5 branes will inevitably intersect as we try to move them past one another [103].

The result of moving non-parallel fivebranes through one another in the presence of an orientifold is well understood. This is the so called Hanany-Witten transition [4]. In type IIB constructions with an orientifold this amounts to the creation/annihilation of a D3 between the NS5 and NS5' depending on the orientifold type, a fact that follows from imposing the conservation of linking number. In the absence of D5 branes the linking number of an NS5 is proportional to the difference of the net D3 brane charges ending on it from the left and right respectively. Following the discussion around (1.1.7) it is easy to see that for the type 0

configuration of figure 1.2 the linking number of the NS5 and NS5' are conserved provided a pair of D3s are created in between them as we go from (a) to (b). This is twice the corresponding situation in type IIB as one would expect from the fact that the charge of $O'3^\pm$ relative to the type 0 D3 is a factor of two greater than the type IIB analogue.

In the next section we discuss the Hanany-Witten setup that leads to the non-SUSY gauge theories of interest with and without flavours.

1.2 3d dualities from non-supersymmetric brane configurations

In this section we consider Hanany-Witten setups that lead to three-dimensional CS theories. See figure 1.3 and 1.4. The construction is analogous to [2]. The difference here, besides being in type 0B, is the presence of the $O'3$ orientifold discussed previously.

In section 1.2.1 we consider the setup of figure 1.3. The low-energy theory of such a configuration is that of non-SUSY analogue of $\mathcal{N} = 2$ CS theories without flavours of (s)quarks. Such a setup turns out to be meaningful for the discussion of 3d dualities without matter. These dualities are also known in the literature as level-rank dualities.

In section 1.2.2 we consider the addition of N_f flavour D5-branes, see figure 1.4. The low-energy theory emerging from such a brane configuration includes quarks and squarks in the fundamental representation of the gauge group.

1.2.1 Level-rank duality

We begin by discussing how level-rank duality is realised in our setup. The discussion follows that of [104], and we provide a more refined account. In particular, we will be more careful about the CS level of the $U(1)$ factor of the gauge group.

The starting point is the brane configuration (a) of figure 1.3 with N_c D3 branes stretched between an NS5 brane and a $(1, k)$ 5-brane. We will refer to this as the *electric* theory. The worldvolume theory is the dimensional reduction of the \mathcal{Y}^- (\boxplus) subject to suitable boundary conditions. There is a $U(N_c)$ gauge field A_μ with a YM term and level k CS interactions, as well as a real scalar σ in the adjoint of $U(N_c)$ and two antisymmetric (complex) Dirac fermions in the \boxplus and the $\bar{\boxplus}$ of $U(N_c)$, respectively. The Lagrangian takes the following form⁴

$$\begin{aligned} \mathcal{L}_{N_f=0}^{(E)} = & \frac{1}{g_e^2} \text{Tr} \left[-\frac{1}{2} (F_{\mu\nu})^2 + (D_\mu \sigma)^2 + i\bar{\lambda} \not{D} \lambda + i\bar{\tilde{\lambda}} \not{D} \tilde{\lambda} - i\bar{\lambda} \sigma \lambda - i\bar{\tilde{\lambda}} \sigma \tilde{\lambda} + D^2 \right] \\ & + \frac{k}{4\pi} \text{Tr} \left[\epsilon^{\mu\nu\rho} \left(A_\mu \partial_\nu A_\rho - \frac{2i}{3} A_\mu A_\nu A_\rho \right) + 2D\sigma - \bar{\lambda}\lambda - \bar{\tilde{\lambda}}\tilde{\lambda} \right]. \end{aligned} \quad (1.2.1)$$

⁴Such a Lagrangian is understood as descending from its parent $\mathcal{N} = 2$ counterpart. In the large N limit we expect to recover a supersymmetric YM-CS theory. The following rule is expected to hold: $\boxplus \oplus \bar{\boxplus} \rightarrow \text{Adj}$.

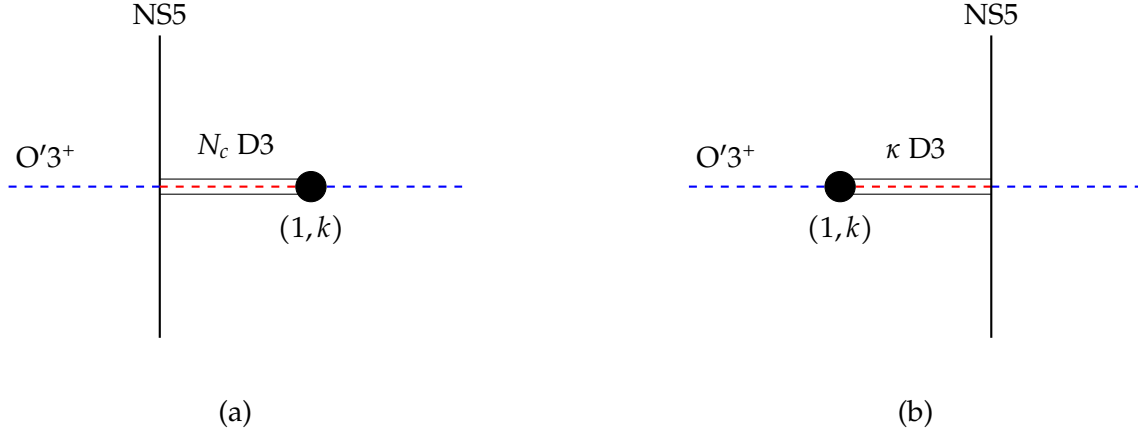


Figure 1.3. The brane setup for the (a) electric and (b) magnetic theory which give rise to level-rank duality.

Here $F_{\mu\nu}$ is the gauge field strength and $D_\mu \equiv \partial_\mu - iA_\mu$ is the covariant derivative. The covariant derivative is understood to act on the various fields in the representations of $U(N_c)$ they belong to. D is the auxiliary field of the vector multiplet borrowed from the supersymmetric parent theory. It belongs to the adjoint representation of the gauge group just like the gauge field and scalar gaugino.

Table 1.3. The field content of the worldvolume theories of the brane constructions in figure 1.3

| | | | |
|-------------------|-----------------|-------------|------------------|
| | $U(N_c)_k$ | | $U(\kappa)_{-k}$ |
| A_μ | Adj | a_μ | Adj |
| σ | Adj | s | Adj |
| λ | \square | l | \square |
| $\tilde{\lambda}$ | $\bar{\square}$ | \tilde{l} | $\bar{\square}$ |

It is straightforward to obtain the Seiberg dual of this theory following e.g. [2, 103] with a slight modification that takes into account the effect discussed in figure 1.2. After reshuffling the NS5 and $(1, k)$ fivebrane we arrive at the configuration (b) in figure 1.3, where the number of colour D3s is now $\kappa \equiv k - N_c + 2$. We refer to this as the *magnetic* theory. The worldvolume theory is now that of a gauge field a_μ with YM term and level $-k$ CS interactions as well as a real adjoint scalar s and antisymmetric Dirac fermions l and \tilde{l} . The Lagrangian is

$$\begin{aligned} \mathcal{L}_{N_f=0}^{(M)} = & \frac{1}{g_m^2} \text{Tr} \left[-\frac{1}{2} (f_{\mu\nu})^2 + (D_\mu s)^2 + i\tilde{l}\not{D}l + i\tilde{l}\not{D}\tilde{l} - i\tilde{l}s l - i\tilde{l}s\tilde{l} + D^2 \right] \\ & + \frac{k}{4\pi} \text{Tr} \left[\epsilon^{\mu\nu\rho} \left(a_\mu \partial_\nu a_\rho - \frac{2i}{3} a_\mu a_\nu a_\rho \right) + 2Ds - \tilde{l}l - \tilde{l}\tilde{l} \right]. \end{aligned} \quad (1.2.2)$$

We are interested in the IR dynamics of these theories. In the absence of supersymmetry, the scalars on the two sides are expected to acquire a 1-loop mass of the order of the cutoff [104]

$$m_\sigma^2 \sim g_e^2 \Lambda, \quad m_s^2 \sim g_m^2 \Lambda. \quad (1.2.3)$$

As in the discussion following (1.1.5) this translates to an attractive force between the branes and the orientifolds, signalling perturbative stability of the configuration. At energies well below the cutoff scales, the scalars are decoupled and do not play a role. Note that the scalars also have tree level CS masses, but we expect them to be subleading due to the stringy nature of the masses in (1.2.3). After integrating out the scalars we are left with gauge fields and antisymmetric fermions, both of which have tree-level CS masses $M_{CS} = \pm g^2 k$ where the sign of the mass follows from the sign of the bare CS levels in (1.2.1) and (1.2.2). Due to the lack of supersymmetry, also the gauginos (the antisymmetric fermions) get a mass at one-loop and can be integrated out. Integrating out the antisymmetric fermions shift the levels of the $U(1)$ and $SU(N_c)$ (resp. $SU(\kappa)$) factors of the gauge group by disproportionate amounts. As a result the IR of the electric theory is a $U(N_c)_{K_1, K_2}$ CS TQFT where

$$K_1 = k - N_c + 2 \equiv \kappa, \quad K_2 = k - 2N_c + 2 \equiv \kappa - N_c. \quad (1.2.4)$$

While the IR of the magnetic theory is described by a $U(\kappa)_{L_1, L_2}$ CS TQFT with

$$L_1 = -k + \kappa - 2 = -N_c, \quad L_2 = -k + 2\kappa - 2 = -N_c + \kappa. \quad (1.2.5)$$

Putting everything together we end up with the TQFTs $U(N_c)_{\kappa, \kappa - N_c}$ and $U(\kappa)_{-N_c, -N_c + \kappa}$. In fact, these theories are dual to each other. Therefore, in the IR, we recover the following level-rank duality

$$U(N_c)_{\kappa, \kappa - N_c} \longleftrightarrow U(\kappa)_{-N_c, -N_c + \kappa}. \quad (1.2.6)$$

1.2.2 Including flavours

We can include flavours in the discussion by adding D5 branes to the setup, the world-volume directions spanned by the flavour D5 branes are as in table 1.2. The IR phases of the electric theory turn out to be richer than the cases studied above and are nicely encoded in terms of the dual magnetic theory. We begin by analysing each theory separately semi-classically before mapping out the phase diagram.

Electric theory

The flavoured electric theory is realised on the brane configuration (a) of figure 1.4. The worldvolume theory on the D3 branes now includes N_f complex scalars Φ and N_f Dirac

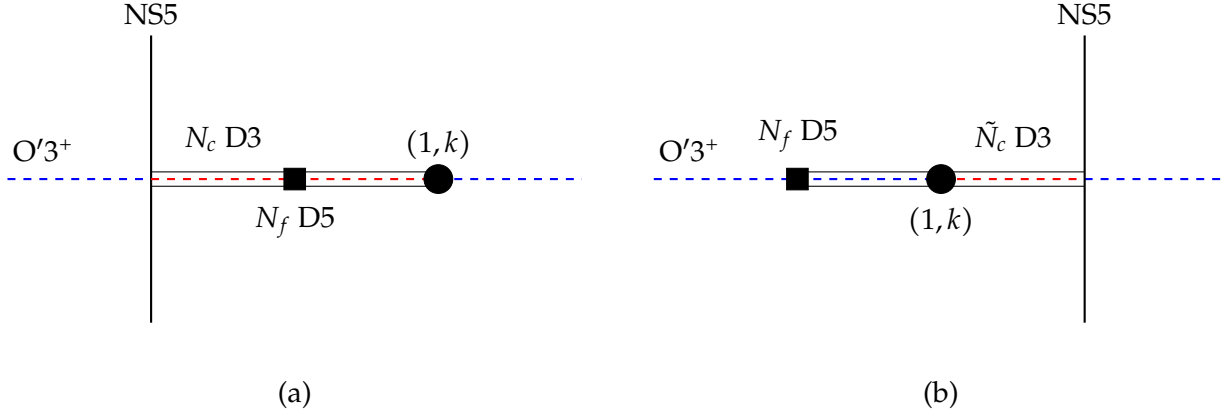


Figure 1.4. The brane setup for the (a) electric and (b) magnetic theory of our proposal. Here $\tilde{N}_c = N_f + k + 2 - N_c$

Table 1.4. The field content of the electric and magnetic theory.

| Electric Theory | | | Magnetic Theory | | |
|-------------------|-----------------|-----------|-----------------|-----------------------|-----------------|
| | $U(N_c)_k$ | $SU(N_f)$ | | $U(\tilde{N}_c)_{-k}$ | $SU(N_f)$ |
| A_μ | Adj | · | a_μ | Adj | · |
| σ | Adj | · | s | Adj | · |
| λ | \square | · | l | \square | · |
| $\tilde{\lambda}$ | $\bar{\square}$ | · | \tilde{l} | $\bar{\square}$ | · |
| Φ | $\bar{\square}$ | \square | ϕ | \square | $\bar{\square}$ |
| Ψ | \square | \square | ψ | $\bar{\square}$ | $\bar{\square}$ |
| | | | M | · | Adj |
| | | | χ | · | \square |
| | | | $\tilde{\chi}$ | · | $\bar{\square}$ |

fermions Ψ . The relevant flavour symmetry emerging from the branes is an $SU(N_f)$ group. The representations of the scalars and fermions with respect to the gauge and flavour groups are listed in table 1.4. These are essentially determined by their coupling to the antisymmetric gauginos, see later (1.2.8).

The tree level Lagrangian is given by

$$\mathcal{L}^{(E)} = \mathcal{L}_{N_f=0}^{(E)} + \mathcal{L}_{\text{matter}}, \quad (1.2.7)$$

where $\mathcal{L}_{N_f=0}^{(E)}$ is, as before, given by (1.2.1). The additional flavour terms are described by

$$\begin{aligned} \mathcal{L}_{\text{matter}} = & |D_\mu \Phi_i^a|^2 + i\bar{\Psi}^{ai} (\not{D}\Psi)_{ai} - \bar{\Phi}_a^i (\sigma^2)_b^a \Phi_i^b + \bar{\Phi}_a^i (D^2)_b^a \Phi_i^b \\ & - \Psi_{ai} \sigma_b^a \bar{\Psi}^{bi} - (i\lambda_{[ab]} \Phi_i^a \bar{\Psi}^{bi} + i\tilde{\lambda}^{[ab]} \bar{\Phi}_a^i \Psi_{bi} + \text{h.c.}) . \end{aligned} \quad (1.2.8)$$

Here $a, b = 1, \dots, N_c$ are colour indices and $i, j = 1, \dots, N_f$ are flavour indices. The interactions with the gauginos fix the representations of the (s)quark fields to be as in table 1.4.

The fate of the scalar σ of the gauge multiplet of the electric theory is similar to the flavourless case. The one-loop corrections to the scalar propagator get positive contributions from its coupling to itself and to the gauge field and negative contributions from its coupling to the gaugino λ . Since there are more bosonic than fermionic degrees of freedom, the vacuum $\langle \sigma \rangle = 0$ is stable; σ does not play a role in the IR dynamics of the theory and can be integrated out.

A similar story pans out for the squark Φ . Indeed, the squark couples to the gauge field A_μ , the scalar σ and the gaugino λ . Since there are more bosonic than fermionic degrees of freedom, one expects the squark to acquire a positive mass $M_\Phi^2 > 0$ and decouple from the IR physics.

For a non-zero level $k \neq 0$, the gauge field and the gaugino acquire a Chern-Simons mass $M_{\text{CS}} = g^2 k$. We therefore expect the IR physics to be dominated by the topological CS theory coupled to N_f fundamental quarks, i.e. QCD₃ with N_f quark flavours.⁵ The IR levels of the electric theory are shifted by the gaugino as in (1.2.4), as well as the fundamental quarks. In summary, using the dictionary (1.0.3) we have

$$\text{electric IR:} \quad \text{U}(N_c)_{K, K-N_c} \oplus N_f \text{ fermions} , \quad (1.2.9)$$

which is nothing but the left hand side of (1.0.1).

On the other hand, when $k = 0$, the IR theory is that of YM theory coupled to the gaugino and the fundamental quarks. It is less straightforward to say anything concrete about the IR dynamics of this theory.

Magnetic theory

The flavoured magnetic theory lives on the configuration (b) of figure 1.4. It is obtained from the flavoured electric theory by the standard Giveon-Kutasov move [2, 103] modified so as to account for the brane creation described in figure 1.2. One can easily verify that the

⁵Integrating out the gauge sector is somewhat more natural in the semiclassical regime $k \gg 1$. We expect this to remain true also at finite k , unless something drastic happens.

resulting number of colour branes between the NS5 and the $(1, k)$ fivebrane is

$$\tilde{N}_c = N_f + k - N_c + 2 \equiv N_f + \kappa . \quad (1.2.10)$$

The magnetic field content is given in table 1.4. This can be obtained in a similar fashion to the electric theory, i.e. by subjecting the theory on the D3 branes in table 1.1 to the appropriate boundary conditions. We have a gauge multiplet identical to the magnetic theory of the $N_f = 0$ case. The matter multiplet consists of a complex scalar ϕ and a Dirac fermion ψ . Their representations with respect to the gauge and flavour groups are given in table 1.4. There are in addition new degrees of freedom, which have no analogue on the electric side, corresponding to the motion of the flavour D3 branes along the $x^{8,9}$ directions. These give rise to two gauge singlets; the meson M which is an $SU(N_f)$ adjoint and its fermionic partners, the ‘‘mesinos’’ χ transforming as \square of $SU(N_f)$ and $\tilde{\chi}$ transforming as $\overline{\square}$ of $SU(N_f)$.

The tree level Lagrangian for this theory is

$$\mathcal{L}^{(M)} = \mathcal{L}_{N_f=0}^{(M)} + \mathcal{L}_{\text{matter}} , \quad (1.2.11)$$

where $\mathcal{L}_{N_f=0}^{(M)}$ is as in (1.2.2). The matter Lagrangian is

$$\begin{aligned} \mathcal{L}_{\text{matter}} = & |D_\mu \phi_a^i|^2 + i\bar{\psi}(\not{D}\psi)^{ai} - \bar{\phi}_i^a (s^2)_a^b \phi_b^i + \bar{\phi}_i^a D_a^b \phi_{bi} - \psi^{ai} (s)_a^b \bar{\psi}_{bi} \\ & - \left(i\tilde{l}^{[ab]} \phi_a^i \bar{\psi}_{bi} + il_{[ab]} \bar{\phi}_i^a \psi^{bi} + \text{h.c.} \right) + |\partial_\mu M_j^i|^2 + i\tilde{\chi}^{\{ij\}} \not{\partial} \chi_{\{ij\}} \\ & - y^2 \bar{\phi}_i^a \phi_a^i \bar{\phi}_j^b \phi_b^j - y^2 \phi_a^i \bar{M}_i^j M_j^k \bar{\phi}_k^a - y \left(\chi_{\{ij\}} \phi_a^i \psi^{aj} + \tilde{\chi}^{\{ij\}} \bar{\phi}_i^a \bar{\psi}_{aj} + \text{h.c.} \right) \\ & - y \left(\psi^{ai} M_i^j \bar{\psi}_{aj} + \text{h.c.} \right) . \end{aligned} \quad (1.2.12)$$

Note that in addition to the magnetic gauge coupling g_m , we now have another coupling constant y which controls interactions between the (s)quarks and the meson multiplet.

The scalar s of the magnetic gauge multiplet gets a positive mass and decouples, just as it did in the flavourless case. This signals the stability of the colour branes near the orientifold.

The squark ϕ couples to the gauge multiplet as well as the meson multiplet. There are more bosonic than fermionic degrees of freedom in the gauge multiplet, and more fermionic than bosonic degrees of freedom in the meson multiplet. Therefore, the squark acquires a 1-loop mass of the form

$$M_\phi^2 \sim (-y^2 + g_m^2) \Lambda . \quad (1.2.13)$$

The two effects compete and the squark may become massive or tachyonic. Since at large k the gauge field becomes heavy and decouples we operate under the assumption that in this limit the squark is tachyonic.

The matter Lagrangian (1.2.12) for the magnetic theory includes a coupling between the meson field and the scalar quarks

$$y^2 \phi_a^i \bar{M}_i^j M_j^k \bar{\phi}_k^a. \quad (1.2.14)$$

If the meson acquires a vev of the form $\langle \bar{M}_i^j M_j^k \rangle = u^2 \delta_i^k$ the squark ϕ becomes massive. If the squark acquires a vev $\langle \phi_a^i \rangle = v \delta_a^i$, and flavour symmetry is unbroken, the mesons become massive. Therefore, the most likely scenario is that in all phases [83]

$$M_\phi^2 M_M^2 < 0. \quad (1.2.15)$$

In the following we will always work with this assumption in mind. This will be crucial in obtaining the phase diagram of QCD₃.

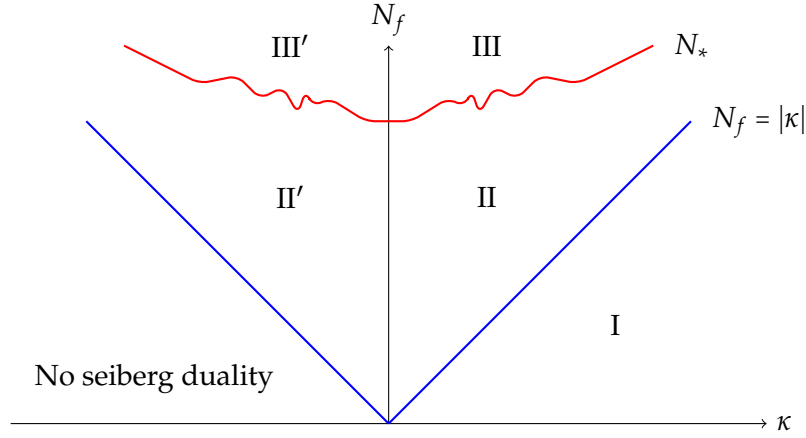
1.3 Phase diagram

As we saw in (1.2.9), the IR theory on the electric brane configuration is precisely QCD₃. In this section we argue that the conjectured phase diagram of QCD₃ can be understood in terms of the dual magnetic description. Many of the features are similar to the symplectic case analysed in [83]. For this reason we will be somewhat brief and focus only on the details which are new to the unitary theory.

1.3.1 Region I: Bosonization

We start with the region of the parameter space where $\kappa \equiv k + 2 - N_c \geq N_f$. This corresponds to region I in the phase diagram of figure 1.5. In this region the rank of the magnetic gauge group $\tilde{N}_c = N_f + \kappa$ is automatically positive. Following the discussion around (1.2.13), the N_f squarks are assumed to be tachyonic throughout this region. This is reasonable as one can go to arbitrarily large values of k while keeping N_f fixed. In this regime the gauge sector becomes heavy and decouples from the dynamics. The main contribution to the mass of the squark (ϕ) comes from the meson multiplet, which is indeed negative. Thus, our main assumption is that this remains true as we move to finite k .

Let us then assume that the magnetic squarks condense. In the brane configuration, this corresponds to Higgsing N_f colour D3 branes via reconnection to N_f flavour D3 branes. This is the Higgs mechanism in the string theory language. The world-volume of the N_f Higgsed D3 branes no longer supports a gauge multiplet as they end on D5s from one side and end on the NS5 brane from the other. However, we still have κ colour D3 branes which support a $U(\kappa)_{-k}$ gauge theory with massive gauge field and massive gauginos. The CS mass is still proportional to k , and we can integrate out the gauge field and gauginos at energies below $g^2 k$. The reconnection preserves the original $U(N_f)$ global symmetry. We will shortly argue,

Figure 1.5. Phase diagram of QCD₃.

from the field theory side, that there are N_f scalars in the fundamental after the Higgsing. In the brane set-up these can only come from open strings stretched between the colour branes and N_f Higgsed D3 branes.

Let us try to understand the phenomenon described in the last paragraph in terms of the field theory description of the magnetic theory. Indeed, the Higgsing corresponds to giving a colour-flavour locking vev to the magnetic squark without breaking the global $U(N_f)$. The gauge symmetry breaking pattern is given by

$$U(\kappa + N_f) \rightarrow U(\kappa), \quad (1.3.1)$$

leaving the gauginos in the \square and $\bar{\square}$ of the Higgsed gauge group as well as N_f fundamental squarks. The N_f magnetic quarks become massive due to Yukawa terms. In addition, the meson and the mesino all become massive due to interactions like (1.2.14) and can be integrated out.

The IR levels get shifted after integrating out the gaugino according to (1.2.5) so that, using the dictionary (1.0.3), the IR of the magnetic theory in this region of the parameter space is described by

$$\text{magnetic IR: } U\left(K + \frac{N_f}{2}\right)_{-N_c, -N_c + K + \frac{N_f}{2}} \oplus N_f \text{ scalars.} \quad (1.3.2)$$

Such a bosonic dual is described in the IR by a Lagrangian that contains, in addition to a CS term with appropriate levels and coupling between the scalars and gauge field, also self-interactions for the squarks. These correspond to mass terms of the form $\bar{\phi}_i^a \phi_a^i$ as well as quartic interaction of the form (single-trace) $(\bar{\phi}_i^a \phi_a^j)(\bar{\phi}_j^b \phi_b^k)$ and (double-trace) $(\bar{\phi}_i^a \phi_a^i)^2$. These

terms can be generated, if not already present, by the RG flow consistently with global symmetries.

As a final step, tuning the mass terms both in the electric IR theory in (1.2.9) and in the magnetic IR theory in (1.3.2), we recover a well-established duality. This is nothing but the duality (1.0.1).

1.3.2 Symmetry breaking

When $N^* > N_f > \kappa$, which corresponds to region II and II' in the phase diagram of figure 1.5, we expect rather different dynamics for the system and we anticipate breaking of the flavour symmetry. As we shall see, the physics in these regions is still captured by a tachyonic squark, colour-flavour locking and brane reconnection, but the implications and the resulting physics will be different with respect to region I. Note that the electric theory we discuss is a $U(N_c)$ gauge theory, while the result in ref.[6] is for $SU(N_c)$.

Region II'

Let us begin with region II' in the phase diagram of figure 1.5. In this region $\kappa < 0$. Therefore, on the magnetic side, there are less colour D3 branes than flavour D3 branes: $\tilde{N}_c = N_f + \kappa < N_f$. We will assume that the squarks condense also in this case. Nonetheless, squark condensation leads in this case to a fully Higgsed gauge group. Once again this is realised in string theory by reconnecting $N_f + \kappa$ colour and flavour D3 branes (we stress that $\kappa < 0$ here). After the Higgsing, we are left with $|\kappa|$ flavour D3 branes stretched between the D5 brane and the $(1, k)$ fivebrane, as well as the $N_f + \kappa$ connected D3 branes. The latter no longer support a gauge multiplet and therefore gauge symmetry is fully broken.

The global symmetry now consists of a $U(N_f + \kappa)$ factor corresponding to the symmetry on the $N_f + \kappa$ reconnected branes as well as a $U(\kappa)$ factor from the remaining flavour D3 branes. Using the dictionary (1.0.3) we have that in this region the global symmetry breaking pattern is

$$SU(N_f) \rightarrow S \left[U \left(\frac{N_f}{2} + K \right) \times U \left(\frac{N_f}{2} - K \right) \right]. \quad (1.3.3)$$

This symmetry breaking pattern is the one anticipated in [6]. As a consequence, the IR physics of this phase is described in terms of the Grassmannian

$$\mathcal{M} \left(K + \frac{N_f}{2}, N_f \right) = \frac{SU(N_f)}{S \left[U \left(\frac{N_f}{2} + K \right) \times U \left(\frac{N_f}{2} - K \right) \right]} \quad (1.3.4)$$

corresponding to the symmetry breaking pattern given in (1.3.3). Such a Grassmannian will

be essentially parametrised by⁶

$$N_f^2 - 1 - [(N_f + \kappa)^2 + \kappa^2 - 1] = 2|\kappa|(N_f - |\kappa|) = 2\left(\frac{N_f}{2} + K\right)\left(\frac{N_f}{2} - K\right) \quad (1.3.5)$$

massless Nambu-Goldstone bosons. We identify the Nambu-Goldstone bosons as the massless modes of open strings stretched between the two stacks of flavour branes.

Region II

When $0 < \kappa < N_f < N^*$ (or $0 < K + \frac{N_f}{2} < N_f < N^*$), after reconnection the theory in the IR is

$$\mathrm{U}\left(K + \frac{N_f}{2}\right)_{-N_c, -N_c + K + \frac{N_f}{2}} \oplus N_f \phi. \quad (1.3.6)$$

Naively, we seem to have a puzzle: instead of obtaining a theory of massless Nambu-Goldstone bosons we obtain bosonization. The NG theory we are seeking is nothing but the effective description of (1.3.6) for large negative masses of the squarks ϕ . According to the field theory analysis of Komargodski and Seiberg [6] upon condensation of the squarks we land on the symmetry breaking phase.

Indeed, after reconnection, the scalars in the bosonic dual (1.3.6) correspond to scalar modes of the open strings in the brane configuration. Therefore our proposal is that these scalars are tachyonic and are to be stabilised via open string tachyon condensation. We do not know whether a nice geometric picture emerges after this condensation. Regardless, in the field theory limit one eventually lands on the Grassmannian $\mathcal{M}(N_f, \kappa)$. This picture is consistent with the mass deformations of the brane setup, already discussed in [83].

1.4 Comments about QED₃

The discussion of the phase diagram in the preceding sections holds for a general number of colours N_c . However, “accidents” happen when $N_c = 1, 2$ that modify parts of the discussion. In the case of $N_c = 2$ the electric gaugino is a singlet of the SU(2) factor of the gauge group, but it carries charge 2 under the abelian factor. Because of this, some intermediate steps taken to arrive at the general phase diagram in figure 1.5 are slightly modified, the end result is however unaffected and the phase diagram of figure 1.5 is the correct picture for $N_c \geq 2$.

On the other hand, we start to see deviations from the general picture of figure 1.5 for $N_c = 1$ i.e. QED₃. In particular, as we shall see momentarily, when $k = 0$ there is no symmetry

⁶In order to be consistent with the UV symmetries one must also include CS terms in the effective description. The required modification is discussed in detail in [6].

breaking phase. This in turn suggests that no symmetry breaking can occur for non-zero k since the window for which a Grassmannian phase exists in the IR is maximised for $k = 0$ [6].

1.4.1 QED_3 with vanishing CS-term

When the electric gauge group is $U(1)$, there is no electric gaugino. Therefore, the IR of the electric theory is $U(1)_0$ theory coupled to N_f fermions. The magnetic dual has a gauge group $U(N_f + 1)$ with vanishing CS level at tree-level. Previously, squark condensation lead to masses being generated for the quarks, meson and the mesino, due to the presence of Yukawa interactions. However, in this case after reconnection we have a $U(1)$ gauge theory with no CS term and N_f massless Dirac fermions. The reason that in this specific case the fermions do not acquire a mass is that there is no gluino when the gauge group is $U(1)$ and no Yukawa term. In the absence of supersymmetry and without fine-tuning the squarks acquire a mass. So we end up with a magnetic theory that admits the same matter content as the electric theory, namely a dual $U(1)$ theory with N_f dual quarks.

The brane setup is such that the flavour branes coincide and hence flavour symmetry remains unbroken. Thus, our magnetic theory predicts no spontaneous breaking of $U(N_f)$. This is consistent with existing conjectures about the IR behaviour of QED_3 [105].

Chapter 2

Magnetic quivers for 5d SCFTs

The program to study Higgs branches of 5d theories via their magnetic quivers, was initiated in [54, 106], following earlier work [107, 108] observing similar connections. 5-brane webs also play an important role in constructing the 3d quiver gauge theories associated to the Higgs branch. A set of rules were established in [69, 109] to derive the magnetic quivers directly from the 5-brane web. In particular, stable intersection number from substructure of 5-brane web at Higgs branch, captures the multiplicity of edges connecting nodes of the 3d quiver [109]. This was later extended to brane webs with O5-planes in [55, 55, 63].

It will be convenient for us to make a distinction between quivers which are made entirely of unitary gauge nodes, and those which can also have orthogonal and/or symplectic gauge nodes in addition. We will refer to the former as unitary and the latter as orthosymplectic (OSp) quivers respectively. The primary focus of this paper is orthosymplectic magnetic quivers.

A convenient tool to study the moduli space of 3d $\mathcal{N} = 4$ theories is the Hilbert series, which enumerates gauge invariant operators graded by their conformal dimension. The Coulomb branch Hilbert series can be computed using the monopole formula [110], while the Higgs branch Hilbert series can be evaluated using the Molien-Weyl formula [47]. The Coulomb branch Hilbert series is sensitive to the pattern of symmetry enhancement discussed above, so long as one finds a way to refine the computation. This is a longstanding challenge in the case of OSp quivers due to a current lack of understanding of such computations.¹ One of the main results of this paper is the refined Hilbert series, and therefore the enhanced magnetic symmetry of the OSp quivers under our study. Together with the other tools of the Plethystic programme [112, 113], the Hilbert series can be used to give an algebraic description of the moduli space as a variety. We will in particular make use of the notion of highest weight generators (HWGs) developed in [114] in order to write down closed form expressions for the Coulomb branch Hilbert series of the OSp magnetic quivers under our consideration.

¹This difficulty is related to the notion of hidden FI parameters in OSp quivers, see e.g. [111].

We uncover an interesting phenomenon which is common to all models under our consideration; the moduli space of the $O\text{Sp}$ quivers that we study generically factorizes into two decoupled sectors, each of which has an alternative description, in terms of the moduli space of a single connected unitary quiver. An upshot of this result is that we can write exact highest weight generating functions (HWGs) encoding the Coulomb branch Hilbert series of several families of orthosymplectic quivers using known results for the individual factors. This result ultimately follows from fact that the $O\text{Sp}$ quivers that we study serve as magnetic quivers to 5d $\mathcal{N} = 1$ SCFTs which are the UV fixed point of a 5d IR gauge theory whose gauge group is a product of $SO(4)$ factors, and with matter representations transforming as either spinors or conjugate spinors of each $SO(4)$ factor. Since $SO(4)$ is locally isomorphic to $SU(2) \times SU(2)$, and a spinor and conjugate spinor transform under different $SU(2)$ factors, each such theory can be reformulated as a product of two decoupled theories, each of which has a gauge group that is a product of $SU(2)$ s. The theories containing $SO(4)$ factors can be engineered using a single type IIB brane web with the inclusion of $O5$ -planes, which can then be used to obtain an $O\text{Sp}$ magnetic quiver [55, 63]. On the other hand the formulation in terms of the product of theories with $SU(2)$ factors is engineered by two independent brane webs, giving rise to two magnetic quivers, which will be unitary by construction [109].

We note that an analogous factorization phenomenon happens for 4d $\mathcal{N}=2$ theories of class-S of D-type. In this context, it is well known that there are cases in which a single three-punctured sphere describes the direct sum of 2 SCFTs, each of which also admits a realization in A-type class-S [115–118]. Indeed, we identify some 4d $\mathcal{N}=2$ theories of D-type class-S which exhibit this factorization, and for which the orthosymplectic 3d mirror theories correspond to the magnetic quiver derived from the 5-brane webs with $O5$ -plane. Likewise, the 3d mirror of the two A-type factors also corresponds to the unitary magnetic quiver derived from the 5-brane web without $O5$ -plane.

In this paper we initiate a study of the Higgs branch of 5d SCFTs engineered using brane webs with $O7^+$ -planes. The relevance of this study is the following. The usual brane web description of 5d SCFTs [11] can be enriched with the inclusion of orientifold planes. There are two types of orientifold planes whose inclusion in the brane web leads to consistent 5d SCFTs, namely $O5$ -planes [17, 21] and $O7$ -planes [16]. Magnetic quivers for 5-brane webs with $O5$ -planes have already been explored in [55, 56, 63], but an analogous study of brane webs with $O7$ -planes is so far missing from the literature. There are two variants of the $O7$ -plane, namely the $O7^+$ and $O7^-$. The latter of these is non-perturbatively resolved into a pair of (p, q) 7-branes at strong string coupling [119, 120], leading therefore to an ordinary brane web. On the other hand the $O7^+$ plane is an exact configuration and so will give rise to novel magnetic quivers.

The strategy for proposing the magnetic quivers is the following. We focus on $SO(N)$

gauge theories with N_v hypermultiplets in the vector representation. This is a natural set of theories to study, as they admit a realization with a brane-web involving an $O7^+$ plane, and also another realization with a brane-web involving $O5^-/\widetilde{O5}^-$ -planes. Since the magnetic quivers for the latter can be obtained using the techniques of [55, 63] they serve as a consistency check for our proposal for the magnetic quivers obtained from the web with $O7^+$ -plane.

As a main result, we find that the magnetic quivers for the webs with $O7^+$ -planes are always framed non-simply-laced quivers. The derivation of the magnetic quivers was performed with some educated guesswork loosely motivated by intuition stemming from S-duality of type IIB, and some existing results on non-simply laced quivers and brane systems [106]. What gives these conjectural magnetic quivers a firm basis is the agreement of their CB Hilbert series with that computed from the magnetic quivers for the same theory, derived from an $O5$ -plane construction.

2.1 Tools from the plethystic programme

In this section we review the material we need for the computation of the Hilbert series. The discussion will be minimal and will cover only those aspects necessary for the subsequent section. For more details the reader can consult the original papers. The literature on this material is vast, but we will mostly follow [47, 65, 110, 112, 114]. In the following subsections we consider a 3d $\mathcal{N} = 4$ theory with gauge group G of rank r and n_H hypermultiplets transforming under the representation R_i of G ($i = 1, \dots, n_H$).

2.1.1 What is a Hilbert series?

The primary object of interest in algebraic geometry is an algebraic variety X , defined as the set of zeros of a system of polynomial equations

$$X := \{F_i(x_1, \dots, x_k) = 0\} \subset \mathbb{C}^k, \quad i \in \{1, \dots, \text{codim}(X)\}. \quad (2.1.1)$$

To a variety X , one associates its coordinate ring, the ring of polynomials holomorphic in the coordinates of X . The strategy is then to learn about properties of X , by studying its coordinate ring. In an abuse of notation, we denote both the variety and its coordinate ring by X , and it should be clear from context, which object is being referred to in a given computation. If a ring X admits a graded decomposition of the sort

$$X = \bigoplus_{A \in I} X_A, \quad (2.1.2)$$

then we can define the Hilbert series of X as

$$\text{HS}_X(t) = \sum_A \dim(X_A) t^A, \quad |t| < 1 \quad (2.1.3)$$

Let us demonstrate this by examples. Consider, perhaps trivially, the space \mathbb{C}^2 . The coordinate ring of this space is $\mathbb{C}[x, y]$, i.e. the ring of polynomials in two variables with complex coefficients. The coordinate ring $\mathbb{C}[x, y]$, has a natural decomposition, graded by homogeneous degree

$$\mathbb{C}[x, y] = \mathbb{C} \oplus \mathbb{C}(x + y) \oplus \mathbb{C}(x^2 + y^2 + xy) \oplus \dots \quad (2.1.4)$$

The Hilbert series in this case is straightforward to compute

$$\text{HS}_{\mathbb{C}^2}(t) = 1 + 2t + 3t^2 + \dots = \sum_{n=1}^{\infty} n t^{n-1} = \frac{1}{(1-t)^2} \quad (2.1.5)$$

Now consider $\mathbb{C}^2/\mathbb{Z}_2$, where we quotient out by the \mathbb{Z}_2 action which inverts the coordinates $\mathbb{Z}_2 : (x, y) \rightarrow (-x, -y)$. Clearly, any monomial of odd homogeneous degree will not be invariant under such a symmetry. Therefore, the coordinate ring is given by

$$\frac{\mathbb{C}[x, y]}{\mathbb{Z}_2} = \mathbb{C} \oplus \mathbb{C}(x^2 + y^2 + xy) \oplus \mathbb{C}(x^4 + y^4 + x^3y + x^2y^2 + xy^3) \oplus \dots, \quad (2.1.6)$$

and so the Hilbert series takes the following form

$$\text{HS}_{\mathbb{C}^2/\mathbb{Z}_2}(t) = \sum_{n=0}^{\infty} (2n+1)t^{2n} = \frac{(1-t^4)}{(1-t^2)^3} \quad (2.1.7)$$

2.1.2 Coulomb branches

The bosonic fields in a 3d $\mathcal{N} = 4$ vector multiplet consist of a gauge field and 3 real scalars. Upon dualising the gauge field to a scalar we have 4 scalars at our disposal, which can be pairwise complexified. These are the coordinates on the Coulomb branch at large vevs. Each of these complex scalars forms the scalar component of an $\mathcal{N} = 2$ chiral superfield. For small vevs one needs to replace the complex scalar containing the dual photon by a BPS monopole operator [121], which can again be thought of as the bottom component of an $\mathcal{N} = 2$ chiral multiplet. The quantum coordinates of the Coulomb branch are therefore the BPS monopole V_m of magnetic charge m and the adjoint scalar ϕ . The Hilbert series (HS) for the Coulomb branch of a good or ugly (in the sense of [121]) 3d $\mathcal{N} = 4$ theory is then computed by the

monopole formula [110]

$$\text{HS}(t, z) = \sum_{m \in \Lambda_m^{\mathbb{G}^V} / \mathcal{W}_{\mathbb{G}^V}} z^{J(m)} t^{2\Delta(m)} P_G(t, m), \quad (2.1.8)$$

where the sum is over the magnetic lattice of the gauge group G , we refer to [65] for a detailed account. $\Delta(m)$ is the conformal dimension of the monopole operator with magnetic charge m , and is given by

$$\Delta(m) = - \sum_{\alpha \in \Delta^+} |\alpha(m)| + \frac{1}{2} \sum_{i=1}^{n_H} \sum_{\rho_i \in R_i} |\rho_i(m)|, \quad (2.1.9)$$

where Δ^+ is the set of positive roots and ρ_i are the weights of the representation R_i . The classical dressing factor $P_G(t, m)$ counts invariants built out of the adjoint scalars ϕ

$$P_G(t, m) = \prod_{i=1}^r \frac{1}{1 - t^{2d(i)}}, \quad (2.1.10)$$

where $d(i)$ are the degrees of the Casimir invariants of the gauge symmetry $H \subset G$ which is the unbroken part of the original gauge symmetry in the presence of a monopole operator V_m of charge m . Finally z denote the fugacities of the topological symmetry whose exponent $J(m)$ denotes the topological current.

When the quiver consists only of unitary nodes, without the addition of flavors, there is typically an overall $U(1)$ which is decoupled. At the level of the HS computation, the decoupling of the overall $U(1)$ can be implemented in two ways. One can either treat one $U(N)$ gauge node as $SU(N)$ since the beginning, or one can treat it as $U(N)$ when computing the monopole dimension formula, and then set to zero one of the magnetic charges of such $U(N)$ at the moment of computing the Hilbert Series. Furthermore, the choice of the specific node at which the overall $U(1)$ decouples is immaterial. We will see that both these features cease to be true if we relax the original hypothesis that the quiver is simply-laced.

Coulomb branch Hilbert series for non-simply laced quivers

Let us consider now a case in which the quiver itself is unitary and non-simply laced. With this we mean that two nodes can be connected by n oriented lines. In the usual non-simply laced case, a straight line between two gauge nodes is interpreted as a bifundamental hypermultiplet. In the non-simply laced case, there is up to date no clear interpretation of the oriented multiple-line, at the field theory level. Despite this, it was proposed in [106] that one can still compute the Coulomb Branch Hilbert series of such a quiver. First of all, the

matter contribution to the dimension formula must be modified as follows²:

$$\Delta_{\text{hyp}} = \begin{cases} \frac{1}{2} \sum_{i=1}^M \sum_{j=1}^N |2m_i - n_j| & \begin{array}{c} M \\ \circ \longrightarrow \circ \\ N \end{array} \\ \frac{1}{2} \sum_{i=1}^M \sum_{j=1}^N |m_i - n_j| & \begin{array}{c} M \\ \circ \text{---} \circ \\ N \end{array} \end{cases} . \quad (2.1.11)$$

Secondly, it turns out that for a unitary non-simply laced quiver with no flavor nodes there is still an overall $U(1)$ that needs to be decoupled. However, now the choice of where to decouple the overall $U(1)$ is crucial. Decoupling it at different nodes will result in different CB Hilbert series. Therefore one denotes with the squircle \square the location at which the overall $U(1)$ has to be decoupled. See [122] for more details on this point.

Not just the node at which the decoupling is done, but also *how* this procedure is done is important. In the simply-laced case we could have decoupled the overall $U(1)$ both by treating a $U(N)$ node as an $SU(N)$ when writing the monopole dimension formula, or at a later stage. In this second option, one writes the monopole dimension formula as if all nodes are unitary, and then simply does not sum over one of the magnetic charges when computing (2.1.8), namely, one sets $m_i = 0$ for a given fugacity m_i . We argue that the two prescriptions are not in general equivalent, and in particular when the quiver is non-simply laced, the second option is the correct one.

The reason for this is very evident working in the fugacity base of $U(1) \times SU(N)$. For simplicity, let us consider $N = 2$. Let q be the fugacity associated to $U(1)$ and p that associated to $SU(2)$. The change of base that connects these fugacities to the usual ones is [123]:

$$\begin{cases} m_1 = p + q \\ m_2 = p - q \end{cases} . \quad (2.1.12)$$

From this we see that setting to zero m_1 means forcing $p = q$. This means decoupling a $U(1)_{\text{diag}}$ which is *not* the $U(1)$ factor in the product $U(1) \times SU(2)$, but rather it is a diagonal $U(1)_{\text{diag}}$ between the $U(1)$ factor of $U(1) \times SU(2)$ and the Cartan $U(1)_{\text{car}}$ of $SU(2)$. On the other hand, treating the $U(2)$ node as $SU(2)$ from the beginning would correspond to set to zero p when writing the monopole dimension formula. The two operations are clearly different. In the simply laced case the end result of the HS computation will not depend on which option is chosen, however this is just an accident. In the simply-laced case the result will depend on this choice, and throughout this paper we find consistent results if and only if the diagonal $U(1)$ is the one to be ungauged.

²In case of multiplicity n , we replace the number 2 in $|2m_i - n_j|$ with the number n .

2.1.3 Higgs branches

The Higgs branch of a 3d $\mathcal{N} = 4$ theory is parametrised by vevs of the scalar components of the hypermultiplets. When dealing with a gauge theory, each such operator will be in an irrep of G . The Higgs branch operators are therefore those constructed by considering all symmetrised tensor powers of these irreps. The symmetrisation is done in order to be consistent with Pauli statistics. To avoid overcounting, the relations among these scalar operators due to the superpotential need to be imposed. One will then need to project onto the gauge singlet states in order for the resulting operators to be well defined gauge invariant operators. The Higgs branch Hilbert series is therefore computed using the Molien-Weyl formula [47]

$$\text{HS}^{\mathcal{H}}(t) = \int_G d\mu_G \frac{\text{PE} \left[\sum_{i=1}^{n_H} \chi_{R_i}(x)t \right]}{\text{PE} \left[\chi_{\text{Adj}}(x)t^2 \right]}, \quad (2.1.13)$$

where $\chi_{R_i}(x)$ is the character of the representation R_i of G under which the scalars in the i -th hypermultiplet transform, χ_{Adj} is the character of the adjoint representation of G , the representation carried by the relations. The function $\text{PE}[\cdot]$ is the plethystic exponential, defined via

$$\text{PE} [f(z_1, \dots, z_r)] = \exp \left(\sum_{k=1}^{\infty} \frac{1}{k} f(z_1^k, \dots, z_r^k) \right), \quad (2.1.14)$$

it is a symmetrising function that generates the characters of the symmetrised tensor powers of χ_{R_i} . Finally the projection onto gauge invariant operators is achieved by integrating over the group manifold using the Haar measure. In a suitable basis, the Haar measure can be taken to be

$$\int_G d\mu_G = \frac{1}{(2\pi i)^r} \prod_{i=1}^r \oint_{|x_i|=1} \frac{dx_i}{x_i} \prod_{\alpha \in \Delta^+} \left(1 - \prod_{k=1}^r x_k^{\alpha_k} \right). \quad (2.1.15)$$

2.1.4 Highest weight generating functions

The refined Hilbert series for a given theory can be generically expanded as Taylor series in t such that the coefficients are sum of the characters of representations of global symmetry of the theory. In general, given a global symmetry of rank r , the refined Hilbert series can be expanded as:

$$\sum_{n_1=0}^{\infty} \sum_{n_2=0}^{\infty} \cdots \sum_{n_r=0}^{\infty} \chi_{[f_1, f_2, \dots, f_r]} t^{\eta}, \quad (2.1.16)$$

where each of f_1, \dots, f_r and η can be some polynomial function in variables n_1, \dots, n_r . The notation $\chi_{[f_1, \dots, f_r]}$ is the character of the irrep of the global symmetry whose highest weight is $f_1 \Lambda_1 + \dots + f_r \Lambda_r$, where f_i are the Dynkin labels of the irrep and Λ_i are the fundamental weights of the global symmetry group. A convenient way to repackage the same information is in terms of highest weight generating functions or HWGs [114]. One introduces a set

of fugacities $\{\mu_1, \dots, \mu_r\}$, called highest weight fugacities, and one writes the characters in terms of μ_i according to the map

$$\chi_{[f_1, \dots, f_r]} \leftrightarrow \mu_1^{f_1} \dots \mu_r^{f_r}. \quad (2.1.17)$$

With this map, the Hilbert series becomes a formal power series which can be resummed, the corresponding generating function is termed as its HWG:

$$\text{HWG} = \sum_{n_1=0}^{\infty} \dots \sum_{n_r=0}^{\infty} \mu_1^{f_1} \dots \mu_r^{f_r} t^\eta. \quad (2.1.18)$$

Notation. To avoid the cluttering of the quiver diagrams, in what follows, we will use a color coding to represent the unitary and orthosymplectic nodes as given below:

| Node type | U(n) | SO(m) | USp($2k$) |
|-----------|----------|-----------|-------------|
| Gauge | ○ n | ● m | ● $2k$ |
| Flavor | □ n | ■ m | ■ $2k$ |

(2.1.19)

In the above, the circular nodes denote the gauge group while the square nodes represent a global (rather than gauge) symmetry group. In this work, we will have three kinds of links connecting the nodes: solid line, dashed line and wavy line. These links transform under the representations of the nodes it connects with the following dictionary.

| Link type | Interpretation |
|-----------|--|
| ○ — ○ | hypermultiplet transforming in the bifundamental representation |
| ○ — ● | hypermultiplet transforming in the bifundamental representation |
| ○ — ● | hypermultiplet transforming in the bifundamental representation |
| ● — ● | half-hypermultiplet transforming in the bifundamental representation |
| ○ - - - ○ | hypermultiplet in the fundamental-fundamental representation |
| ○ ~ ~ ~ □ | charge 2 hypermultiplet |

(2.1.20)

In order to avoid confusion, we will denote 5d (electric) quivers as $\dots - G - G_j - \dots$ and use square braces $[F]$ to denote flavor nodes.

2.2 Factorised 3d $\mathcal{N} = 4$ orthosymplectic quivers

In this section we present sequences of orthosymplectic magnetic quivers whose moduli space is the product of two decoupled sectors, each of which enjoys a description as the moduli space of a unitary quiver. Each sequence is parameterised by an integer N which is

the sequence number, and labelled $E_m \times E_n$, in accordance with the Coulomb branch isometry of the $N = 1$ case. For $N = 1$, some of the theories become particularly simple such that we can prove the equivalence of the orthosymplectic quiver with the two unitary quivers. The $E_m \times E_n$ orthosymplectic quiver with sequence number 1 corresponds to the magnetic quiver for infinite coupling limit of 5d $\mathcal{N} = 1$ SO(4) gauge theory with $m - 1$ hypermultiplets in the spinor representation denoted by \mathfrak{s} and $n - 1$ hypermultiplets in the conjugate spinor representation of SO(4) denoted by \mathfrak{c} . Correspondingly the dual unitary quivers with sequence number 1 correspond to magnetic quivers for infinite coupling limit of 5d $\mathcal{N} = 1$ SU(2)×SU(2) gauge theory with $m - 1$ hypermultiplets in the $(\mathbf{F}, \mathbf{1})$ and $n - 1$ hypermultiplets in the $(\mathbf{1}, \mathbf{F})$ representation of SU(2)×SU(2), where we denote by \mathbf{F} the fundamental representation of associated gauge group. One can engineer these theories using 5-brane webs with O5-planes [17], as well as using ordinary brane webs [11]. This pattern generalizes for higher sequence numbers, namely one can provide an intuition for the reason that the orthosymplectic quivers factorise into two decoupled sectors by viewing them as magnetic quivers of a 5d theory. We will therefore employ this perspective in the following. We will use $\text{EQ}_{m,n}$ to denote the 5d OSp electric quivers for the $E_m \times E_n$ sequence, while we use the notation EQ_m to denote the 5d unitary electric quivers to which the former factorise. Similarly, we will denote the OSp magnetic quivers of the $E_m \times E_n$ sequence by $\text{MQ}_{m,n}$, while we denote the unitary components to which they factorise by MQ_m . Occasionally there will be more than one generalisation of a given sequence for higher sequence numbers, in which case we will distinguish the different sequences by a prime.

2.2.1 The $E_1 \times E_1$ sequence

Consider the 5-brane web constructed by collapsing $2N$ NS5 branes on top of an O5-plane that is asymptotically O5⁺ as in figure 2.1. By resolving this web to go on the Coulomb branch one can identify the following low energy quiver description,

$$\text{EQ}_{1,1} = \overbrace{\text{SO}(4) - \text{USp}(0) - \text{SO}(4) - \dots - \text{USp}(0) - \text{SO}(4)}^{2N-1}. \quad (2.2.1)$$

One can recast this theory, by using the accidental Lie algebra isomorphism $\mathfrak{so}(4) \cong \mathfrak{su}(2) \times \mathfrak{su}(2)$ as a product of two decoupled 5d quiver gauge theories:

$$\text{EQ}_{1,1} = (\text{EQ}_1)^2 = \left(\overbrace{\text{SU}(2) - \text{SU}(2) - \text{SU}(2) - \dots - \text{SU}(2)}^N \right)^2. \quad (2.2.2)$$

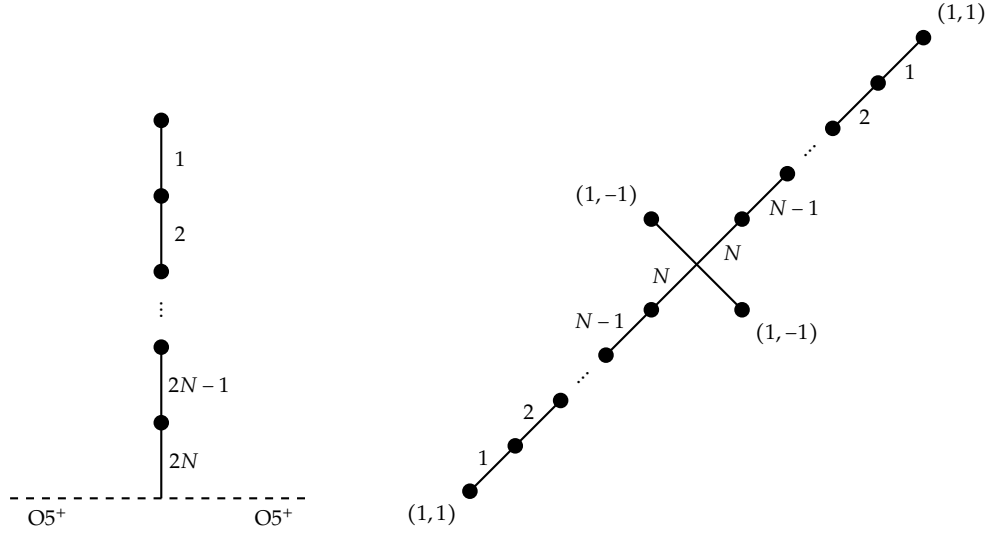


Figure 2.1. Brane webs engineering $EQ_{1,1}$ (left) and EQ_1 (right). The numbers near each 5-brane denote the number of coincident 5-branes in the stack in that segment. Black dots denote 7-branes of charge (p, q) .

Since this description involves only special unitary gauge groups, we should be able to engineer it using (two copies of) ordinary brane webs, i.e. without using $O5$ -planes. It turns out there are a few possible candidates as there are distinct webs for $SU(2)$ gauge theory with discrete theta angles $\theta = 0$ and $\theta = \pi$. In order to identify the correct web diagram, we scanned through all the possibilities and eliminated inconsistent choices by trial and error, by counting the Higgs branch dimension of the different candidate web diagrams and requiring the answer to match with the result of the same computation performed on the brane web with $O5$ -plane. We found that, modulo $SL(2, \mathbb{Z})$ and Hanany-Witten moves, the unitary web diagram in figure 2.1 is the unique choice satisfying the aforementioned criterion.

At this point we need to clarify which aspect of the two theories (2.2.1) and (2.2.2) are expected to be the same. This is because we used an isomorphism at the level of Lie algebra, ignoring any issues related to the global structure of the gauge group (with the exception of the choice of discrete theta angle mentioned above). In particular, any information related to local operators in the two theories is likely to agree, while questions about e.g. line and surface operators in general will be sensitive to the global structure of the gauge group. Our primary interest in these theories is in their Higgs branch, which is parameterised by local operators, and thus should agree regardless of any subtle differences such as those alluded to above.

Having constructed web diagrams for $EQ_{1,1}$ and EQ_1 in figure 2.1, we can now proceed

Even more remarkable, is that the agreement between the quivers (2.2.3) and (2.2.4) is also valid on the Higgs branch. From the 5d perspective there is no a priori reason why this should be so, but it can be confirmed by an explicit calculation of the unrefined Hilbert series

$$\prod_{q=2}^{2N} (1-t^{2q}) \int d\mu_{C_N} \text{PE} \left[\chi_{[0,1,0,\dots,0]_{C_N}} t^2 + 4\chi_{[1,0,\dots,0]_{C_N}} t \right]. \quad (2.2.7)$$

Let us evaluate this integral for $N = 2$. The measure over the $\text{USp}(4)$ group can be taken to be

$$\int d\mu_{C_2} = \oint_{|x_1|=1} \frac{dx_1}{2\pi i x_1} \oint_{|x_2|=1} \frac{dx_2}{2\pi i x_2} (1-x_1^2)(1-x_2)(1-\frac{x_1^2}{x_2})(1-\frac{x_2^2}{x_1^2}), \quad (2.2.8)$$

while the characters for the fundamental and second rank antisymmetric representation of $\text{USp}(4)$ are given respectively by⁴

$$\begin{aligned} \chi_{[1,0]_{C_2}} &= x_1 + \frac{x_2}{x_1} + \frac{x_1}{x_2} + \frac{1}{x_1}, \\ \chi_{[0,1]_{C_2}} &= x_2 + \frac{x_1^2}{x_2} + 1 + \frac{x_2}{x_1^2} + \frac{1}{x_2}, \end{aligned} \quad (2.2.9)$$

Thus the expression we need to evaluate is

$$\begin{aligned} &\prod_{q=2}^4 (1-t^{2q}) \oint_{|x_1|=1} \frac{dx_1}{2\pi i x_1} \oint_{|x_2|=1} \frac{dx_2}{2\pi i x_2} (1-x_1^2)(1-x_2)(1-\frac{x_1^2}{x_2})(1-\frac{x_2^2}{x_1^2}) \times \\ &\times \frac{1}{(1-x_2 t^2)(1-\frac{x_1^2}{x_2} t^2)(1-t^2)(1-\frac{x_2}{x_1^2} t^2)(1-\frac{t^2}{x_2})(1-x_1 t)^4(1-\frac{x_2}{x_1} t)^4(1-\frac{x_1}{x_2} t)^4(1-\frac{t}{x_1})^4}. \end{aligned} \quad (2.2.10)$$

This integral can now be evaluated using residues to arrive at the following Hilbert series

$$\text{HS}_{1,1}^{\mathcal{H}}|_{N=2} = \frac{(1-t^6)^2(1-t^8)^2}{(1-t^4)^6(1-t^2)^6}. \quad (2.2.11)$$

We recognise this as the Coulomb branch Hilbert series of two copies of $\text{U}(2)$ with 4 fundamental hypermultiplets [110], which is the mirror of the $N = 2$ quiver of (2.2.4). Therefore we see that the agreement between the OSp quiver (2.2.3) and unitary quiver (2.2.4) holds also on the Higgs branch.

⁴These characters are computed as follows. For a weight $w = [w_1, w_2] \equiv w_1 \Lambda_1 + w_2 \Lambda_2$ appearing in the weight system of a representation R of C_2 , the corresponding monomial in the character will be $x_1^{w_1} x_2^{w_2}$. For example, the weights appearing in the weight system of fundamental representation of C_2 are $\{[1,0], [-1,1], [1,-1], [-1,0]\}$ where each weight is written in the fundamental weight basis. Thus the character for fundamental representation will be simply $x_1^1 x_2^0 + x_1^{-1} x_2^1 + x_1^1 x_2^{-1} + x_1^{-1} x_2^0$.

2.2.2 The $E_1 \times E_3$ sequence

In the previous subsection, we saw that the Higgs branch of the fixed point limit of 5d $SO(4)$ gauge theory, factorises to two copies of the Higgs branch of the 5d pure $SU(2)$ gauge theory. It is natural to ask whether this pattern holds if we include matter transforming under $SO(4)$. The two matter representations which are straightforward to obtain from the brane web are the vector of $SO(4)$ and the two spinor representations of opposite chirality. Since the vector of $SO(4)$ corresponds to bifundamental of $SU(2) \times SU(2)$, this will not lead to the desired factorised theory. However, each of the two spinor representations, denoted by \mathbf{s} and \mathbf{c} respectively, will only transform under one of the two $SU(2)$ factors in $SO(4)$. In this and subsequent subsections, we will exploit this well-known fact.

Consider the orientifold web diagram presented in figure 2.2. The corresponding IR quiver gauge theory description is given by the electric quiver

$$EQ_{1,3} = \overbrace{[1 \mathbf{s}] - SO(4) - USp(0) - SO(4) - \dots - USp(0) - SO(4) - [1 \mathbf{s}]}^{2N-1} . \quad (2.2.12)$$

By using the isomorphism $\mathfrak{so}(4) \cong \mathfrak{su}(2) \times \mathfrak{su}(2)$, we can rewrite this theory as a product of

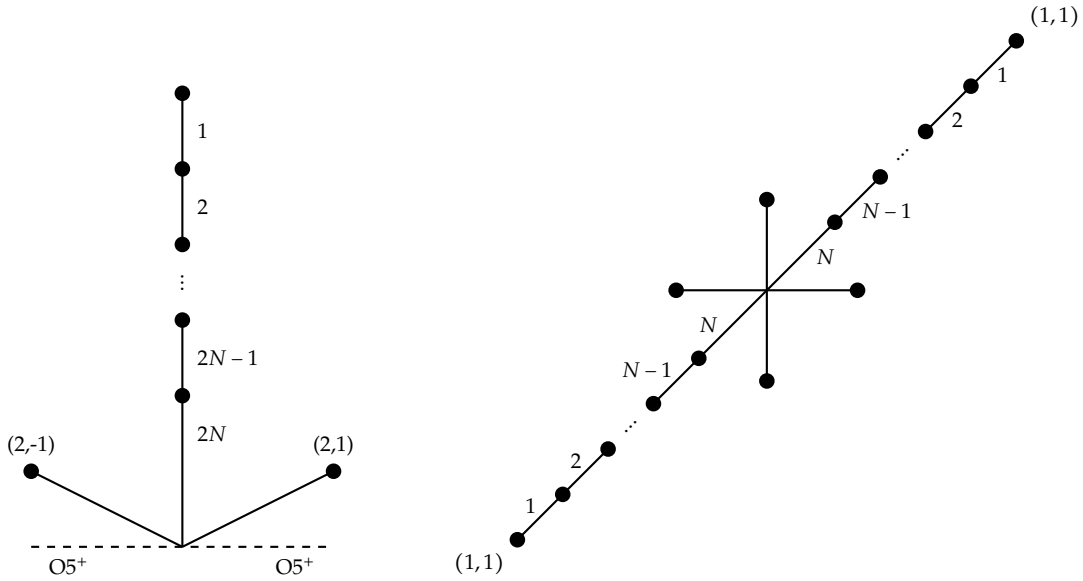


Figure 2.2. Brane webs engineering $EQ_{1,3}$ (left) and EQ_3 (right). For the unitary brane web engineering EQ_1 , see figure 2.1.

the following electric quivers.

$$\text{EQ}_{1,3} = \text{EQ}_1 \times \text{EQ}_3 = \overbrace{\text{SU}(2) - \text{SU}(2) - \dots - \text{SU}(2)}^N \times \overbrace{\text{SU}(2) - \text{SU}(2) - \dots - \text{SU}(2)}^N \quad (2.2.13)$$

\downarrow
 $[1\mathbf{F}]$

\downarrow
 $[1\mathbf{F}]$

The unitary brane web for EQ_1 is given in figure 2.1, while the unitary brane web for EQ_3 is presented in figure 2.2. The orientifold web in figure 2.2 admits two maximal subdivisions. Accordingly the Higgs branch of this theory is the union of two cones, given by the two OSp magnetic quivers in table 2.1. On the other hand, we expect these magnetic quivers to be equivalent to the product $\text{MQ}_1 \times (\text{MQ}_3^{(\text{I})} \cup \text{MQ}_3^{(\text{II})})$, with the latter factor obtained from the unitary web for EQ_3 in figure 2.2. As a further non-trivial check, we can compute the Coulomb branch Hilbert series of the unitary and OSp quivers. The unitary quivers MQ_1 along with $\text{MQ}_3^{(\text{I})}$ and $\text{MQ}_3^{(\text{II})}$ have known HWGs [61].

We are now in a position to write down the HWGs for the OSp magnetic quivers in table 2.1. The final result for the first cone reads

| MS | OSp | Unitary |
|---------------------------------|-----|---------|
| $\text{MQ}_{1,3}^{(\text{I})}$ | | |
| $\text{MQ}_{1,3}^{(\text{II})}$ | | |

Table 2.1. OSp and unitary representation of the two cones on the Higgs branch of $\text{EQ}_{1,3}$. The unitary quivers appearing in the extreme right of the two rows of the table are respectively $\text{MQ}_3^{(\text{I})}$ and $\text{MQ}_3^{(\text{II})}$.

$$\text{HWG}_{1,3}^{(\text{I})} = \text{PE} \left[\sum_{k=1}^N \mu_k \mu_{2N-k} t^{2k} \right] \text{PE} \left[t^2 + (q + q^{-1}) v_N t^{N+1} + \sum_{k=1}^N v_k v_{2N-k} t^{2k} - v_N^2 t^{2N+2} \right], \quad (2.2.14)$$

where μ and ν are the highest weight fugacities for $SU(2N) \times SU(2N)$ while q keeps track of the $U(1)$ charge. The HWG for the second cone reads

$$\begin{aligned} \text{HWG}_{1,3}^{(\text{II})} &= \text{PE} \left[\sum_{k=1}^N \mu_k \nu_{2N-k} t^{2k} \right] \\ &\times \text{PE} \left[t^2 + (\nu_{N+1} q + \nu_{N-1} q^{-1}) t^{N+1} + \sum_{k=1}^{N-1} \nu_k \nu_{2N-k} t^{2k} - \nu_{N+1} \nu_{N-1} t^{2N+2} \right]. \end{aligned} \quad (2.2.15)$$

This was verified upon comparison with the result of an unrefined Hilbert series computation on the OSp side.

We can also compute the Higgs branch HS for $\text{MQ}_{1,3}^{(1)}$ for $N = 2$ exactly. The computation is very similar to that of the Higgs branch of $\text{MQ}_{1,1}$ discussed around (2.2.7). We need to evaluate the following integral

$$\prod_{q=1}^4 (1 - t^{2q}) \int d\mu_{C_2} \int d\mu_{U(1)} \text{PE} \left[\chi_{[0,1]}^{C_2} t^2 + 2\chi_{[1,0]}^{C_2} (q + q^{-1})t + (q^2 + q^{-2})t \right] \quad (2.2.16)$$

Evaluating this integral by finding the residues one arrives at the following

$$\text{HS}_{1,3,(1)}^{\mathcal{H}} = \frac{(1-t+t^2)(1+t^4)(1+t^3+t^4+t^5+t^6+t^7+t^{10})}{(1-t)^8(1+t)^6(1+t^2)^3(1+t+t^2+t^3+t^4)}. \quad (2.2.17)$$

This is to be compared with the product of the Higgs branch HS of the two unitary quivers appearing in the first row of table 2.1. We already know the result for one of these, which is identical to MQ_1 of (2.2.4). Its Higgs branch HS was discussed in the previous section and is given by the square root of the expression in (2.2.11). The Higgs branch HS of the other quiver in the first row of table, 2.1, which we dub $\text{MQ}_3^{(1)}$ is straightforward to compute. Specialising to the case $N = 2$, we need to evaluate the following integral

$$\begin{aligned} &\int d\mu_{U(2)}(x, q_x) \int d\mu_{U(1)}(u) H_{T[SU(2)]}^2(x) H_{\text{glue}}^{U(2)}(x, q_x) \times \\ &\quad \times H_{[2]-[1]}(x, q_x) H_{[2]-[1]}(x, q_x, u) H_{[1]-[1]}(u) H_{\text{glue}}^{U(1)}(u) \\ &= \oint_{|x|=1} \frac{dx}{2\pi i x} (1-x^2) \oint_{|q_x|=1} \frac{dq_x}{2\pi i q_x} \oint_{|u|=1} \frac{du}{2\pi i u} (1-t^2)^2 (1-t^4)^2 \times \\ &\quad \times \text{PE} \left[(x^2 + 1 + x^{-2})t^2 + (x + x^{-1})(q_x + q_x^{-1})(u + u^{-1})t + (u + u^{-1})t + (x + x^{-1})(q_x + q_x^{-1})t \right]. \end{aligned} \quad (2.2.18)$$

Evaluating this integral by computing its residues results in

$$\text{HS}_{3,(1)}^{\mathcal{H}} = \frac{(1+t^3+t^4+t^5+t^6+t^7+t^{10})}{(1-t)^4(1+t)^2(1+t^2)(1+t+t^2)(1+t+t^2+t^3+t^4)}. \quad (2.2.19)$$

Together with the result for the HB of MQ_1 , this precisely reproduces the computation on the OSp side (2.2.17).

2.2.3 The $E_3 \times E_3$ sequence

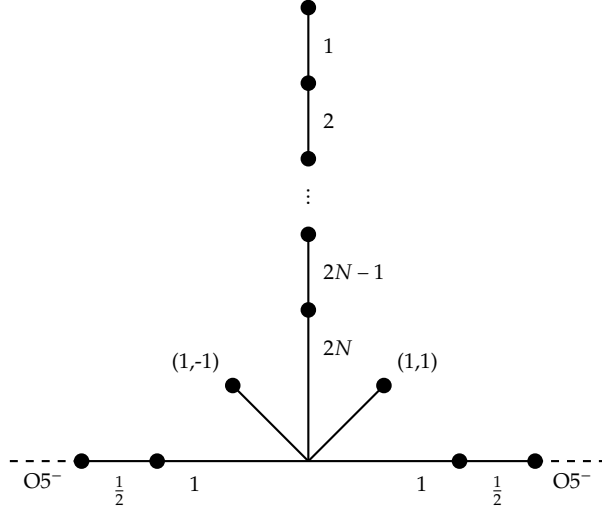


Figure 2.3. Orientifold web for $\text{EQ}_{3,3}$.

The $E_3 \times E_3$ sequence corresponds to the fixed point limit of the electric quiver

$$\text{EQ}_{3,3} = (\text{EQ}_3)^2 = \overbrace{\text{SO}(4) - \text{USp}(0) - \text{SO}(4) - \dots - \text{USp}(0) - \text{SO}(4)}^{2N-1} \cdot \quad (2.2.20)$$

$$\begin{array}{ccc} \text{SO}(4) & & \text{SO}(4) \\ | & & | \\ [1\mathbf{s} + 1\mathbf{c}] & & [1\mathbf{s} + 1\mathbf{c}] \end{array}$$

The orientifold web which engineers this theory is given in figure 2.3. This brane web admits three maximal subdivisions leading to the three OSp magnetic quivers in table 2.2. It can be understood as a limiting case of the $Y_N^{1,1}$ theory in [55]. One can provide a purely unitary description of this theory in terms of the following electric quiver:

$$\text{EQ}_{3,3} = \text{EQ}_3^2 = \left(\overbrace{\text{SU}(2) - \text{SU}(2) - \dots - \text{SU}(2)}^N \right)^2, \quad (2.2.21)$$

$$\begin{array}{ccc} \text{SU}(2) & & \text{SU}(2) \\ | & & | \\ [1\mathbf{F}] & & [1\mathbf{F}] \end{array}$$

which can be engineered by taking two copies of the unitary web shown in figure 2.2. This

brane web admits two maximal subdivisions whose magnetic quivers were discussed in the previous subsection. Since we are taking two copies, a third cone arises when we take a different maximal subdivision for each web diagram. This leads us to the unitary magnetic quivers in table 2.2.

| MS | OSp | Unitary |
|--------------------|-----|---|
| $MQ_{3,3}^{(I)}$ | | $\left(\begin{array}{c} 1 \quad 1 \\ \diagdown \quad \diagup \\ \cdots \quad \cdots \\ 1 \quad N \quad \cdots \quad 1 \end{array} \right)^2$ |
| $MQ_{3,3}^{(II)}$ | | $\left(\begin{array}{c} 1 \quad 1 \\ \diagdown \quad \diagup \\ \cdots \quad \cdots \\ 1 \quad N-1 \quad N-1 \quad N-1 \quad \cdots \quad 1 \end{array} \right)^2$ |
| $MQ_{3,3}^{(III)}$ | | |

Table 2.2. Unitary and OSp magnetic quivers for the $E_3 \times E_3$ sequence.

We can now infer the HWG for the OSp quivers in table 2.2 by taking those of the corresponding unitary magnetic quivers as building blocks. This reasoning leads us to conjecture

the following HWG for the three cones in table 2.2

$$\begin{aligned}
 \text{HWG}_{3,3}^{(I)}(t^2) &= \text{PE} \left[t^2 + (\mu_N q_1 + \mu_N q_1^{-1}) t^{N+1} + \sum_{k=1}^N (\mu_k \mu_{2N-k} t^{2k}) - \mu_N^2 t^{2N+2} \right] \\
 &\quad \times \text{PE} \left[t^2 + (\nu_N q_2 + \nu_N q_2^{-1}) t^{N+1} + \sum_{k=1}^N (\nu_k \nu_{2N-k} t^{2k}) - \nu_N^2 t^{2N+2} \right] \\
 \text{HWG}_{3,3}^{(II)}(t^2) &= \text{PE} \left[t^2 + (\mu_{N+1} p + \mu_{N-1} p^{-1}) t^{N+1} + \sum_{k=1}^{N-1} \mu_k \mu_{2N-k} t^{2k} - \mu_{N+1} \mu_{N-1} t^{2N+2} \right] \\
 &\quad \times \text{PE} \left[t^2 + (\nu_{N+1} q + \nu_{N-1} q^{-1}) t^{N+1} + \sum_{k=1}^{N-1} \nu_k \nu_{2N-k} t^{2k} - \nu_{N+1} \nu_{N-1} t^{2N+2} \right] \\
 \text{HWG}_{3,3}^{(III)}(t^2) &= \text{PE} \left[t^2 + (\mu_{N+1} p + \mu_{N-1} p^{-1}) t^{N+1} + \sum_{k=1}^{N-1} \mu_k \mu_{2N-k} t^{2k} - \mu_{N+1} \mu_{N-1} t^{2N+2} \right] \\
 &\quad \times \text{PE} \left[t^2 + (q + q^{-1}) \nu_N t^{N+1} + \sum_{k=1}^N \nu_k \nu_{2N-k} t^{2k} - \nu_N^2 t^{2N+2} \right]. \tag{2.2.22}
 \end{aligned}$$

Here μ and ν are the fugacities for the two $\text{SU}(2N)$ groups and p and q are the $\text{U}(1)$ charges.

2.2.4 The $E'_3 \times E'_3$ sequence

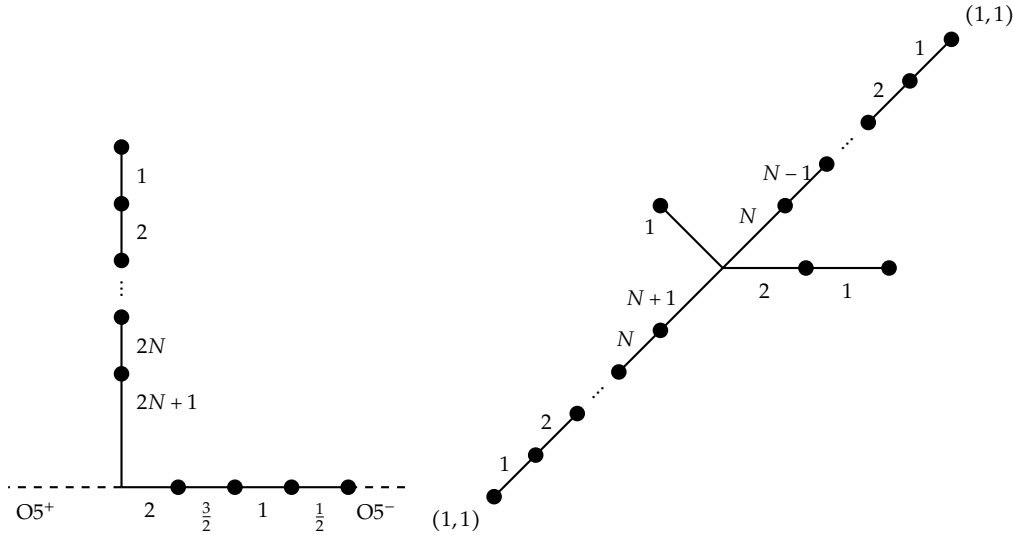


Figure 2.4. Brane webs for $\text{EQ}_{3',3'}$ (left) and $\text{EQ}_{3'}$ (right).

There is another sequence whose first member has an $E_3 \times E_3$ symmetry. We will refer to this as the $E'_3 \times E'_3$ sequence. In figure 2.4 we present the orientifold web that engineers the

| MS | OSp | Unitary |
|----------------------|-----|---|
| $MQ_{3',3'}^{(I)}$ | | $\left(\begin{array}{c} 1 \\ \diagup \quad \diagdown \\ N \quad N \\ \vdots \quad \vdots \\ 1 \quad 1 \end{array} \right)^2$ |
| $MQ_{3',3'}^{(II)}$ | | $\left(\begin{array}{c} N-1 \quad N-1 \\ \diagup \quad \diagdown \\ N-1 \quad N-1 \\ \vdots \quad \vdots \\ 1 \quad 1 \end{array} \right)^2$ |
| $MQ_{3',3'}^{(III)}$ | | |

Table 2.3. Magnetic quivers for the $E'_3 \times E'_3$ sequence

unitary quivers to obtain the HWGs for the OSp quivers. In order to do this, let us point out the following useful fact; one of the unitary quivers appearing in the second and third row of table 2.4, is itself a product of two unitary quivers:

$$\begin{array}{c} N-1 \quad N-1 \\ \diagup \quad \diagdown \\ N-1 \quad N-1 \\ \vdots \quad \vdots \\ 1 \quad 1 \end{array} = \begin{array}{c} N-1 \quad N-1 \\ \diagup \quad \diagdown \\ N-1 \quad N-1 \\ \vdots \quad \vdots \\ 1 \quad 1 \end{array} \times \begin{array}{c} 1 \\ \parallel \\ 1 \end{array}, \quad (2.2.25)$$

where the right hand side of the above is obtained after ungauging the overall decoupled $U(1)$ in the original quiver. The first quiver in the right hand side of the above is a height

2 nilpotent orbit, whose HWG is presented in [61], while the second quiver is just $\mathcal{N} = 4$ QED with 2 electrons. Turning to the second and third row, we again see that for $N = 1$ the correspondence between the unitary and OSp quivers is obvious, which one may view as a further robustness of our proposal.

Now we have all the necessary ingredients to write down HWGs for the OSp quivers

$$\begin{aligned} \text{HWG}_{3',3'}^{(\text{I})} &= \text{PE} \left[\sum_{k=1}^N (\mu_k \mu_{2N+1-k} + \nu_k \nu_{2N+1-k}) t^{2k} \right], \\ \text{HWG}_{3',3'}^{(\text{II})} &= \text{PE} \left[\sum_{k=1}^{N-1} (\mu_k \mu_{2N+1-k} + \nu_k \nu_{2N+1-k}) t^{2k} + (\rho^2 + \lambda^2) t^2 \right], \\ \text{HWG}_{3',3'}^{(\text{III})} &= \text{PE} \left[\sum_{k=1}^N \mu_k \mu_{2N+1-k} t^{2k} + \sum_{j=1}^{N-1} \nu_j \nu_{2N+1-j} t^{2j} + \rho^2 t^2 \right]. \end{aligned} \quad (2.2.26)$$

This proposal has been checked by a direct computation of the unrefined Hilbert series of the OSp quiver.

2.2.5 The $E'_3 \times E_4$ sequence

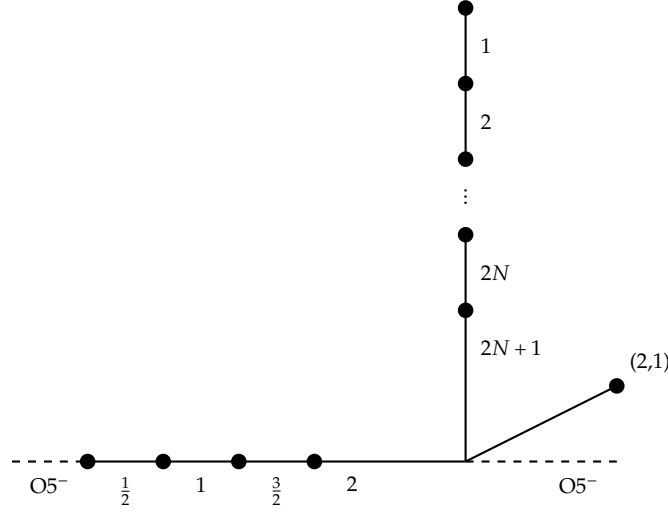
The $E'_3 \times E_4$ sequence is the magnetic quiver for the fixed point limit of the 5d IR electric quiver

$$\text{EQ}_{3',4} = \overbrace{\text{SO}(4) - \text{USp}(0) - \text{SO}(4) - \dots - \text{USp}(0) - \text{SO}(4)}^{2N-1} \begin{array}{c} | \\ [1\mathbf{s}] \end{array} \quad \begin{array}{c} | \\ [2\mathbf{s} + 2\mathbf{c}] \end{array}. \quad (2.2.27)$$

It can be engineered by the orientifold web diagram presented in figure 2.6. Alternatively we may reformulate the electric theory $\text{EQ}_{3,4}$ as a product of two unitary electric quivers

$$\text{EQ}_{3',4} = \text{EQ}_{3'} \times \text{EQ}_4 = \overbrace{\text{SU}(2) - \text{SU}(2) - \dots - \text{SU}(2)}^N \begin{array}{c} | \\ [2\mathbf{F}] \end{array} \times \overbrace{\text{SU}(2) - \text{SU}(2) - \dots - \text{SU}(2)}^N \begin{array}{c} | \\ [1\mathbf{F}] \end{array} \quad \begin{array}{c} | \\ [2\mathbf{F}] \end{array}, \quad (2.2.28)$$

where $\text{EQ}_{3'}$ is engineered by the unitary web in figure 2.4, while the unitary web engineering EQ_4 is the one in figure 2.7. Given these webs, the magnetic quivers can be extracted using the rules in [55]. The Higgs branch of $\text{EQ}_{3',4}$ at the fixed point is the union of two cones, whose magnetic quivers are given in table 2.4. The HWG that we propose for the OSp

Figure 2.6. Orientifold web for $\text{EQ}_{3',4}$.

quivers are

$$\begin{aligned}
 \text{HWG}_{3',4}^{(\text{I})} &= \text{PE} \left[\sum_{i=1}^N \mu_i \mu_{2N+1-i} t^{2i} + (v^2 + 1)t^2 + v(\mu_N q + \mu_{N+1} q^{-1})t^{N+1} - v^2 \mu_N \mu_{N+1} t^{2N+2} \right] \\
 &\quad \times \text{PE} \left[\sum_{k=1}^N \rho_k \rho_{2N+1-k} t^{2k} \right] \\
 \text{HWG}_{3',4}^{(\text{II})} &= \text{PE} \left[\sum_{i=1}^N \mu_i \mu_{2N+1-i} t^{2i} + (v^2 + 1)t^2 + v(\mu_N q + \mu_{N+1} q^{-1})t^{N+1} - v^2 \mu_N \mu_{N+1} t^{2N+2} \right] \\
 &\quad \times \text{PE} \left[\sum_{k=1}^N \lambda_k \lambda_{2N+1-k} t^{2k} \right] \text{PE} [\eta^2 t^2]
 \end{aligned} \tag{2.2.29}$$

These expressions are consistent with the unrefined Hilbert series for low values of N .

2.2.6 The $E_4 \times E_4$ sequence

The $E_4 \times E_4$ sequence are the magnetic quivers for the fixed point limit of the 5d electric quiver

$$\text{EQ}_{4,4} = [1s + 1c] - \overbrace{\text{SO}(4) - \text{USp}(0) - \text{SO}(4) - \dots - \text{USp}(0) - \text{SO}(4)}^{2N-1} - [2s + 2c] \quad . \tag{2.2.30}$$

| MS | OSp | Unitary |
|--------------------|-----|---------|
| $MQ_{3',4}^{(I)}$ | | |
| $MQ_{3',4}^{(II)}$ | | |

Table 2.4. Magnetic quivers for the two cones of the Higgs branch of $EQ_{3',4}$.

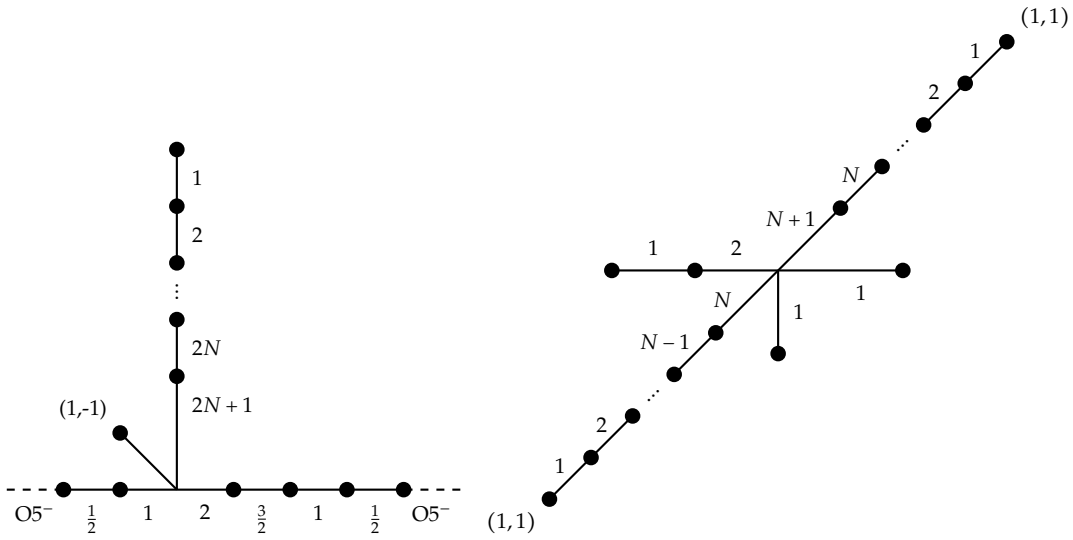


Figure 2.7. Brane webs for $EQ_{4,4}$ (left) and EQ_4 (right).

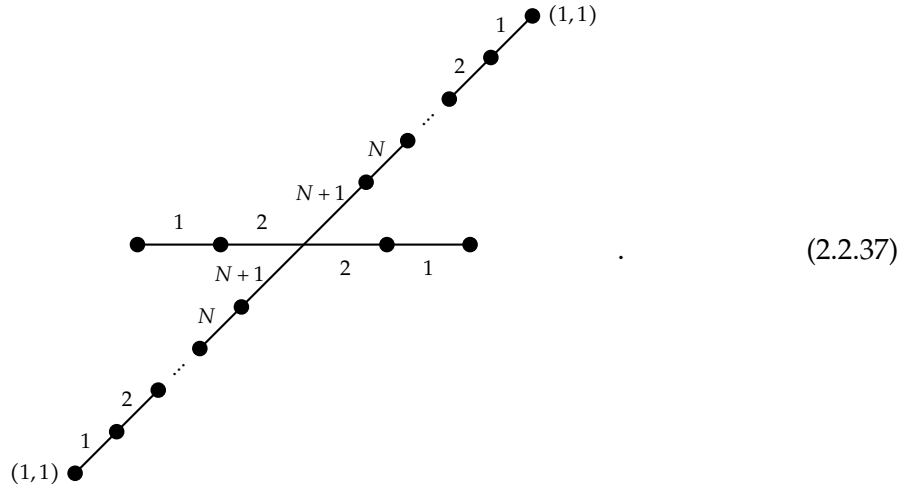
We present the orientifold web that engineers this theory in figure 2.7. Alternatively we can write $EQ_{4,4}$ as the product of two unitary electric quivers

$$EQ_{4,4} = EQ_4^2 = \left(\begin{array}{c} \overbrace{SU(2) - SU(2) - \dots - SU(2)}^N \\ \hline \begin{array}{cc} [1\mathbf{F}] & [2\mathbf{F}] \end{array} \end{array} \right)^2, \quad (2.231)$$

Alternatively, we can rewrite $\text{EQ}_{5,5}$ as the product of two unitary electric quivers

$$\text{EQ}_{5,5} = \text{EQ}_5^2 = \left(\overbrace{\text{SU}(2) - \text{SU}(2) - \dots - \text{SU}(2)}^N \right)_{\substack{\downarrow \\ [\mathbf{2F}]}}^2, \quad (2.2.36)$$

each of which is engineered by taking one copy of the following unitary brane web



From the brane webs in (2.2.35) and (2.2.37), we obtain the two corresponding magnetic quivers which then imply

$$\text{MQ}_{5,5} = \text{MQ}_5^2 = \left(\begin{array}{c} \circ 1 \\ \vdots \\ \circ 2N+1 \\ \bullet 2N+2 \\ \circ 2 \quad \circ 2 \quad \circ 4 \quad \circ 2 \quad \circ 2 \end{array} \right) = \left(\begin{array}{ccccc} & 1 & 2 & 1 & \\ & \circ & \circ & \circ & \\ & & | & & \\ \circ & \dots & \circ & \dots & \circ \\ 1 & & N+1 & & 1 \end{array} \right)^2. \quad (2.2.38)$$

The unitary quiver appearing here has been studied previously, and its HWG was given in [54]. We can now obtain the HWG for the OSp quiver by simply squaring that expression to

obtain

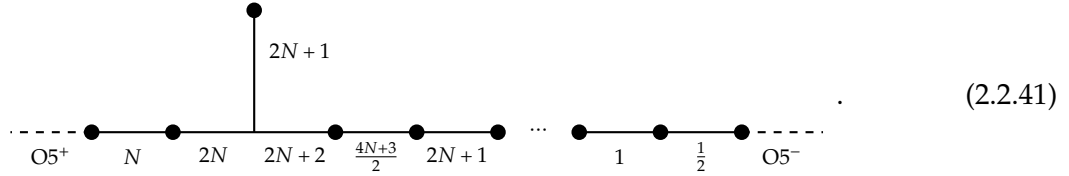
$$\begin{aligned} \text{HWG}_{5,5} = & \text{PE} \left[\sum_{i=1}^{N+1} \mu_i \mu_{2N+2-i} t^{2i} + (v_1^2 + v_2^2) t^2 + t^4 + v_1 v_2 \mu_{N+1} (t^{N+1} + t^{N+3}) - v_1^2 v_2^2 \mu_{N+1}^2 t^{2N+6} \right] \\ & \times \text{PE} \left[\sum_{i=1}^{N+1} \lambda_i \lambda_{2N+2-i} t^{2i} + (\rho_1^2 + \rho_2^2) t^2 + t^4 + \rho_1 \rho_2 \lambda_{N+1} (t^{N+1} + t^{N+3}) - \rho_1^2 \rho_2^2 \lambda_{N+1}^2 t^{2N+6} \right]. \end{aligned} \quad (2.2.39)$$

2.2.8 The $E'_5 \times E'_5$ sequence

The $E_{5'} \times E_{5'}$ sequence is obtained by considering the fixed point limit of the following 5d electric quiver:

$$\text{EQ}_{5',5'} = \overbrace{\text{SO}(4) - \text{USp}(0) - \text{SO}(4) - \dots - \text{USp}(0) - \text{SO}(4)}^{2N-1} - [4\mathbf{s} + 4\mathbf{c}] \quad , \quad (2.2.40)$$

which can be engineered using the orientifold web:

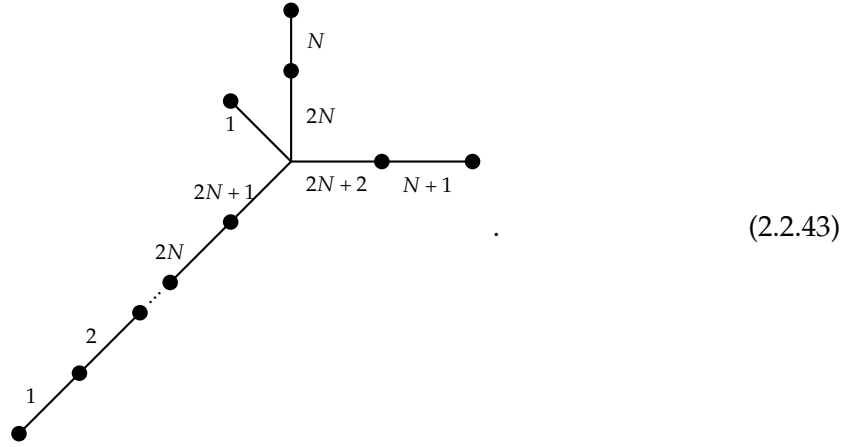


$$(2.2.41)$$

Alternatively we may rewrite $\text{EQ}_{5',5'}$ as two copies of a single electric quiver with $\text{SU}(2)$ gauge nodes, namely

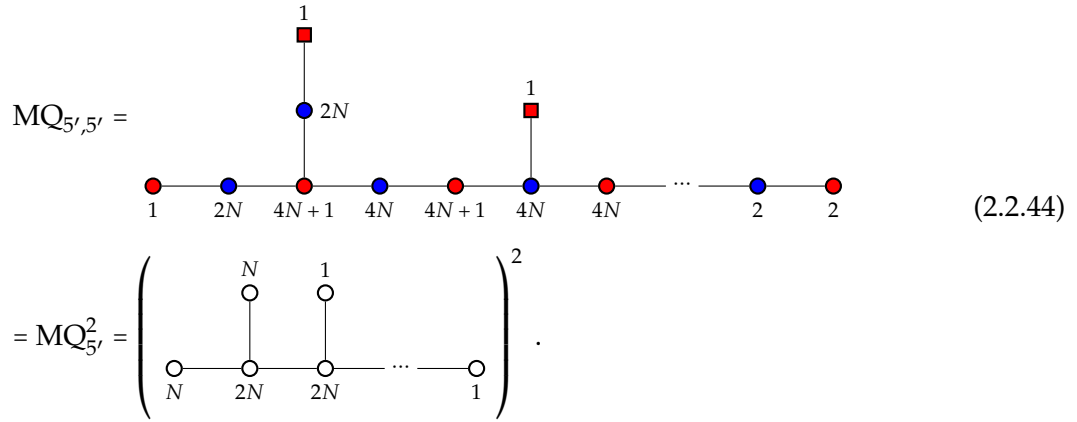
$$\text{EQ}_{5'}^2 = \left(\overbrace{\text{SU}(2) - \text{SU}(2) - \dots - \text{SU}(2)}^N \begin{array}{c} | \\ [4\mathbf{F}] \end{array} \right)^2 \quad , \quad (2.2.42)$$

each copy of which can now be engineered using an ordinary brane web:



(2.2.43)

This leads us to conjecture the equivalence of the following 3d magnetic quivers



(2.2.44)

We now want to write down the HWG for the Coulomb branch Hilbert series of $MQ_{5',5'}$, via the conjectured relation to the unitary quiver. The HWG for the unitary quiver $MQ_{5'}$ can be found in [125] (also see table 18 of [126]). Consequently, the HWG for $MQ_{5',5'}$ is obtained by squaring this result, namely

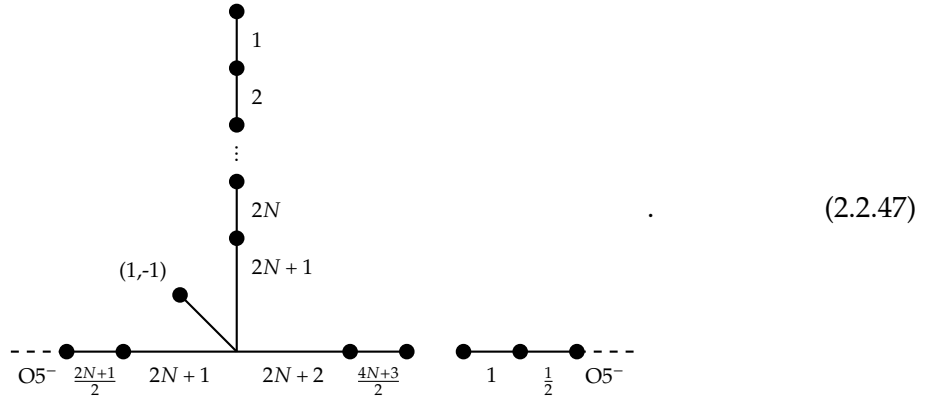
$$HWG_{5',5'} = PE \left[\sum_{k=1}^N (\mu_{2k} + \nu_{2k}) t^{2k} \right] . \tag{2.2.45}$$

2.2.9 The $E_{5'} \times E_6$ sequence

The $E_{5'} \times E_6$ sequence is obtained by taking the fixed point limit of the 5d electric quiver given by

$$\text{EQ}_{5',6} = \overbrace{[1\mathbf{s}] - \text{SO}(4) - \text{USp}(0) - \text{SO}(4) - \dots - \text{USp}(0) - \text{SO}(4) - [4\mathbf{s} + 4\mathbf{c}]}^{2N-1}, \quad (2.2.46)$$

which can be engineered by the following orientifold web diagram



Alternatively we may reformulate $\text{EQ}_{5',6}$ as the product of two unitary electric quivers

$$\text{EQ}_{5',6} = \text{EQ}_{5'} \times \text{EQ}_6 = \overbrace{\text{SU}(2) - \text{SU}(2) - \dots - \text{SU}(2)}^N \times \overbrace{\text{SU}(2) - \text{SU}(2) - \dots - \text{SU}(2)}^N, \quad (2.2.48)$$

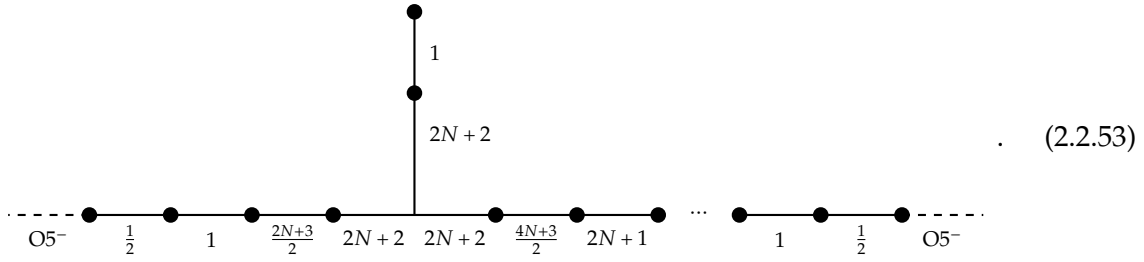
$\begin{array}{ccc} \downarrow & & \downarrow \\ [4\mathbf{F}] & & [1\mathbf{F}] \quad [4\mathbf{F}] \end{array}$

2.2.10 The $E_6 \times E_6$ sequence

The electric quiver for the IR limit of the $E_6 \times E_6$ sequence reads

$$EQ_{6,6} = \overbrace{[1\mathbf{s} + 1\mathbf{c}] - \text{SO}(4) - \text{USp}(0) - \text{SO}(4) - \dots - \text{USp}(0) - \text{SO}(4) - [4\mathbf{s} + 4\mathbf{c}]}^{2N-1} . \quad (2.2.52)$$

It can be engineered using the following orientifold web



Alternatively we may present the electric quiver as a product of two unitary quivers:

$$EQ_{6,6} = EQ_6^2 = \left(\overbrace{\text{SU}(2) - \text{SU}(2) - \dots - \text{SU}(2)}^N \right)^2, \quad (2.2.54)$$

$\begin{array}{c} \text{SU}(2) \\ | \\ [1\mathbf{F}] \end{array} \quad \dots \quad \begin{array}{c} \text{SU}(2) \\ | \\ [4\mathbf{F}] \end{array}$

where each copy is engineered by the web diagram in (2.2.49). We can then obtain the magnetic quivers from the brane webs in (2.2.53) and (2.2.49), that lead us to the conjecture that

$$MQ_{6,6} = MQ_6^2 = \left(\begin{array}{c} \text{O} \ 1 \\ | \\ \text{O} \ 2N+2 \\ | \\ \text{O} \ 1 \\ | \\ \text{O} \ N+1 \\ | \\ \text{O} \ 2N+1 \\ | \\ \text{O} \ 1 \end{array} \right)^2 . \quad (2.2.55)$$

$\begin{array}{c} \text{O} \ 1 \\ | \\ \text{O} \ 2N+2 \\ | \\ \text{O} \ 1 \\ | \\ \text{O} \ N+1 \\ | \\ \text{O} \ 2N+1 \\ | \\ \text{O} \ 1 \end{array}$

This has an immediate corollary which allows us to extract the HWG for the OSp quiver appearing above by squaring the known result [54] for the unitary quiver:

$$\begin{aligned} \text{HWG}_{6,6} = & \text{PE} \left[\sum_{i=1}^N \mu_{2i} t^{2i} + t^2 + (\mu_{2N+2} q_1 + \mu_{2N+3} q_1^{-1}) t^{N+1} \right] \\ & \times \text{PE} \left[\sum_{i=1}^N \nu_{2i} t^{2i} + t^2 + (\nu_{2N+2} q_2 + \nu_{2N+3} q_2^{-1}) t^{N+1} \right]. \end{aligned} \quad (2.2.56)$$

Indeed the unrefined Hilbert series for the OSp quiver for $N = 1$ was computed in [65], and is in agreement with our claim. For higher values of N we were not able to perform an explicit computation due to the high rank of the OSp quiver. This is one instance in which our conjecture proves powerful, as it gives an exact expression for the Hilbert series of a quiver which would otherwise be very challenging to compute.

We further point out an interesting fact about this theory, namely the existence of a 4d $\mathcal{N} = 2$ theory with very similar properties. As noticed in [115], there is one class-S theory of D_4 type in which a single three-punctured sphere realizes a product SCFT, where both factors are the E_6 Minahan-Nemeschansky (MN) theory [127]. We recall that the E_6 Minahan-Nemeschansky theory is a 4d $\mathcal{N} = 2$ SCFT of rank 1, with flavor symmetry group E_6 , and central charges

$$a_{E_6} = \frac{41}{24}, \quad c_{E_6} = \frac{13}{6}, \quad (2.2.57)$$

We report the partitions labeling the punctures in table 2.5, together with their contribution to the effective number of hypermultiplets and vector multiplets.

| Nahm partition | $(\delta n_h, \delta n_v)$ |
|----------------|----------------------------|
| $[1^8]$ | $(112, 100)$ |
| $[3^2, 1^2]$ | $(72, 69)$ |
| $[3^2, 1^2]$ | $(72, 69)$ |

Table 2.5. Table containing the data defining the punctures for the 4d $E_6 \times E_6$ theory.

From this data it is easy to compute the central charges a and c of this theory, finding

$$a_{E_6 \times E_6} = \frac{41}{12}, \quad c_{E_6 \times E_6} = \frac{13}{3} \quad (2.2.58)$$

as it should be for two copies of the E_6 MN theory. By applying the procedure to write the 3d mirror for this theory we find that the full puncture $[1^8]$ is associated to the quiver tail (2.2.59) while the puncture $[3^2, 1^2]$ is associated to the quiver tail (2.2.60),

Now we use the alternative description of the $\text{EQ}_{7,7}$ as a product of a pair of linear quivers with $\text{SU}(2)$ nodes, namely

$$\text{EQ}_{7,7} = \text{EQ}_7^2 = \left(\overbrace{\text{SU}(2) - \text{SU}(2) - \dots - \text{SU}(2)}^N \right)^2. \quad (2.2.64)$$

Each individual factor can be engineered using the following unitary 5-brane web

(2.2.65)

The magnetic quiver one obtains from this unitary web leads us to the following conjecture

$$\text{MQ}_{7,7} = \text{MQ}_7^2 = \left(\begin{array}{ccccccc} & & & N+1 & & & \\ & & & \circ & & & \\ & & & | & & & \\ \circ & \circ & \circ & \circ & \circ & \dots & \circ \\ 1 & 2 & N+2 & 2N+2 & 2N+1 & & 1 \end{array} \right)^2. \quad (2.2.66)$$

The HWG for the unitary quiver appearing above was conjectured in [54]. We will use this result and square it to obtain the HWG for the OSp quiver $\text{MQ}_{7,7}$ (2.2.63):

$$\begin{aligned} \text{HWG}_{7,7} = & \text{PE} \left[\sum_{i=1}^{N+1} \mu_{2i} t^{2i} + t^4 + v^2 t^2 + v \mu_{2N+4} (t^{N+1} + t^{N+3}) + \mu_{2N+4}^2 t^{2N+4} - v^2 \mu_{2N+4} t^{2N+6} \right] \\ & \times \text{PE} \left[\sum_{i=1}^{N+1} \lambda_{2i} t^{2i} + t^4 + \rho^2 t^2 + \rho \lambda_{2N+4} (t^{N+1} + t^{N+3}) + \lambda_{2N+4}^2 t^{2N+4} - \rho^2 \lambda_{2N+4} t^{2N+6} \right]. \end{aligned} \quad (2.2.67)$$

We further point out an interesting fact about this theory, namely the existence of a 4d $\mathcal{N} = 2$ theory with very similar properties. As noticed in [115], there is one class-S theory of D_5 type in which a single three-punctured sphere realizes a product SCFT, where both factors are the E_7 Minahan-Nemeschansky theory [128]. We recall that the E_7 Minahan-Nemeschansky theory is a 4d $\mathcal{N} = 2$ SCFT of rank 1, with flavor symmetry group E_7 , and central charges

$$a_{E_7} = \frac{59}{24}, \quad c_{E_7} = \frac{19}{6}. \quad (2.2.68)$$

We report the partitions labeling the punctures in table 2.6, together with their contribution to the effective number of hypermultiplets and vector multiplets.

| Nahm partition | $(\delta n_h, \delta n_v)$ |
|----------------|----------------------------|
| $[1^{10}]$ | (240, 220) |
| $[5^2]$ | (104, 102) |
| $[3^2, 1^4]$ | (184, 177) |

Table 2.6. Table containing the data defining the punctures for the 4d $E_7 \times E_7$ theory.

From this data it is easy to compute the central charges a and c of this theory, finding

$$a_{E_7 \times E_7} = \frac{59}{12}, \quad c_{E_7 \times E_7} = \frac{19}{3} \quad (2.2.69)$$

as it should be for two copies of the E_7 MN theory.

By applying the procedure to write the 3d mirror for this theory we find that the full puncture $[1^{10}]$ is associated to the quiver tail (2.2.70), the puncture $[3^2, 1^4]$ is associated to the quiver tail (2.2.71), and the puncture $[5^2]$ is associated to the quiver tail (2.2.72),

$$\begin{array}{cccccccccc} \bullet & \bullet & \bullet & \bullet & \bullet & \bullet & \bullet & \bullet & \square \\ 2 & 2 & 4 & 4 & 6 & 6 & 8 & 8 & 10 \end{array} \quad (2.2.70)$$

$$\begin{array}{cccccc} \bullet & \bullet & \bullet & \bullet & \square \\ 2 & 2 & 4 & 8 & 10 \end{array} \quad (2.2.71)$$

$$\begin{array}{ccc} \bullet & \square \\ 4 & 10 \end{array} \quad (2.2.72)$$

Gluing the three tails together results in the magnetic quiver for the 5d $E_7 \times E_7$ depicted in (2.2.63) for $N = 1$. Therefore the magnetic quiver of the 5d $E_7 \times E_7$ theory is the 3d mirror theory of the 4d $E_7 \times E_7$ theory above described. It is then tempting to conjecture that the 5d $E_7 \times E_7$ theory reduces to 4d to this D_5 type class-S theory, giving two copies of E_7 Minahan-Nemeschansky.

Having derived the magnetic quiver for the $E_7 \times E_7$ sequence from the brane web, for any $N \in \mathbb{N}$, we can use the same argument as the paragraphs above to conjecture that all class-S theories of D_{2N+3} type given by a three punctured sphere with regular punctures given by $[1^{4N+6}]$, $[2N+1, 2N+1, 1^4]$, $[2N+3, 2N+3]$ will be a factorized SCFT. We conjecture that it will decompose into two copies of three punctured A_{2N+1} spheres, with regular punctures given by $[1^{2N+2}]$, $[N+1, N+1]$, $[N, N, 1, 1]$. It will be interesting to further check this proposal.

2.2.12 An outlier: the $E_8 \times E_8$ theory

While not explicitly written⁵ in [115], it is easy to use the methods of such paper to find a choice of punctures in the D_6 theory, such that we realize the product of two copies of the E_8 Minahan-Nemeschansky theory [128]. We recall that the E_8 Minahan-Nemeschansky theory is a 4d $\mathcal{N} = 2$ SCFT of rank 1, with flavor symmetry group E_8 , and central charges

$$a_{E_8} = \frac{95}{24}, \quad c_{E_8} = \frac{31}{6}. \quad (2.2.73)$$

We report the partitions labeling the punctures which we believe engineer this product SCFT in table 2.7, together with their contribution to the effective number of hypermultiplets and vector multiplets.

| Nahm partition | $(\delta n_h, \delta n_v)$ |
|----------------|----------------------------|
| $[1^{12}]$ | (440, 410) |
| $[3, 1^9]$ | (400, 380) |
| $[9, 1^3]$ | (120, 118) |

Table 2.7. Table containing the data defining the punctures for the 4d $E_8 \times E_8$ theory.

As a check that such 4d theory is really the product of two copies of the E_8 Minahan-Nemeschansky theory, we compute the central charges from the data defining the punctures. We get

$$a_{E_8 \times E_8} = \frac{95}{12}, \quad c_{E_8 \times E_8} = \frac{31}{3} \quad (2.2.74)$$

as it should be for two copies of the E_8 MN theory. We also check that there exist no other choice of three punctures, in the D_6 theory, that realizes these correct central charges.

By applying the procedure to write the 3d mirror for this theory we find that the full puncture $[1^{12}]$ is associated to the quiver tail (2.2.75), the puncture $[3, 1^9]$ is associated to the

⁵But surely noticed by the authors of such paper. See for example [116] and [117] for discussions about product SCFTs in class-S.

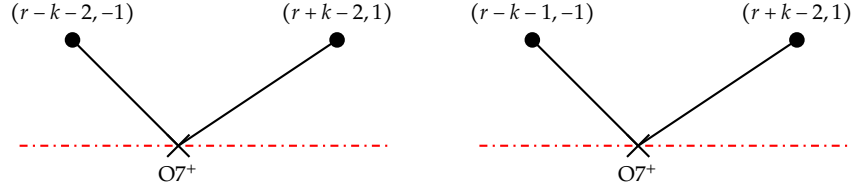


Figure 2.8. Brane webs for pure $\text{SO}(N)$ gauge theory at the infinite gauge coupling limit for the case where $N = 2r$ (left) and $N = 2r + 1$ (right).

in figure 2.8 is mapped to itself with $k \rightarrow k + 1$. Note that the brane web looks slightly different depending on whether the gauge algebra is of B-type or D-type. We would first like to understand how to read off the Higgs branch directions from these web diagrams. For the $\text{SO}(2r)$ theory in figure 2.8, one can separate the $(r - k - 2, -1)$ and the $(r + k - 2, 1)$ 5-branes along the Higgs branch directions giving rise to a Higgs branch of unit quaternionic dimension. That this is a one-dimensional space rather than a two dimensional one is due to the fact that the moduli correspond to the relative positions of the two independent subwebs. Equivalently one has the freedom to fix the position of one of the subwebs to the origin of the transverse space. This is unlike the situation one would encounter when dealing with brane webs with O5-planes due to the fact that the O5-plane provides a reference point, and the number of available directions is equal to the number of independent subwebs. But since an O7-plane spans all the directions transverse to the plane in which the web is drawn, i.e. it is not localised to any point along the Higgs branch directions it cannot serve as a reference point and the total available Higgs branch directions are one less than the number of independent subwebs. For the $\text{SO}(2r + 1)$ theory a similar statement holds for the $(r - k - 1, -1)$ and the $(r + k - 2, 1)$ 5-branes. The naive prescription for obtaining the magnetic quiver, had the O7^+ -plane not been present, would be [109] to assign a $\text{U}(1)$ gauge node to each subweb and connect them together by as many hypermultiplets as the Schwinger product, or bare stable intersection⁶ of the (p, q) charges of the independent subwebs in figure 2.8, with the knowledge that an overall $\text{U}(1)$ acts trivially, corresponding to the freedom to fix the position of one independent subweb to the origin. On the other hand, it is known [129] that the Higgs branch of the infinite gauge coupling limit of a 5d $\mathcal{N} = 1$ super Yang-Mills theory with gauge group G should be given by the orbifold $\mathbb{C}^2/\mathbb{Z}_{h_G^\vee}$, where h_G^\vee denotes the dual Coxeter number of the group G . Moreover, the Coulomb branch of 3d $\mathcal{N} = 4$ QED with n_1 charge one hypermultiplets and n_2 charge 2 hypermultiplets is $\mathbb{C}^2/\mathbb{Z}_{n_1+2n_2}$. If we further require the Higgs branch dimension of the magnetic quiver to be equal to the rank of the 5d

⁶We refer the reader to [109] for the precise definition

theory, then the magnetic quiver is uniquely determined to be

$$\mathcal{H}_\infty(\mathrm{SO}(N)) = \mathbb{C}^2 / \mathbb{Z}_{h_{\mathrm{SO}(N)}^V} = \mathcal{C}^{3\mathrm{d}} \left(\begin{array}{c} 4 - \lfloor \frac{N}{2} \rfloor + \lceil \frac{N}{2} \rceil \\ \square \\ | \\ \circ \text{---} \text{---} \square \lfloor \frac{N-6}{2} \rfloor \\ 1 \end{array} \right), \quad (2.3.1)$$

where $\lfloor x \rfloor, \lceil x \rceil$ denote the floor and ceiling function respectively, and are defined by

$$\lfloor x \rfloor = \max \{ n \in \mathbb{Z} \mid n \leq x \}, \quad \lceil x \rceil = \min \{ n \in \mathbb{Z} \mid n \geq x \}. \quad (2.3.2)$$

Our task now is to recover (2.3.1) from the data in the brane webs of figure 2.8. Let us first take the Schwinger product of the (p, q) charges of the two independent subwebs in each of the webs in figure 2.8 to find

$$\begin{aligned} \left| \det \begin{pmatrix} (r-k-2) & -1 \\ (r+k-2) & 1 \end{pmatrix} \right| &= 2r-4 \\ \left| \det \begin{pmatrix} (r-k-1) & -1 \\ (r+k-2) & 1 \end{pmatrix} \right| &= 2r-3 \end{aligned} \quad (2.3.3)$$

Upon comparison with (2.3.1) we propose that the number of charge 2 hypermultiplets be given by the formula

$$n_{\text{charge } 2} = \left\lfloor \frac{\mathrm{SI}_0 - 2}{2} \right\rfloor, \quad (2.3.4)$$

where SI_0 refers to the bare stable intersection number, i.e. those computed in (2.3.3). The number of charge one hypermultiplets, is fixed to be 4 in the case of $N = 2r$ and 3 in the case when $N = 2r + 1$. We do not currently have a good microscopic understanding of these hypermultiplets, but this should not stop us from proposing the magnetic quivers. At this point the reader might question our assumption that only charge 1 or charge 2 hypers could appear in the magnetic quiver. However, in the next section we provide examples where an OSp dual is known and comparison of the HS of the non-simply-laced and OSp quivers leads to a justification of this assumption.

2.3.2 $\mathrm{SO}(N)$ with $N_v \leq N - 5$

Having gained some intuition about the Higgs branch of pure $\mathrm{SO}(N)$ theory at infinite coupling, we can now proceed with more involved cases. We can add matter in the vector representation of $\mathrm{SO}(N)$ by adding D7 branes to the brane configuration as in figure 2.9. To read off the magnetic quiver, we first perform a few Hanany-Witten moves [130] by moving all flavour D7s, say, to the left of the $(r-k-2, -1)$ (resp. $(r-k-1, -1)$) 5-brane in figure 2.9. This

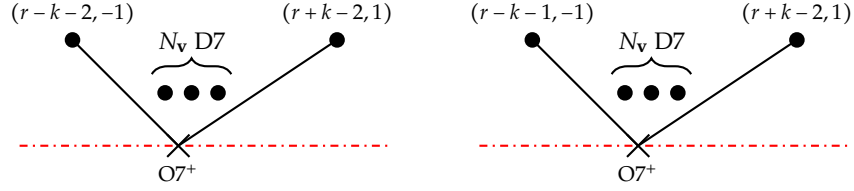


Figure 2.9. Brane webs for pure $SO(N)$ gauge theory with N_v hypermultiplets in the vector representation at the infinite gauge coupling limit for the case where $N = 2r$ (left) and $N = 2r + 1$ (right).

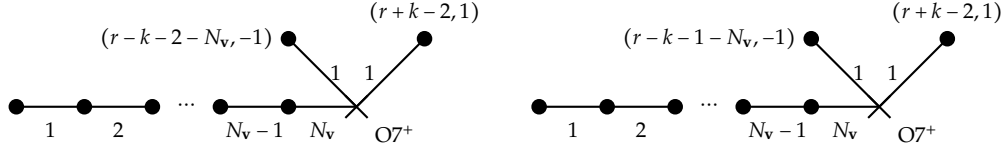
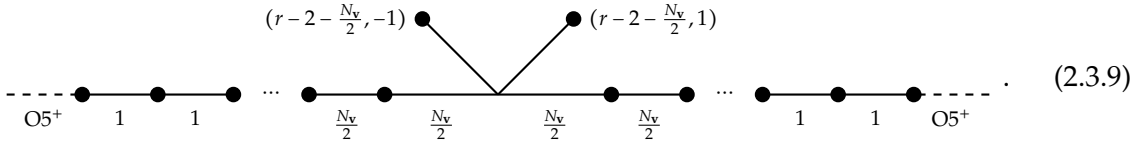


Figure 2.10. Brane webs for $SO(N)+N_v$ hypermultiplets in the vector representation at infinite gauge coupling after taking all mass parameters to zero for $N = 2r$ (left) and $N = 2r + 1$ (right). From here onwards we will not indicate the monodromy cut associated with the 7-brane explicitly for ease of presentation.

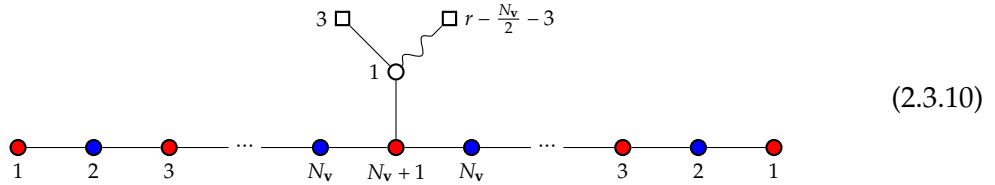
creates N_v D5 branes and further changes the charge of the $(r-k-2, -1)$ (resp. $(r-k-1, -1)$) 7-brane to $(r-k-2-N_v, -1)$ (resp. $(r-k-1-N_v, -1)$) for $N = 2r$ (resp. $N = 2r + 1$). As a final step we set all the mass parameters in the web to zero and separate the D7 branes along the horizontal direction in the web diagram. The end result of this process is depicted in figure 2.10. We immediately identify the independent subwebs to be the D5 branes extended between the adjacent pairs of D7 branes, D5 branes extended between the $O7^+$ -plane and the D7 closest to it in addition to the $(r+k-2, 1)$ 5-brane and the $(r-k-2-N_v, -1)$ (resp. $(r-k-1-N_v, -1)$) for $N = 2r$ (resp. $N = 2r + 1$). Each of the aforementioned subwebs corresponds to a unitary gauge node whose rank is determined by the number of 5-branes in the stack. We need to decouple an overall $U(1)$ to reflect the fact that the Higgs branch directions only care about the relative positions of the aforementioned independent subwebs and we are free to fix the position of one of the subwebs to be at the origin. We will decouple the $U(1)$ node corresponding to the $(r+k-2, 1)$ node. There is a single link connecting any two nodes corresponding to subwebs which end on the same 7-brane from the opposite side, except for those lying on either side of the 7-brane immediately to the left of the $O7^+$ -plane in figure 2.10, which are connected by a double bond. This is essentially the T-dual of the brane system and magnetic quiver in [106]. There are charge 1 and charge 2 hypermultiplets attached to nodes corresponding to subwebs that end on the $O7^+$. The number of charge 2 hyps is given by the formula (2.3.4), where we take their SI with the subweb which we have frozen to the origin. The number of charge 1 hyps are fixed by requiring the HS to agree with dual OSp quivers, to be mentioned momentarily. The magnetic quiver that we propose in

$$N = 2r$$

An immediate consistency check to see whether our conjectured magnetic quiver for $\text{SO}(N)$ with $N_v \leq N - 5$ (2.3.5), (2.3.6) is to compare its Coulomb branch Hilbert series with the orthosymplectic magnetic quiver for the same theory obtained from an O5-plane construction. Let us focus on $N = 2r$ as this is the best understood case. The brane web for $\text{SO}(2r)$ gauge theory with $N_v \leq N - 5$ takes on a slightly different form depending on whether N_v is odd or even. In the case when $N_v \in 2\mathbb{Z}$ the brane web is given by



The magnetic quiver that one reads off from this brane web using the methods of [55, 56] is



Let us compute its Coulomb branch Hilbert series for $N_v = 2$. Following the Hall-Littlewood and gluing technique developed in [131, 132], the expression we need to evaluate is the following

$$\sum_{m=0}^{\infty} P_{\text{SU}(2)}(m, t) \text{HS}_{T[\text{SO}(3)]}^2(m, t) \left(\sum_{-m}^{-m} + \sum_{-m+1}^0 + \sum_1^m + \sum_{m+1}^{\infty} \right) \frac{t^{\Delta(m, n, N)}}{1-t}, \quad (2.3.11)$$

where $P_{\text{SU}(2)}$ is the dressing factor for the central $\text{SO}(3)$ gauge group, the factor $\frac{1}{1-t}$ is the dressing factor for the $\text{U}(1)$ gauge group. The Hilbert series for each $T[\text{SO}(3)]$ leg in the presence of a background magnetic charge is given by

$$\text{HS}_{T[\text{SO}(3)]}(m, t) = \frac{t^{\frac{m}{2}} (1 + m + t - mt)}{(1-t)^2}. \quad (2.3.12)$$

Finally, the conformal dimension, for generic values of $N = 2r$ takes the form

$$\Delta(m, n, N) = -|m| + \frac{1}{2} (|n - m| + |n + m| + |n| + (N - 5)|n|) \quad (2.3.13)$$

$$= \begin{cases} -m - \frac{nN}{2} + n & -\infty < n \leq -m \\ -(N - 4)\frac{n}{2} & m < n \leq 0 \\ (N - 4)\frac{n}{2} & 0 < n \leq m \\ (N - 2)\frac{n}{2} - m & m < n < \infty \end{cases} \quad (2.3.14)$$

Putting all of this together and evaluating the summations in (2.3.11) we obtain the following:

$$\begin{aligned} \text{HS}_{N_v=2}(t, N) &= \frac{1}{(1 - t^2)^7 (1 - t^{N-2})^4} \left[1 + 4t^2 + 4t^4 + t^6 + 6t^{N-2} - 16t^{N+2} - 4t^{N+4} \right. \\ &\quad \left. - 6t^{2N-4} - 22t^{2N-2} - 6t^N + 22t^{2N} - 6t^{3N} + 6t^{2N+2} \right. \\ &\quad \left. + 4t^{3N-6} + 16t^{3N-4} + 6t^{3N-2} - t^{4N-8} - 4t^{4N-6} - 4t^{4N-4} - t^{4N-2} \right]. \end{aligned} \quad (2.3.15)$$

A similar computation for the $N_v = 4$ case leads to

$$\begin{aligned} \text{HS}|_{N=10} &= 1 + 37t^2 + 675t^4 + 8130t^6 + 73131t^8 + 526815t^{10} + 3179939t^{12} + \mathcal{O}(t^{13}) \\ \text{HS}|_{N=12} &= 1 + 37t^2 + 675t^4 + 8130t^6 + 73047t^8 + 524505t^{10} + 3147881t^{12} + \mathcal{O}(t^{13}) \\ \text{HS}|_{N=14} &= 1 + 37t^2 + 675t^4 + 8130t^6 + 73047t^8 + 524421t^{10} + 3145571t^{12} + \mathcal{O}(t^{13}) \end{aligned} \quad (2.3.16)$$

We note that these results are in agreement with (2.3.7), (2.3.8).

The brane web for $\text{SO}(2r)$ gauge theory with $N_v \leq N - 5$ and $N_v \in 2\mathbb{Z} + 1$ is given by

$$(r - 2 - \frac{N_v+1}{2}, -1) \quad (r - 2 - \frac{N_v-1}{2}, -1) \quad (2.3.17)$$

The corresponding magnetic quiver, obtained following the methods of [55, 56] is

$$3 \quad r - \frac{N_v-1}{2} - 3 \quad (2.3.18)$$

Notice that the central $\text{USp}(N_v + 1)$ node appearing in this magnetic quiver is bad in the

sense of Gaiotto and Witten [121]. Due to this technical reason we are not able to perform an explicit computation of its Coulomb branch Hilbert series. There is however an alternative consistency check one could perform for $N_v = 1$, by comparing the Higgs branch Hilbert series. Note that in this limit, the non-simply-laced edge in (2.3.6) disappears and such a computation is accessible. Concretely, one has to compare the Molien-Weyl formula for the $N = 2r$, $N_v = 1$ limit of (2.3.6)

$$\oint_{|p|=1} \frac{dp}{2\pi ip} \oint_{|q|=1} \frac{dq}{2\pi iq} \frac{\text{PE} \left[\left(\frac{p}{q} + \frac{q}{p} \right) t + (p + p^{-1})t + (r-3)(q^2 + q^{-2})t + 3(q + q^{-1})t \right]}{\text{PE} [2t^2]}, \quad (2.3.19)$$

with the Molien-Weyl formula for the $N_v = 1$ limit of (2.3.18)

$$\sum_{p \in \{1, -1\}} \oint_{|q|=1} \frac{dq}{2\pi iq} \oint_{|u|=1} \frac{du}{2\pi iu} (1 - u^2) \times \frac{\text{PE} \left[(q + q^{-1})[1]_u t + (r-3)(q^2 + q^{-2})t + 3(q + q^{-1})t + (2 + p + p^{-1})[1]_u t \right]}{\text{PE} \left[(1 + [2]_u) t^2 \right]}. \quad (2.3.20)$$

Indeed, evaluating these integrals by computing their residues one finds an exact agreement. We collect the results for several values of N in table 2.8.

| N | $\text{HS}_{\mathcal{H}}(t)$ |
|-----|--|
| 6 | $\frac{1+t+6t^2+9t^3+15t^4+12t^5+15t^6+9t^7+6t^8+t^9+t^{10}}{(1-t)^6(1+t)^4(1+t^2)^3}$ |
| 8 | $\frac{1+t+7t^2+21t^3+39t^4+58t^5+90t^6+110t^7+118t^8+110t^9+90t^{10}+58t^{11}+39t^{12}+21t^{13}+7t^{14}+t^{15}+t^{16}}{(1-t)^8(1+2t+2t^2+t^3)^4(1+t+t^2+t^3+t^4)}$ |
| 10 | $\frac{1+t+10t^2+35t^3+82t^4+171t^5+324t^6+517t^7+740t^8+961t^9+1113t^{10}+1158t^{11}+1113t^{12}+\dots\text{palindrome}\dots+t^{22}}{(1-t)^{10}(1+t)^4(1+t^2)^5(1+t+t^2+t^3+t^4)^2}$ |

Table 2.8. Higgs branch Hilbert series of (2.3.6) and (2.3.18) for $N_v = 1$ and various values of N .

Finally, let us mention that for the $\text{SO}(6)+1\mathbf{v}$, namely for the case when $N = 6$ and $N_v = 1$, there is also a unitary web description, that of $\text{SU}(4)_0+1 \mathbf{AS}$, depicted in figure 2.11. Indeed the magnetic quiver one obtains from this ordinary web diagram at infinite coupling is

$$(2.3.21)$$

where the two quivers above are related by decoupling an overall $\text{U}(1)$, and furthermore the quiver on the right matches our proposed magnetic quiver for $\text{SO}(6)+1\mathbf{v}$ (2.3.6) on the nose. This provides us with yet another consistency check.

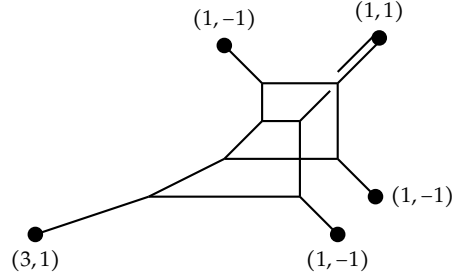
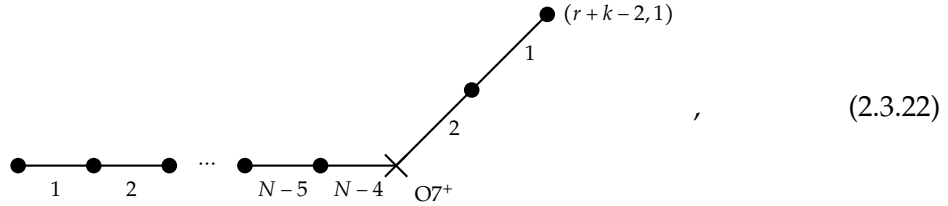


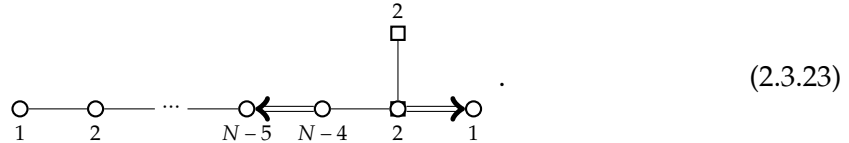
Figure 2.11. Brane web for $SU(4)_{0+1}AS$.

2.3.3 $SO(N)$ with $N_v = N - 4$ flavours

Let us now consider $SO(N)$ gauge theories with $N_v = N - 4$ hypermultiplets in the vector representation. The starting configurations are the web diagrams in figure 2.9 with $N_v = N - 4$ flavour D7 branes. The Higgs branch directions are most easily read off, by performing a few Hanany-Witten moves which we now describe. One first moves all flavour D7 branes through, say, the left 5-brane, creating N_v D5 branes in the process and changing the charge of the 5 brane which crosses their monodromy cut. In the $SO(2r)$ (resp. $SO(2r + 1)$) web in figure 2.9 this results in the $(r - k - 2, -1)$ (resp. $(r - k - 1, -1)$) being converted into an $(r + k - 2, 1)$ leading, after tuning all mass parameters to zero, to the following web diagram



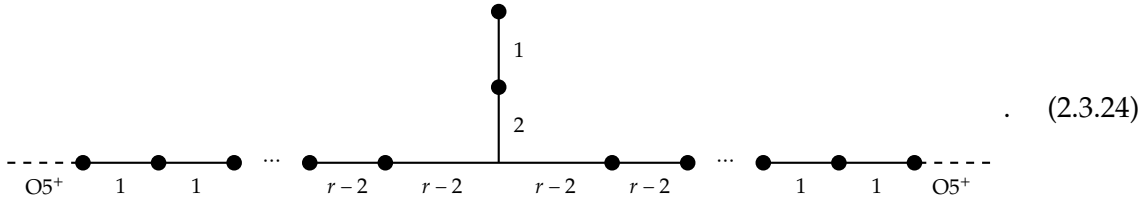
from here, following a similar logic that led us to the magnetic quiver (2.3.6) from the brane web in figure 2.10, we obtain the following magnetic quiver



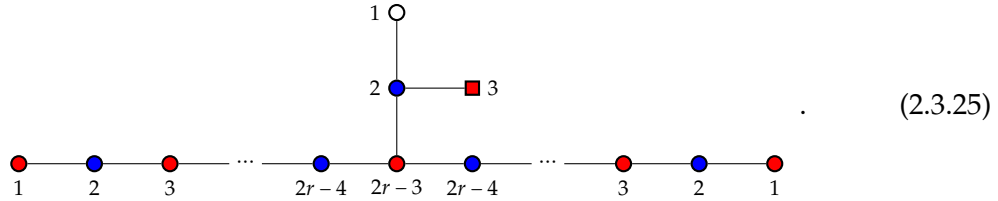
Notice that generically the only unbalanced node is the squircle, which suggests the Coulomb branch isometry in the generic case to be $usp(2N - 8) \oplus su(2)$. The only exception to this happens for $N = 4$. As we will describe in more detail below, in this case the moduli space is actually two copies of $\mathbb{C}^2/\mathbb{Z}_2$ and hence one has an $su(2) \oplus su(2)$ Coulomb branch symmetry. Note that the number of flavours attached to the squircle is due to the $O7^+$ -plane. The reason

that this is 2, rather than 4 as in the previous cases, is purely fixed by trial and error and by the requirement to match the computation on the OSp side as outlined below. For now let us conjecture this quiver and slowly build up the evidence in its support.

We can compare the Coulomb branch of (2.3.23) for $N = 2r$, with the OSp magnetic quiver for $SO(2r)$ with $N_v = 2r - 4$, obtained from the brane web of this theory which uses $O5^+$ -planes:



The magnetic quiver one obtains from this web diagram is given by



We computed the Coulomb branch HS for the two quivers in (2.3.23) and (2.3.25) and found agreement. We provide the results for small values of N below.

$N=4$

For $N = 4$ this theory is the pure $SO(4)$ so it can be engineered as two copies of pure $SU(2)$ without the need of an $O7$ plane. From this an analysis the ordinary magnetic quiver expected, gives two copies of C^2/Z_2 [56]. The CB HS that we expect is then

$$HS|_{N=4} = \frac{1 + 2t^2 + t^4}{(1 - t^2)^4} \tag{2.3.26}$$

Indeed, we computed the CB HS of (2.3.23) for $N = 4$ and we find a match.

$N=5$

When $N = 5$, the 5d theory in question is $SO(5)+1v$, which is the same as $USp(4)+1AS$. The latter theory can be engineered using an ordinary brane web which we depict in figure 2.12.

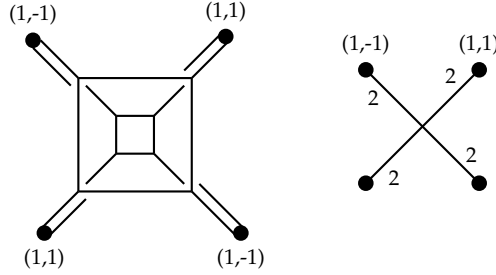


Figure 2.12. Brane web for $USp(4)+1 \text{ AS}$

The magnetic quiver that one reads from the brane web at infinite coupling is

$$\begin{array}{c} \circ \\ \parallel \\ \circ \\ 2 \quad 2 \end{array} . \quad (2.3.27)$$

Note that this quiver is bad in the sense of Gaiotto and Witten and so we cannot compute its Coulomb branch. However, we can make a prediction about what its Coulomb branch Hilbert series would be, utilising the non-simply-laced description. There is actually a third quiver, which should also have the same CB HS, as first discussed in [55]. This is the $O\text{Sp}$ magnetic quiver for $SO(5)+1\mathfrak{v}$, obtained from the brane web using $\widetilde{O5^+}$ -plane. In particular, we claim the following three quivers to have identical Coulomb branch HS

$$\begin{array}{c} 2 \\ \square \\ | \\ \circ \\ 1 \quad 2 \quad \rightarrow \quad \circ \\ 1 \end{array} \longleftrightarrow \begin{array}{c} 3 \\ \square \\ | \\ \circ \\ 1 \quad 2 \quad 3 \\ \bullet \quad \bullet \end{array} \longleftrightarrow \begin{array}{c} 2 \\ \circ \\ \parallel \\ \circ \\ 2 \end{array} \quad (2.3.28)$$

The HS one computes for the non-simply-laced quiver in (2.3.28) is

$$\text{HS}|_{N=5} = \frac{1 + t + 3t^2 + 6t^3 + 8t^4 + 6t^5 + 8t^6 + 6t^7 + 3t^8 + t^9 + t^{10}}{(1-t)^6(1+t)^4(1+t+t^2)^3} . \quad (2.3.29)$$

We recognise this as the HS for the reduced moduli space of two- $SU(2)$ instantons on \mathbb{C}^2 [133].

$N=6$

This theory is $SO(6)$ with 2 vectors. Since this theory is isomorphic to $SU(4)_0 + 2 \text{ AS}$, we can extract a unitary magnetic quiver from a brane system that doesn't involve $O7$ planes. The brane web for $SU(4)_0 + 2 \text{ AS}$ is depicted in figure 2.13. From this brane web one can readily

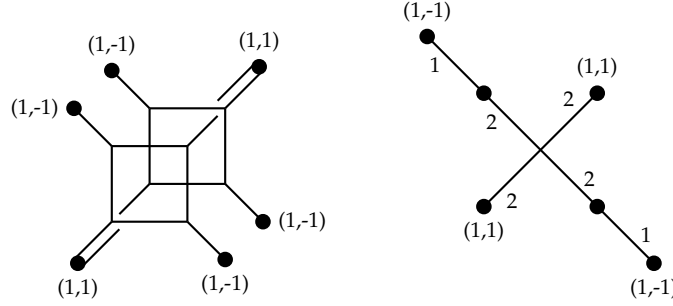


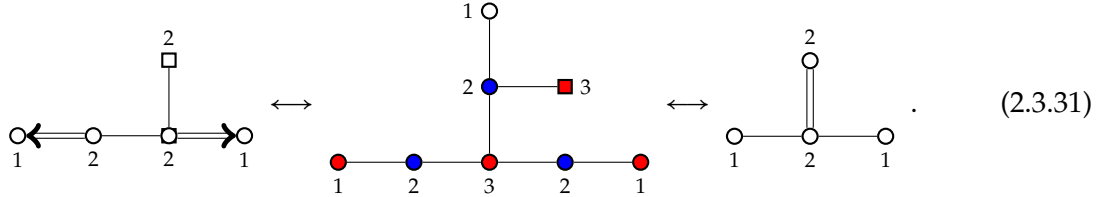
Figure 2.13. Brane web for $SU(4)_{0+2} AS$

obtain the following magnetic quiver



(2.3.30)

We therefore claim that the following three quivers should have the same Coulomb branch



(2.3.31)

The expected CB HS for the magnetic quiver is then

$$HS|_{N=6} = \frac{1 + 8t^2 + 40t^4 + 107t^6 + 199t^8 + 234t^{10} + 199t^{12} + \dots \text{palindrome} \dots + t^{20}}{(1 - t^2)^{10}(1 + t^2)^5} \tag{2.3.32}$$

We computed the CB HS of (2.3.23) for $N = 6$ and we find a match.

2.3.4 $SO(N)$ with $N_v = N - 3$

We now analyse the final possible family of theories, $SO(N)$ gauge theories with $N_v = N - 3$ hypermultiplets in the vector representation. This is the highest possible number of vector matter that has a UV completion in 5d. The web diagram for the fixed point limit can be obtained by adding D7 branes to the pure gauge theory cases as in figure 2.9. To read off the Higgs branch directions we first perform the following sequence of Hanany-Witten moves. First, one has to move all $2r - 3$ (resp. $2r - 2$) D7s to, say, the left of the $(r - k - 2, -1)$ (resp.

$(r - k - 1, -1)$ 5-brane in the web for the $SO(2r)$ (resp. $SO(2r + 1)$) theory in figure 2.9. In doing so, the $(r - k - 2, -1)$ and $(r - k - 1, -1)$ 5-branes are both converted into an $(r + k - 1, 1)$. Next we pull the $(r + k - 1, 1)$ 5-brane through the $(r + k - 2, 1)$ 5-brane, which creates an additional $(r + k - 1, 1)$ 5-brane ending on the $(r + k - 1, 1)$ 7-brane in addition to converting the $(r + k - 2, 1)$ 5-brane into a D5. Setting all mass parameters to zero and separating the D7s to make the Higgs branch directions manifest, we arrive at

(2.3.33)

The magnetic quiver we propose in this case is given by

(2.3.34)

where all the gauge nodes and hypermultiplet contributions are read off following a discussion analogous to that outlined in the previous cases. We stress that the rank of the flavour node attached to the squircle is fixed by the requirement that the CB HS matches that of the $O\text{Sp}$ quiver below. It would be interesting to understand the number of flavours more clearly. Except for the squircle, all other nodes in this quiver all balanced, with the balanced subquiver forming the Dynkin diagram of C_{N-2} , implying that the Coulomb branch isometry is generically $usp(2N - 4)$.

Since $SO(N)$ theory with $N_v = N - 3$ hypers in the vector representation can also be engineered using an $O5$ -plane, we can provide a consistency check of the magnetic quiver (2.3.34). The infinite coupling limit of the web with $O5$ -plane in the case where $N = 2r$ is given by

(2.3.35)

from which one can obtain the following OSp magnetic quiver

(2.3.36)

The computation of the CB HS of this OSp quiver is a close analog of (2.3.11), so let us skip the details and quote the final results

$$\text{HS}|_{r=3} = 1 + 36t^2 + 681t^4 + 8688t^6 + 83376t^8 + 640695t^{10} + 4110730t^{12} + \mathcal{O}(t^{13}) \quad (2.3.37)$$

$N = 4$

For the $N = 4$ case this theory is $\text{SO}(4)$ with one vector, which can be realized without an orientifold plane as $\text{SU}(2)_0 \times \text{SU}(2)_0$ with a bifundamental. The magnetic quiver for this theory is

(2.3.38)

Which leads us to claim that the following three quivers should have identical Coulomb branches

(2.3.39)

The unitary simply-laced quiver (2.3.38) is the 3d mirror dual of $\text{U}(2)$ with $N_f = 4$ fundamental hypermultiplets. The refined Hilbert series for the CB of (2.3.38) reads

$$\text{HS}(t; x) = \sum_{n_1, n_2} \chi_{[n_1, 2n_2, n_1]}(x) t^{n_1 + 2n_2} . \quad (2.3.40)$$

We computed the unrefined HS for the CB of the non-simply laced quiver of (2.3.34) finding agreement of the results. In fact both the CB HS and the HB HS of the OSp quiver in (2.3.39) and the unitary simply-laced quiver (2.3.38) were computed and found to agree in [55]. We

see that there is actually a third description of the Coulomb branch of these theories in terms of a non-simply-laced quiver.

Chapter 3

Electrostatic description of 3d SCFTs

The conjunction of conformal symmetry and supersymmetry proved to be a very powerful tool to analyse the existence and dynamics of fixed points for field theories in dimension $d + 1$ (with $d = 0, \dots, 5$). In this line, Maldacena's AdS/CFT conjecture [5] played a central role motivating the construction of AdS_D backgrounds in consistent theories of gravity.

For the particular case of half-BPS backgrounds with isometries $SO(2, D - 1) \times SU(2)$, great progress was achieved. In fact, infinite classes of backgrounds of the form $\text{AdS}_D \times S^2 \times \Sigma_{8-D}$ have been constructed for the cases $D = 2, \dots, 7$. For some values of D , these backgrounds are described in terms of a *potential function*. This potential satisfies a Laplace equation, which needs initial and boundary conditions to be well-defined.

It is in these initial or boundary conditions that the healthy character of the background is encoded and where the connection with the dual CFT is made concrete. Indeed, the presence of a 'rank' function (so called as it encodes the ranks of the colour and flavour groups of the field theory) turns out to be the initial condition of the Laplace equation. For the cases $D = 2, 3, 5, 7$ the formalism, backgrounds and dual field theories are respectively described in the papers [134]-[135] (for AdS_2), [136]-[137] (for AdS_3), [138]-[139] (for AdS_5) and [140]-[141] (for AdS_7). The cases $D = 4$ and $D = 6$ corresponding with SCFTs in dimension three and five have a very elegant formulation in terms of holomorphic functions, but the connection with the dual SCFT is a bit more laborious. See [142]-[143] (for AdS_4) and [144]-[145] (for AdS_6) respectively. The case $D = 6$ was recently written in the 'electrostatic' context (Laplace equation and boundary-initial conditions) in [45].

A first goal of this chapter is to complete the picture and write the case of AdS_4 in this electrostatic formalism. In fact, we present a holographic dual formulation of $\mathcal{N} = 4$, $d=3$ superconformal field theories (linear quivers), involving $\text{AdS}_4 \times S^2 \times S^2$ backgrounds in type IIB, which are obtained by reformulating the solution in [142]. The case we deal with in this chapter is that of *balanced* linear quivers, that is for each gauge node the number of fields transforming in the (bi)fundamental is twice the rank of the gauge group (or $N_f = 2N_c$). The contents of this chapter are distributed across the coming sections as follows.

In Section 3.1 we study the background, the defining Laplace PDE, its initial and boundary conditions. Possible singular behaviours in the spacetime are discussed.

In Section 3.2 we study the Page charges. Imposing their quantisation determines the range of some coordinates and the character of the rank function (the initial condition for the Laplace equation), that we determine to be a piecewise, continuous, linear function. We study the associated Hanany–Witten set-up and linking numbers, giving a holographic expression for them. We algorithmically associate a balanced linear quiver with a given supergravity solution. We also find a generic expression for the holographic central charge. This is a purely geometric quantity that counts the number of degrees of freedom of the dual CFT. Usually, this is also identified as proportional to the Free Energy of the CFT when formulated on a three-sphere.

In Section 3.3 we discuss generic examples of linear quivers and study all the quantities defined in Section 3.2: charges, Hanany–Witten set-ups, linking numbers, central charge. We discuss special limits of our examples and compare them with previously found results.

Section 3.4 summarises some known field theoretical aspects of the dual 3d $\mathcal{N} = 4$ SCFTs, dwelling in particular with Mirror symmetry. We present a purely geometric version of Mirror symmetry, mapping balanced quivers into balanced quivers. This geometric correspondence exchanges between NS5 and D5 branes and the dimensions of the Higgs and Coulomb branches of the theories, all being nicely realised as a simple operation in the string description. As a spin-off, we present a (not-mirror) transformation that maps a balanced linear quiver into a different one (still balanced and linear), both sharing the same central charge. Some of the content of this section might illuminate future work and this, together with other possible lines of investigation, are presented in Section 3.5, with a summary of the main results obtained in the paper [74] and some concluding remarks.

3.1 Geometry

We start this section by writing explicitly the infinite family of type IIB supergravity backgrounds we work with.

We are after solutions dual to 3d $\mathcal{N} = 4$ super-conformal field theories. This implies that the background must have isometries $\text{SO}(2,3) \times \text{SU}(2)_C \times \text{SU}(2)_H$ and preserve eight Poincaré supercharges to match the global symmetries of the field theory. Hence, our geometries must contain an AdS_4 factor and a couple of two spheres $S^2_1(\theta_1, \varphi_1)$ and $S^2_2(\theta_2, \varphi_2)$. There are two extra directions labelled by (σ, η) . The presence of $\text{SO}(2,3) \times \text{SU}(2)_C \times \text{SU}(2)_H$ isometries allow for warp factors that depend only on (σ, η) . The background must have the form $\text{AdS}_4 \times S^2_1 \times S^2_2 \times \Sigma_2(\sigma, \eta)$. The Ramond and Neveu-Schwarz fields must also respect the above mentioned isometries.

The preservation of four Poincaré supersymmetries implies that the generic type IIB background can be casted in terms of a function $V(\sigma, \eta)$. In string frame the solution reads

$$\begin{aligned}
ds_{10,st}^2 &= f_1(\sigma, \eta) \left[ds^2(\text{AdS}_4) + f_2(\sigma, \eta) ds^2(S_1^2) + f_3(\sigma, \eta) ds^2(S_2^2) + f_4(\sigma, \eta) (d\sigma^2 + d\eta^2) \right], \\
e^{-2\Phi} &= f_5(\sigma, \eta), \quad B_2 = f_6(\sigma, \eta) \text{Vol}(S_1^2), \quad C_2 = f_7(\sigma, \eta) \text{Vol}(S_2^2), \quad \tilde{C}_4 = f_8(\sigma, \eta) \text{Vol}(\text{AdS}_4), \\
f_1 &= \frac{\pi}{2} \sqrt{\frac{\sigma^3 \partial_{\eta\sigma}^2 V}{\partial_\sigma(\sigma \partial_\eta V)}}, \quad f_2 = -\frac{\partial_\eta V \partial_\sigma(\sigma \partial_\eta V)}{\sigma \Lambda}, \quad f_3 = \frac{\partial_\sigma(\sigma \partial_\eta V)}{\sigma \partial_{\eta\sigma}^2 V}, \quad f_4 = -\frac{\partial_\sigma(\sigma \partial_\eta V)}{\sigma^2 \partial_\eta V}, \\
f_5 &= -16 \frac{\Lambda \partial_\eta V}{\partial_{\eta\sigma}^2 V}, \quad f_6 = \frac{\pi}{2} \left(\eta - \frac{\sigma \partial_\eta V \partial_\eta^2 V}{\Lambda} \right), \quad f_7 = -2\pi \left(\partial_\sigma(\sigma V) - \frac{\sigma \partial_\eta V \partial_\eta^2 V}{\partial_{\eta\sigma}^2 V} \right), \\
f_8 &= -\pi^2 \sigma^2 \left(3\partial_\sigma V + \frac{\sigma \partial_\eta V \partial_\eta^2 V}{\partial_\sigma(\sigma \partial_\eta V)} \right), \quad \Lambda = \partial_\eta V \partial_{\eta\sigma}^2 V + \sigma \left((\partial_{\eta\sigma}^2 V)^2 + (\partial_\eta^2 V)^2 \right). \tag{3.1.1}
\end{aligned}$$

Where the fluxes are defined from the potentials as follows,

$$F_1 = 0, \quad H_3 = dB_2 \quad F_3 = dC_2, \quad F_5 = d\tilde{C}_4 + *d\tilde{C}_4. \tag{3.1.2}$$

Using Mathematica, we have checked that the configuration in eq.(3.1.1) is solution to the Type IIB equations of motion, if the function $V(\sigma, \eta)$ satisfies,

$$\partial_\sigma(\sigma^2 \partial_\sigma V) + \sigma^2 \partial_\eta^2 V = 0. \tag{3.1.3}$$

This infinite family of solutions is equivalent to the backgrounds described by D'Hoker, Estes and Gutperle in [142].

For the backgrounds in eq.(3.1.1) to be well defined, $e^{2\Phi}$ and the metric warping functions must be real and positive. For the class of solutions we analyse in the next sections, we assume the symmetry $V(-\sigma, \eta) = -V(\sigma, \eta)$. Under the 'parity' change $\sigma \rightarrow -\sigma$, the quantity $\Lambda(-\sigma, \eta) = -\Lambda(\sigma, \eta)$. The reader can check that the functions f_1, \dots, f_5 are invariant under this 'parity' transformation. Hence, the solution for negative σ is well defined as long as the one with positive σ is. The required positivity condition for the dilaton and warping functions is

$$-\sigma \frac{\partial_{\eta\sigma}^2 V}{\partial_\eta V} \geq 1. \tag{3.1.4}$$

As a direct result of the above condition we have

$$\begin{aligned} \sigma\Lambda &= \sigma\partial_\eta V\partial_{\eta\sigma}^2 V + (|\sigma\partial_{\eta\sigma}^2 V|^2 + (\sigma\partial_\eta^2 V)^2) \geq \sigma\partial_\eta V\partial_{\eta\sigma}^2 V + |\sigma\partial_\eta V\partial_{\eta\sigma}^2 V| + (\sigma\partial_\eta^2 V)^2 \geq 0, \\ \sigma\frac{\partial_\sigma(\sigma\partial_\eta V)}{\sigma\partial_{\eta\sigma}^2 V} &= 1 + \frac{\partial_\eta V}{\sigma\partial_{\eta\sigma}^2 V} \geq 0. \end{aligned} \quad (3.1.5)$$

The positivity of f_1, f_2, f_3, f_4, f_5 is derived as a consequence of $\sigma\Lambda \geq 0$ and eq.(3.1.4).

3.1.1 Study of the partial differential equation

Let us now study the partial differential equation (3.1.3). Define $V(\sigma, \eta) = \frac{\hat{V}(\sigma, \eta)}{\sigma}$ and $\hat{V}(\sigma, \eta) = \partial_\eta \hat{W}(\sigma, \eta)$. Consider the coordinates to range in $0 \leq \eta \leq P$, where P is a real number, and $-\infty < \sigma < \infty$. The differential equation (3.1.3) must be supplemented by boundary and initial conditions. In terms of $\hat{W}(\sigma, \eta)$ the problem reads

$$\begin{aligned} \partial_\sigma^2 \hat{W}(\sigma, \eta) + \partial_\eta^2 \hat{W}(\sigma, \eta) &= 0, & (\text{almost everywhere}) & \quad (3.1.6) \\ \hat{W}(\sigma, \eta = 0) = 0, \quad \hat{W}(\sigma, \eta = P) &= 0, \\ \partial_\sigma \hat{W}(\sigma = 0^+, \eta) - \partial_\sigma \hat{W}(\sigma = 0^-, \eta) &= -\mathcal{R}(\eta). \end{aligned}$$

As we discuss in the following sections, the function $\mathcal{R}(\eta)$ is the input determined by the dual quiver field theory. Notice that, since \hat{W} is an harmonic function, we have that also \hat{V} is harmonic, which in turn implies (3.1.3).

To solve the problem in eq.(3.1.6), we separate variables and impose the boundary conditions to find,

$$\hat{V}(\sigma, \eta) = \sum_{k=1}^{\infty} a_k \cos\left(\frac{k\pi\eta}{P}\right) e^{-\frac{k\pi|\sigma|}{P}}, \quad \hat{W}(\sigma, \eta) = \sum_{k=1}^{\infty} a_k \left(\frac{P}{k\pi}\right) \sin\left(\frac{k\pi\eta}{P}\right) e^{-\frac{k\pi|\sigma|}{P}}. \quad (3.1.7)$$

We have used that the function $\mathcal{R}(\eta)$ has a Fourier decomposition,

$$\mathcal{R}(\eta) = \sum_{k=1}^{\infty} 2a_k \sin\left(\frac{k\pi\eta}{P}\right), \quad a_k = \frac{1}{P} \int_0^P \mathcal{R}(\eta) \sin\left(\frac{k\pi\eta}{P}\right). \quad (3.1.8)$$

3.1.2 Asymptotic behaviour

Let us briefly study the asymptotic behaviour of our backgrounds. We start with the region $\sigma \rightarrow \pm\infty$. Using the solutions in eq.(3.1.7), for $|\sigma| \rightarrow \infty$, we find,

$$\begin{aligned} ds_{st}^2 \Big|_{\sigma \rightarrow \pm\infty} &\sim \frac{\pi|\sigma|}{2} ds^2(\text{AdS}_4) + \frac{d\eta^2}{2P} + \frac{P}{2a_1} \sin^2\left(\frac{\pi\eta}{P}\right) ds^2(S_1^2) + \frac{\pi|\sigma|}{2} ds^2(S_2^2) + \frac{1}{2P} d\sigma^2, \\ e^{-2\Phi} &\sim \frac{e^{-\frac{2\pi|\sigma|}{P}}}{|\sigma|}. \end{aligned} \quad (3.1.9)$$

Performing a change of coordinates $|\sigma| \rightarrow -\log r$, with r small, one can notice that the metric and the dilaton highlights the presence of a (p, q) five brane [144] with support on $\text{AdS}_4 \times S_2^2$.

Let's now consider the asymptotic behaviour at the physical boundary $\eta \sim 0, P$. We will explicitly deal with the case $\eta \rightarrow 0$ since the discussion for the other boundary is identical. The expressions for $f_i(\sigma, 0)$ can be found in [74]; schematically, we have

$$ds_{st}^2 \Big|_{(0,0)} \sim ds^2(\text{AdS}_4) + d\eta^2 + \eta^2 ds^2(S_1^2) + d\sigma^2 + ds^2(S_2^2), \quad e^{-2\Phi} \sim 1, \quad (3.1.10)$$

where we have omitted functions of σ which are not singular at least for $\sigma \neq 0$. Thus near to $\eta \sim 0$ we have a regular $\text{AdS}_4 \times S^2 \times \mathbb{R}^4$ geometry.

The behaviour in the corner $(\sigma, \eta) = (0, 0)$ requires some more analysis, since in that case the functions $f_i(0, 0)$ can lead to a singular metric. Notice that, however, the dilaton is always finite, so if these singularities are present it would be hard to give them an interpretation in terms of branes. One possibility is to restrict our analysis to the $\mathcal{R}(\eta)$ which leads to a regular metric. We can do that by choosing $\mathcal{R}(\eta)$ to be linear near to $\eta = 0$, so that we have

$$\partial_\eta^2 \mathcal{R}|_{\eta \sim 0} = \partial_{\eta\sigma}^2 \hat{V}|_{(\sigma, \eta) \sim (0, 0)} = 0 \quad \iff \quad \sum_k k^3 a_k = 0. \quad (3.1.11)$$

With this ansatz, the metric has the following asymptotic behavior

$$ds_{st}^2 \Big|_{(0,0)} \sim ds^2(\text{AdS}_4) + d\eta^2 + \eta^2 ds^2(S_1^2) + d\sigma^2 + \sigma^2 ds^2(S_2^2), \quad e^{-2\Phi} \sim 1, \quad (3.1.12)$$

which is a regular $\text{AdS}_4 \times \mathbb{R}^6$ geometry. It is particularly interesting to notice that requiring $\mathcal{R}(\eta)$ to be linear in $(\sigma, \eta) = (0, 0)$ is not actually a restriction but a necessary condition for having the Page charges properly quantised, as we are going to see in the next section.

3.2 Charges and other important quantities

To start, we write the expressions of the Page fluxes $\hat{F}_p = F_p \wedge e^{-B_2}$. For the Ramond and NS5 fields in our configuration of eq.(3.1.1), we have

$$\hat{F}_3 = F_3, \quad \hat{F}_5 = F_5 - \left(B_2 - \frac{\pi\Delta}{2} \text{Vol}(S_1^2) \right) \wedge F_3. \quad (3.2.1)$$

Note that we have performed a large gauge transformation $B_2 \rightarrow (B_2 - \frac{\pi\Delta}{2} \text{Vol}(S_1^2))$, that will be useful below. The Page charges are defined as

$$Q_{Dp/NS5} = \frac{1}{(2\pi)^{7-p} \alpha'} \int_{\Sigma_{8-p}} \hat{F}_{8-p}. \quad (3.2.2)$$

In the following, we will set $\alpha' = 1$. Let us study the charges associated with $H_3, \hat{F}_5, \hat{F}_3$.

NS5 branes charge

First, we analyse the charge of NS5 branes. We choose a three-cycle to perform the integration of H_3 ,

$$\Sigma_3 = [\eta, S_1^2(\theta_1, \varphi_1)]_{\sigma=\pm\infty}. \quad (3.2.3)$$

We then find,

$$Q_{NS5} = \frac{1}{4\pi^2} \int_{\Sigma_3} H_3 = \frac{1}{\pi} \int_0^P \partial_\eta f_6(\sigma \rightarrow \pm\infty, \eta) = P - \left. \frac{\sigma \partial_\eta V \partial_\eta^2 V}{2\Lambda} \right]_{\sigma \rightarrow \pm\infty, 0}^{\sigma \rightarrow \pm\infty, P} = P. \quad (3.2.4)$$

In the last two steps we have summed up the contributions at $\sigma = \pm\infty$. In conclusion, the total number of NS5 branes is proportional to the length of the η -interval.

D3 branes charge

To calculate the number of D3 branes we integrate the expression for the Page flux \hat{F}_5 in eq.(3.2.1). The five manifold on which we integrate \hat{F}_5 is defined as

$$\Sigma_5 = [S_1^2, S_2^2, \sigma]_{\eta=\text{fixed}}. \quad (3.2.5)$$

We implemented a large gauge transformation as in (3.2.1), below we determine the parameter Δ to have a quantised number of D3 branes in each interval of the η -coordinate.

Using the potential \hat{W} defined above eq.(3.1.6) we are able to compactly write the relevant component of \hat{F}_5 as,

$$\begin{aligned} \hat{F}_5|_{\Sigma_5} &= F_5 - (B_2 - \frac{\pi}{2}\Delta \text{Vol}(S_1^2)) \wedge F_3|_{\Sigma_5} = \pi^2 \partial_\sigma (\mathcal{M}_1 + \mathcal{M}_2) \text{Vol}(S_1^2) \wedge \text{Vol}(S_1^2) \wedge d\sigma. \\ \mathcal{M}_1 &= \frac{\eta\sigma(\partial_\eta^2 V)(\partial_\eta V) - \sigma(\partial_\eta V)^2}{\partial_{\eta\sigma}^2 V}, \quad \mathcal{M}_2 = \partial_\sigma (\hat{W} - (\eta - \Delta)\partial_\eta \hat{W}). \end{aligned} \quad (3.2.6)$$

Then, we compute

$$N_{D3} = \frac{1}{(2\pi)^4 \alpha'} \int_{\Sigma_5} \hat{F}_5 = \frac{\pi^2 \times (4\pi)^2}{(2\pi)^4} \int d\sigma \partial_\sigma (\mathcal{M}_1 + \mathcal{M}_2) = 2(\mathcal{M}_1 + \mathcal{M}_2) \Big|_{\sigma=0^+, \eta}^{\sigma \rightarrow \infty, \eta}. \quad (3.2.7)$$

Since \mathcal{M}_i are even, we have considered twice the contribution for $\sigma > 0$.

The reader can check that the contribution of \mathcal{M}_1 is vanishing at $\sigma \rightarrow \infty$ and at $\sigma = 0$. Inspecting the expression for \mathcal{M}_2 shows that it vanishes for $\sigma \rightarrow \infty$. In summary, the charge of D3 branes is given by \mathcal{M}_2 evaluated at $\sigma = 0$, and using the definition of \mathcal{R} in eq.(3.1.8) we get

$$N_{D3} = 2\partial_\sigma (\hat{W} - (\eta - \Delta)\partial_\eta \hat{W}) \Big|_{\sigma=0^+} = \mathcal{R}(\eta) - (\eta - \Delta)\mathcal{R}'(\eta). \quad (3.2.8)$$

This expression indicates that the rank function used as input for the partial differential equation must be piecewise linear. In fact, consider a piecewise linear and continuous function defined in intervals

$$\mathcal{R}(\eta) = \begin{cases} N_1 \eta & 0 \leq \eta \leq 1 \\ N_l + (N_{l+1} - N_l)(\eta - l) & l \leq \eta \leq l+1, \quad l := 1, \dots, P-2 \\ N_{P-1}(P - \eta) & (P-1) \leq \eta \leq P. \end{cases}$$

The expression in eq.(3.2.8) indicates that, after choosing $\Delta = k$ in the interval $[k, k+1]$ there are N_k D3 branes.

D5 brane charge

To calculate the charge of D5 branes, we use

$$N_{D5} = \frac{1}{4\pi^2} \int_{\hat{\Sigma}_3} F_3, \quad \hat{\Sigma}_3 = [\eta, S_2^2(\theta_2, \varphi_2)]_{\sigma=0^+}. \quad (3.2.9)$$

We find,

$$N_{D5} = -\frac{1}{\pi} \int_{\eta_i}^{\eta_f} d\eta \partial_\eta f_7(\sigma = 0^+, \eta) = -\frac{1}{\pi} (f_7(0, \eta_f) - f_7(0, \eta_i)).$$

| | t | x_1 | x_2 | r | θ_1 | φ_1 | θ_2 | φ_2 | σ | η |
|-----|-----|-------|-------|-----|------------|-------------|------------|-------------|----------|--------|
| NS5 | – | – | – | · | · | · | – | – | – | · |
| D5 | – | – | – | – | – | – | · | · | · | · |
| D3 | – | – | – | · | · | · | · | · | · | – |

Table 3.1. The Hanany–Witten set up, indicating the directions over which each brane extends.

The reader can check that

$$N_{D5} = \mathcal{R}'(\eta_i) - \mathcal{R}'(\eta_f). \quad (3.2.10)$$

This result is expressing the number of D5s between the points η_i and η_f as computed by the differences in slope of the rank function at those two points. For a piece-wise continuous and linear rank function as the one obtained in quantising the charge of D3 branes, we find that the charge of D5 branes is also quantised.

In summary, the rank-function is the input for the PDE problem in eq.(3.1.6). To have quantised charges for Neveu-Schwarz five branes, we need the size of the interval P to be an integer—consistently with the boundary conditions in eq.(3.1.6). To have quantised numbers of D3 and D5 branes, the rank function must be a piece-wise linear and continuous function of the form

$$\mathcal{R}(\eta) = \begin{cases} N_1 \eta & 0 \leq \eta \leq 1 \\ N_l + (N_{l+1} - N_l)(\eta - l) & l \leq \eta \leq l + 1, \quad l := 1, \dots, P - 2 \\ N_{P-1}(P - \eta) & (P - 1) \leq \eta \leq P. \end{cases}$$

The number of D3 (colour) branes and D5 (flavour) branes in the interval $[k, k + 1]$ and the total number of branes are given by,

$$N_{D3}[k, k + 1] = N_k, \quad N_{D5}[k, k + 1] = 2N_k - N_{k+1} - N_{k-1}, \quad (3.2.11)$$

$$N_{D3}^{\text{total}} = \int_0^P \mathcal{R}(\eta) d\eta, \quad N_{D5}^{\text{total}} = \mathcal{R}'(0) - \mathcal{R}'(P), \quad N_{NS5}^{\text{total}} = P.$$

3.2.1 Hanany–Witten set-up and linking numbers

The counting of branes described above encodes in the rank function $\mathcal{R}(\eta)$ the ‘kinematic data’ of the dual conformal field theory. The presence of P NS5 branes along the η -direction suggest that we should place one NS5 at each integer value of η . In between the k^{th} and $(k + 1)^{\text{th}}$ NS5-branes, we have N_k D3 branes and $N_{F_k} = 2N_k - N_{k+1} - N_{k-1}$ D5 branes as indicated in eq.(3.2.11). Analysing the Ramond fields \hat{F}_5 and \hat{F}_3 suggests that the branes extend along the directions of space time as indicated in Table 3.1.

In this Hanany–Witten set-up [146], the field theory is realised on the t, x_1, x_2 directions.

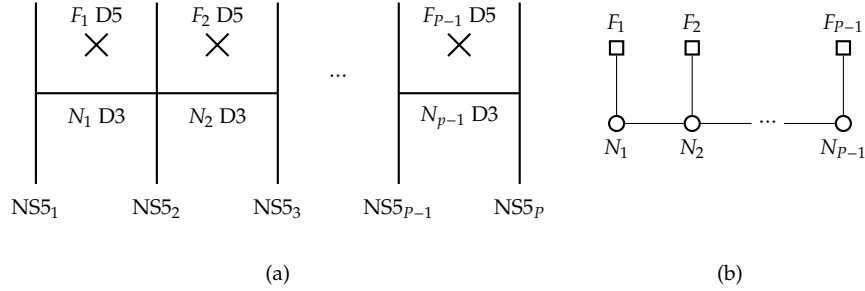


Figure 3.1. The Hanany–Witten brane set up, showing the N_k (colour) D3 branes, the F_k (flavour) D5 branes and the NS5 branes. The associated quiver field theory is also shown.

The D3 branes have one compact direction leading to an effective $(2 + 1)$ -dimensional dynamics, for each stack of N_k branes, that give rise to an $U(N_k)$ gauge group. The D5 branes are effectively realising an $SU(F_k)$ global symmetry, hence correspond to flavour branes. The NS5 branes provide the boundary conditions necessary for the D3 to end on them. We represent the system as in Figure 3.1. One interesting quantity associated with these Hanany–Witten set-ups are the linking numbers. These are topological quantities (invariant under Hanany–Witten moves) associated with Neveu–Schwarz and Ramond five branes. For the i^{th} NS5 brane and the j^{th} D5 brane they are defined in terms of the number of branes to the left and right of a given one,

$$\hat{L}_{NS5i} = (n_{D3}^{\text{right}} - n_{D3}^{\text{left}}) + n_{D5}^{\text{left}}, \quad L_{D5j} = (n_{D3}^{\text{right}} - n_{D3}^{\text{left}}) + n_{NS5}^{\text{right}}. \quad (3.2.12)$$

For the systems described above, the linking numbers can be seen to have the values,

$$\hat{L}_1 = \hat{L}_2 = \dots = \hat{L}_P = \mathcal{R}'(0), \quad L_{D5,j} = P - j. \quad (3.2.13)$$

These satisfy

$$\sum_{i=1}^{N_{NS5}} \hat{L}_i = \sum_{j=1}^{N_{D5}} L_{D5,j} = \hat{N}. \quad (3.2.14)$$

Therefore with each quiver we associate two partitions of the integer \hat{N} . The partitions are made out of the linking numbers of NS5 and D5 branes,

$$\hat{\rho} = (\hat{L}_{NS1}, \hat{L}_{NS2}, \dots, \hat{L}_{NSP}), \quad \rho = (L_{D51}, L_{D52}, \dots, L_{D5}). \quad (3.2.15)$$

The associated quiver field theories are referred to as $T_{\rho}^{\hat{\rho}}[SU(\hat{N})]$. Gaiotto and Witten [121] proposed that these field theories flow to an interacting conformal point at low energies if a relation between partitions $\hat{\rho}^T \geq \rho$ is satisfied. The authors of the work [147] translated this condition into $N_{D5,k} \geq 2N_{D3,k} - N_{D3,k+1} - N_{D3,k-1}$. The formulation we presented in terms of

a rank functions constrains us to the *balanced* quiver for which the equality is satisfied. We leave for future study the unbalanced situation.

3.2.2 Holographic central charge

Let us discuss now the holographic central charge. This is a quantity, instrumental in the tests of the duality between the backgrounds in (3.1.1) and the conformal field theories described in the previous section. The holographic central charge is defined as a weighted version of the volume of the internal manifold (the part of the space that is not AdS₄). The definition of this quantity is carefully discussed in [148]-[149], we refer the reader to those references for the general definitions. The application to our particular case is discussed below.

We use coordinates for AdS₄ such that

$$ds_{AdS_4}^2 = e^{2\rho} dx_{1,2}^2 + d\rho^2. \quad (3.2.16)$$

We quote the relevant quantities that can be read from the metric and dilaton in eq.(3.1.1)

$$\begin{aligned} a &= f_1(\sigma, \eta) e^{2\rho}, \quad b = e^{-2\rho}, \quad d = 2, \\ ds_{int}^2 &= f_1(\sigma, \eta) \left[f_2(\sigma, \eta) ds^2(S_1^2) + f_3(\sigma, \eta) ds^2(S_2^2) + f_4(\sigma, \eta) (d\sigma^2 + d\eta^2) \right], \\ \det[g_{int}] &= f_1^6 f_2^2 f_3^2 f_4^2 \sin^2 \theta_1 \sin^2 \theta_2, \\ V_{int} &= \int_{M_{int}} \sqrt{\det\{g_{int}\} e^{-4\Phi} a^d} = \left[16\pi^2 \int d\sigma d\eta f_1^4 f_2 f_3 f_4 f_5 \right] e^{2\rho} = \mathcal{N} e^{2\rho}, \\ H &= V_{int}^2 = \mathcal{N}^2 e^{4\rho}, \quad H' = 4H, \\ c_{hol} &= \frac{d^d}{G_N} b^{d/2} \frac{H^{\frac{2d+1}{2}}}{(H')^d} = \frac{\mathcal{N}}{4G_N} = \frac{\mathcal{N}}{32\pi^6}. \end{aligned} \quad (3.2.17)$$

We have used $G_N = 8\pi^6 \alpha'^4 g_s^2 = 8\pi^6$ (in units where $\alpha' = g_s = 1$). Using the definitions for the dilaton and the warp factors given in eq.(3.1.1), we have

$$\mathcal{N} = -16\pi^6 \int d\sigma d\eta (\sigma^2 \partial_\eta V) \partial_\sigma (\sigma \partial_\eta V) = -16\pi^6 \int d\sigma d\eta \sigma (\partial_\eta \hat{V}) (\partial_{\sigma\eta}^2 \hat{V}). \quad (3.2.18)$$

Performing explicitly the integral over η and after that the σ -integral¹. We find,

$$\mathcal{N} = 4\pi^7 \sum_{k=1}^{\infty} k a_k^2, \quad c_{hol} = \frac{\pi}{8} \sum_{k=1}^{\infty} k a_k^2. \quad (3.2.19)$$

¹Using that $\int_0^P \sin\left(\frac{k\pi\eta}{P}\right) \sin\left(\frac{l\pi\eta}{P}\right) d\eta = \frac{P}{2} \delta_{k,l}$.

Let us now evaluate explicitly this formula for a generic balanced quiver, characterised by a generic rank function.

Generic balanced quiver

In this section we derive an analytic expression for the holographic central charge in eq.(3.2.19) in the case of a generic quiver field theory. Consider a generic balanced 3d $\mathcal{N} = 4$ linear quiver and its associated rank function

$$\begin{array}{c}
 F_1 \quad F_2 \quad F_{P-1} \\
 \square \quad \square \quad \square \\
 | \quad | \quad | \\
 \circ \quad \circ \quad \dots \quad \circ \\
 N_1 \quad N_2 \quad \dots \quad N_{P-1}
 \end{array}
 ; \quad \mathcal{R}(\eta) = \begin{cases} N_1 \eta & \eta \in [0, 1] \\ \vdots & \\ N_k + (N_{k+1} - N_k)(\eta - k) & \eta \in [k, k+1] \\ \vdots & \\ N_{P-1}(P - \eta) & \eta \in [P-1, P] \end{cases} \quad (3.2.20)$$

From the rank function we can compute the Fourier coefficients as defined in eq.(3.1.8)

$$\begin{aligned}
 a_k &= \frac{1}{P} \sum_{j=0}^{P-1} \int_j^{j+1} [N_j + (N_{j+1} - N_j)(\eta - j)] \sin\left(\frac{k\pi\eta}{P}\right) d\eta, \quad \text{with } N_0 = N_P = 0, \\
 a_k &= \frac{1}{\pi^2 k^2} \sum_{j=0}^{P-1} k\pi \left[N_j \cos\left(\frac{k\pi j}{P}\right) - N_{j+1} \cos\left(\frac{k\pi(j+1)}{P}\right) \right] + \\
 &P(N_{j+1} - N_j) \left[\sin\left(\frac{k\pi(j+1)}{P}\right) - \sin\left(\frac{k\pi j}{P}\right) \right]. \quad (3.2.21)
 \end{aligned}$$

The first line of a_k sums to zero. The second line, can be rewritten as

$$a_k = \frac{P}{\pi^2 k^2} \sum_{j=0}^{P-1} F_j \sin\left(\frac{k\pi j}{P}\right), \quad (3.2.22)$$

where $F_j = 2N_j - N_{j+1} - N_{j-1}$ —here we used the *balanced* character of the quiver. Plugging this into (3.2.19) we obtain our general formula for the holographic central charge to be

$$\begin{aligned}
 c_{hol} &= \frac{P^2}{8\pi^3} \sum_{k=1}^{\infty} \sum_{j,l=0}^{P-1} \frac{F_j F_l}{k^3} \sin\left(\frac{k\pi j}{P}\right) \sin\left(\frac{k\pi l}{P}\right) \\
 &= -\frac{P^2}{32\pi^3} \sum_{k=1}^{\infty} \sum_{j,l=0}^{P-1} \frac{F_j F_l}{k^3} \left(e^{\frac{i\pi k}{P}(j+l)} + e^{-\frac{i\pi k}{P}(j+l)} - e^{\frac{i\pi k}{P}(j-l)} - e^{-\frac{i\pi k}{P}(j-l)} \right) \\
 &= -\frac{P^2}{16\pi^3} \sum_{j,l=0}^{P-1} F_j F_l \text{Re} \left[\text{Li}_3 \left(e^{\frac{i\pi k}{P}(j+l)} \right) - \text{Li}_3 \left(e^{\frac{i\pi k}{P}(j-l)} \right) \right]. \quad (3.2.23)
 \end{aligned}$$

This expression should be compared with equation (70) in the work [143], see also [150]. The authors of [143] derived a generic expression for the Free Energy on a three-sphere of a balanced quiver using localisation and matrix model methods. Just like it occurs in different dimensions, the holographic central charge is proportional to the Free Energy of the CFT on a sphere.

In what follows, we will discuss some illustrative examples of balanced quivers. We will start giving the rank function, compute the Fourier coefficients, the brane charges and the linking numbers of the brane system. We will precisely calculate the holographic central charge emphasising the scaling with the various parameters of the CFT.

3.3 Some examples

The explicit discussion of examples gives the interested reader a better understanding of the formalism we developed. Also, it allows a more intuitive comprehension of the field theory kinematic and dynamical aspects. Below, we compute the various quantities for which we derived generic expressions in the previous sections. We discuss these quantities in examples of increasing level of sophistication.

3.3.1 Generic triangular rank function

Our first example is described by the rank function

$$\mathcal{R}(\eta) = \begin{cases} N\eta & 0 \leq \eta \leq S \\ \frac{NS}{(P-S)}(P-\eta) & S \leq \eta \leq P, \end{cases}$$

where we require $N/(P-S)$ to be integer, this condition will be needed to have properly quantised Page charges. The first derivative of the rank function is

$$\mathcal{R}'(\eta) = \begin{cases} N & 0 \leq \eta \leq S \\ -\frac{NS}{(P-S)} & S \leq \eta \leq P, \end{cases}$$

and $\mathcal{R}'' = \frac{NP}{(P-S)}\delta(\eta - S)$. The quiver and Hanany–Witten set-up associated with the rank function are given in Figure 3.2.

The charge of D3 and D5 in each interval can be read from the rank function and its

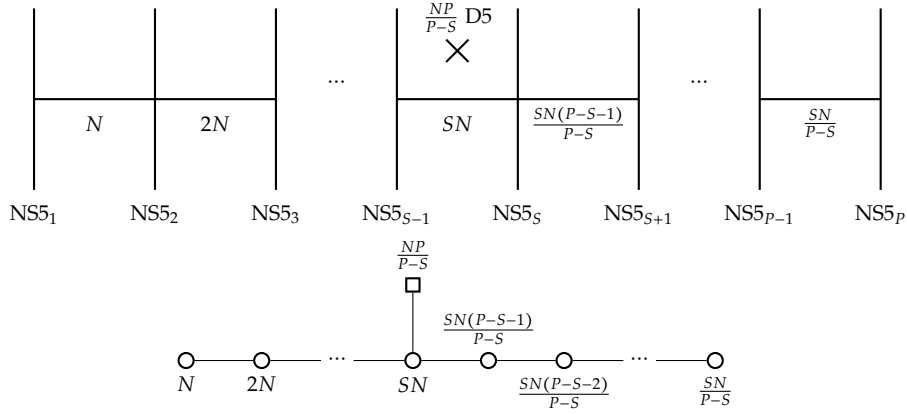


Figure 3.2. The Hanany–Witten and quiver associated with a generic triangular rank function. As usual, vertical lines represent NS-five branes. Horizontal lines and circular nodes denote D3 branes and crosses and square nodes indicate D5 branes.

second derivative. The total number of branes follows from eq.(3.2.11)

$$Q_{D3}^{\text{total}} = \int_0^P \mathcal{R}(\eta) d\eta = \sum_{j=1}^S jN + \sum_{j=1}^{P-S} \frac{NS}{(P-S)} (P-S-j) = \frac{NPS}{2}, \quad (3.3.1)$$

$$Q_{D5}^{\text{total}} = \mathcal{R}'(0) - \mathcal{R}'(P) = \frac{PN}{(P-S)}, \quad Q_{NS5}^{\text{total}} = P.$$

For this family of quivers we calculate the Fourier coefficient of the rank function using eqs.(3.1.8), (3.2.21). We find,

$$a_k = \frac{NP^2}{(P-S)\pi^2 k^2} \sin\left(\frac{k\pi S}{P}\right). \quad (3.3.2)$$

The linking numbers can be computed using the definitions in eq.(3.2.12), the Hanany–Witten set-up of Figure 3.2, and the holographic expressions in eq.(3.2.13),

$$\hat{L}_{NS5_1} = \hat{L}_{NS5_2} = \dots = \hat{L}_{NS5_P} = \mathcal{R}'(0) = N, \quad (3.3.3)$$

$$L_{D5_1} = L_{D5_2} = \dots = L_{D5_{PN/(P-S)}} = P - i = P - S.$$

These values satisfy the relation in eq.(3.2.14), $\sum_{NS5} \hat{L}_i = \sum_{D5} L_j = NP$. These numbers define two partitions of $\hat{N} = NP$,

$$\hat{\rho} = (N, N, N, N, \dots, N) = ([N]^P), \quad \rho = (P-S, P-S, \dots, P-S) = \left([P-S]^{\frac{PN}{(P-S)}}\right), \quad (3.3.4)$$

and the quiver in Figure 3.2 represents the theory $T_{\hat{\rho}}^{\hat{\rho}}[\text{SU}(NP)]$.

We can compute the holographic central charge using eq.(3.2.19) and the Fourier coefficient in eq.(3.3.2),

$$c_{hol} = \frac{N^2 P^4}{32\pi^3 (P-S)^2} \left[2\zeta(3) - 2\text{Re} \text{Li}_3\left(e^{\frac{2\pi i S}{P}}\right) \right]. \quad (3.3.5)$$

This family of quivers have some interesting special cases. Indeed, consider the case $S = (P - 1)$, the expressions derived in eqs.(3.3.1)-(3.3.5) are valid. Interestingly, in the holographic limit (P being very large), we find

$$\lim_{P \rightarrow \infty} c_{hol} = \frac{N^2 P^2}{8\pi} \log P. \quad (3.3.6)$$

Another interesting case is the ‘symmetric quiver’ for which $2S = P$. In this case we find,

$$\lim_{P \rightarrow \infty} c_{hol} = \frac{7N^2 P^2}{16\pi^3} \zeta(3). \quad (3.3.7)$$

It is also interesting the case in which S is some fixed integer, not scaling with P . The holographic limit for this situation gives,

$$\lim_{P \rightarrow \infty} c_{hol} = \frac{N^2 S^2}{8\pi} \log(P). \quad (3.3.8)$$

The expression of the holographic central charge and its limiting cases clearly display the non-perturbative character of the result. Let us analyse a more elaborated example.

3.3.2 Generic trapezoidal rank function

The rank function corresponding to this more sophisticated example is,

$$\mathcal{R}(\eta) = \begin{cases} N\eta & 0 \leq \eta \leq M \\ NM & M \leq \eta \leq M+S \\ \frac{MN}{Q}(M+S+Q-\eta) & M+S \leq \eta \leq M+S+Q. \end{cases}$$

In this case $P = M + S + Q$ and we also require that MN is a even multiple of Q . The second derivative of the rank function is

$$\mathcal{R}'' = N\delta(\eta - M) + \frac{MN}{Q}\delta(\eta - S - M). \quad (3.3.9)$$

The quiver and Hanany–Witten set-up associated with the rank function are given in Figure 3.3. The reader can check that for both examples the balanced-quiver condition is satisfied. Let us perform the same calculations we did in the previous example.

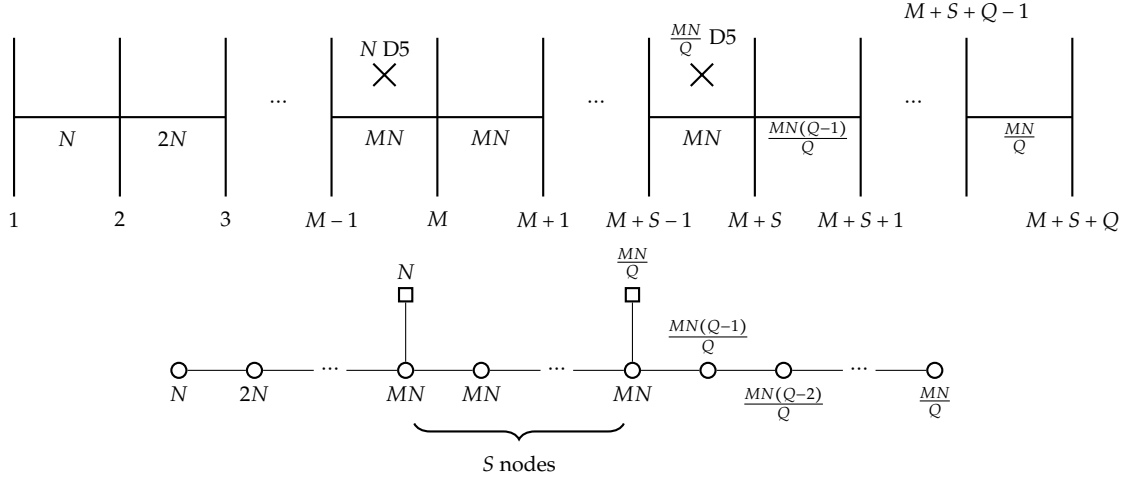


Figure 3.3. The Hanany–Witten set-up and the associated quiver for the trapezoidal rank function. The conventions are those described previously.

The charges of D3 and D5 in each interval can be read from the rank function and its second derivative. The total number of branes follow from eq.(3.2.11)

$$\begin{aligned}
 Q_{D3}^{\text{total}} &= \int_0^P \mathcal{R}(\eta) d\eta = \sum_{j=1}^M jN + NMS + \sum_{j=1}^{Q-1} \frac{NM}{Q} (Q-j) = \frac{NM}{2} (P+S) \\
 Q_{D5}^{\text{total}} &= \mathcal{R}'(0) - \mathcal{R}'(P) = N + \frac{MN}{Q}, \quad Q_{NS5_5}^{\text{total}} = P = M + S + Q.
 \end{aligned} \tag{3.3.10}$$

We calculate the Fourier coefficient of the rank function using eq.(3.2.21). We find,

$$a_k = \frac{NP}{Q\pi^2 k^2} \left[Q \sin\left(\frac{k\pi M}{P}\right) + M \sin\left(\frac{k\pi(M+S)}{P}\right) \right]. \tag{3.3.11}$$

The linking numbers can be computed using the definitions in eq.(3.2.12), the Hanany–Witten set-up of Figure 3.3, and the holographic expressions in eq.(3.2.13),

$$\begin{aligned}
 \hat{L}_{NS5_1} &= \hat{L}_{NS5_2} = \dots = \hat{L}_{NS5_P} = \mathcal{R}'(0) = N, \\
 L_{D5_1} &= L_{D5_2} = \dots L_{D5_N} = P - i = (S+Q), \\
 L_{D51'} &= L_{D52'} = \dots = L_{D5'_{MN/Q}} = P - i = Q.
 \end{aligned} \tag{3.3.12}$$

We have two stacks of D5 branes (distinguished by a 'symbol). These are located at $i = M$ and $i' = M + S$. These values for the linking numbers satisfy the relation in eq.(3.2.14),

$\sum_{NS5} \hat{L}_i = \sum_{D5} L_j = N(M + S + Q) = PN$. These numbers define two partitions of $\hat{N} = NP$,

$$\begin{aligned}\hat{\rho} &= (N, N, N, N, \dots, N) = ([N]^P), \\ \rho &= (S + Q, S + Q, \dots, S + Q; Q, Q, \dots, Q) = \left([S + Q]^N; [Q]^{\frac{MN}{Q}} \right),\end{aligned}$$

and the quiver in Figure 3.3 represents the theory $T_\rho^{\hat{\rho}}[\text{SU}(N(M + S + Q))]$.

We can compute the holographic central charge using eq.(3.2.19) and the Fourier coefficient in eq.(3.3.11),

$$\begin{aligned}c_{hol} &= \frac{N^2(M + Q + S)^2}{16\pi^3 Q^2} \text{Re} \left[(M^2 + Q^2) \zeta(3) - Q^2 \text{Li}_3 \left(e^{\frac{2\pi i M}{P}} \right) - M^2 \text{Li}_3 \left(e^{\frac{2i\pi(M+S)}{P}} \right) \right. \\ &\quad \left. - 2MQ \text{Li}_3 \left(e^{\frac{i\pi(2M+S)}{P}} \right) + 2MQLi_3 \left(e^{\frac{i\pi S}{P}} \right) \right].\end{aligned}\quad (3.3.13)$$

The holographic limit ($P = M + Q + S$ being very large) is more subtle than in the previous example as we can take M very large, keeping fixed Q, S and the other two combinations. We find

$$\begin{aligned}\lim_{M \rightarrow \infty} c_{hol} &= \frac{N^2 M^2}{8\pi} \log(M), \quad Q, S \text{ are fixed.} \\ \lim_{S \rightarrow \infty} c_{hol} &= \frac{N^2 M^2}{8\pi} \log(S^2), \quad Q, M \text{ are fixed.} \\ \lim_{Q \rightarrow \infty} c_{hol} &= \frac{N^2 M^2}{8\pi} \log(Q), \quad M, S \text{ are fixed.}\end{aligned}$$

Another interesting situation is the ‘symmetric quiver’ for which $Q = M$ and $P = 2Q + S$. In this case we find,

$$\begin{aligned}c_{hol} &= \frac{N^2(2Q + S)^2}{32\pi^3} \text{Re} \left[7\zeta(3) - 2\text{Li}_3 \left(e^{\frac{2\pi i Q}{P}} \right) - 2\text{Li}_3 \left(e^{\frac{2i\pi(Q+S)}{P}} \right) + 4\text{Li}_3 \left(e^{\frac{i\pi S}{P}} \right) \right]. \\ \lim_{Q \rightarrow \infty} c_{hol} &= \frac{7}{4\pi^3} Q^2 N^2 \zeta(3), \quad S \text{ is fixed.} \\ \lim_{S \rightarrow \infty} c_{hol} &= \frac{N^2 Q^2}{4\pi} \log(S), \quad Q \text{ is fixed.}\end{aligned}\quad (3.3.14)$$

As a consistency check, notice that the second result in eq.(3.3.14) is the same as that in eq.(3.3.7) for $Q = \frac{P}{2}$ and $S = 0$.

3.4 Mirror Symmetry

Many 3d $\mathcal{N} = 4$ gauge theories enjoy a duality known as mirror symmetry [3, 151]. Our goal in this section is to provide a holographic perspective on mirror symmetry through some of the machinery introduced in the previous sections. In order to keep the discussion self-contained, we will proceed by recalling relevant aspects of 3d $\mathcal{N} = 4$ supersymmetry and introduce the notion of mirror symmetry. We will then go over how mirror symmetry is derived from the Hanany–Witten setup by studying a specific example and provide consistency checks from holography, by matching the holographic central charges of the mirror pair.

The 3d $\mathcal{N} = 4$ supersymmetry algebra admits two short representations known as vector multiplets and hypermultiplets respectively. The bosonic components of a vector multiplet include a gauge field and 3 real scalars, while the bosonic fields in a hypermultiplet are comprised of two complex (or four real) scalars. Under the $SU(2)_C \times SU(2)_H$ R-symmetry, the scalars in the vector multiplet form a $(\mathbf{3}, \mathbf{1})$, while the hypermultiplet scalars form a $(\mathbf{1}, \mathbf{2})$. A 3d $\mathcal{N} = 4$ gauge theory is specified by a choice of gauge group G , to which one associates a vector multiplet in the adjoint representation of G , as well as choice of matter content, specified by hypermultiplets transforming in representation ρ of G . Since Maxwell’s theory in 3d is dual to a periodic scalar, one can trade out the gauge field component of a free vector multiplet with another scalar field. Upon doing so, the field content of a vector multiplet and hypermultiplet now become almost indistinguishable.² The only way one can tell them apart is by their transformation under the R-symmetry group, and the dualised vector multiplet is referred to as a twisted hypermultiplet. This may be viewed as a precursor, or hint of mirror symmetry; mirror symmetry is a non-trivial generalisation of this curious observation about free vector multiplets and hypermultiplets, but now applied to interacting quantum field theories. The moduli space of vacua of a 3d $\mathcal{N} = 4$ theory is generically comprised of a Coulomb branch \mathcal{M}_C , a Higgs branch \mathcal{M}_H and a mixed branch \mathcal{M}_{mix} . The Higgs branch, parameterised by VEVs of scalars in the hypermultiplet, is protected by a holomorphic non-renormalisation theorem [152], and as such is classically exact. The Coulomb branch is classically parameterised by VEVs of scalars in the twisted hypermultiplet, which are the coordinates of the Coulomb branch at large VEVs. However in the quantum theory one has to replace the complex scalar built out of one of the 3 scalars and the dual photon by a BPS monopole operator. Denoting by n_h and n_v the number of hypermultiplets and vector multiplets respectively, the quaternionic dimension of the Higgs and Coulomb branches for

²One might be worried about the fact that the dual scalar is a compact scalar. Indeed the dual photon is an S^1 -valued scalar, where the radius of the S^1 is proportional to the gauge coupling g^2 . However, in the infra-red limit $g^2 \rightarrow \infty$ this scalar decompactifies and one has 4 real-valued scalars in the vectormultiplet.

a generic linear quiver (3.2.20) are given by

$$\begin{aligned} \dim(\mathcal{M}_C) &= n_v = \sum_{i=1}^{P-1} N_i^2; \\ \dim(\mathcal{M}_H) &= n_h - n_v = \sum_{i=1}^{P-1} N_i F_i + \sum_{i=1}^{P-2} N_i N_{i+1} - \sum_{i=1}^{P-1} N_i^2, \end{aligned} \quad (3.4.1)$$

where in the second line, the first sum is the contribution of fundamental hypers attached to each node, whereas the second sum counts bi-fundamental hypers between neighbouring gauge nodes. Gauge theories in 3d enjoy a topological or magnetic symmetry associated with the current

$$J_{\text{top}} = \star \text{tr}(F), \quad (3.4.2)$$

whose conservation follows from the Bianchi identity. For quiver theories of the type we are interested in (3.2.20), there is one such conserved current for each gauge group factor and so the magnetic symmetry is classically $G_C^{\text{cl}} = \text{U}(1)^{P-1}$, while the flavour symmetry is given by $G_H = \text{S} \left[\prod_{i=1}^{P-1} \text{U}(F_i) \right]$, together with the R-symmetry the full classical 0-form global symmetry of quiver theories of the type (3.2.20) is

$$\text{U}(1)^{P-1} \times \text{S} \left[\prod_{i=1}^{P-1} \text{U}(F_i) \right] \times \text{SU}(2)_C \times \text{SU}(2)_H. \quad (3.4.3)$$

In the quantum theory, the magnetic symmetry can be enhanced to a non-abelian symmetry. In [121] Gaiotto and Witten conjectured the pattern of enhancement of the magnetic symmetry by analysing the monopole spectrum. Their conjecture states that for a quiver of the type in eq.(3.2.20), whenever a chain of n_i adjacent nodes are balanced, there is an enhancement of the form $\text{U}(1)^{n_i} \subset \text{SU}(n_i + 1)$. Hence the full quantum 0-form symmetry of such quivers takes the form

$$\text{U}(1)^{P-1 - \sum_{I \in B} n_I} \times \prod_{I \in B} \text{SU}(n_I + 1) \times \text{S} \left[\prod_{i=1}^{P-1} \text{U}(F_i) \right] \times \text{SU}(2)_C \times \text{SU}(2)_H, \quad (3.4.4)$$

where the index I takes values in the set B of chains of balanced nodes. Mirror symmetry then relates pairs of 3d $\mathcal{N} = 4$ theories where the flavour symmetry on one side is manifest as the magnetic or topological symmetry on the magnetic side. Moreover the two R-symmetry factors as well as the Coulomb and Higgs branches are also exchanged under mirror symmetry.

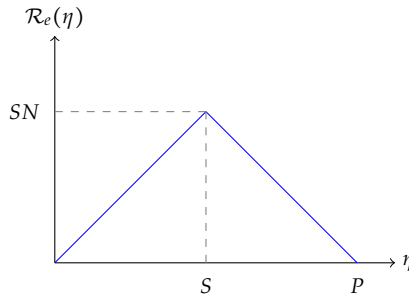
From the type IIB perspective, mirror symmetry is a consequence of S-duality [146]. The flavour symmetry of the low energy 3d theory is given by the gauge symmetry on the D5s, while its topological symmetry in the string embedding corresponds to the gauge symmetry

3.4.1 Geometry and Mirror Symmetry

In other formulations of holographic duals to $\mathcal{N} = 4$ three dimensional SCFTs, mirror symmetry manifests itself as S-duality. This is the case for the formulation of [142], [147], based on two holomorphic functions $\mathcal{A}_1, \mathcal{A}_2$. Our formulations corresponds to the choice $\mathcal{A}_2 \sim z$, and it is in this choice that the connection between S-duality and mirror symmetry fades away in our formulation. Indeed, one can check that by choosing $\mathcal{A}_1 \sim z$, one obtains the background S-dual to $\mathcal{A}_2 \sim z$. The goal of this section is to discuss how mirror symmetry is geometrically realised in the formulation presented in Section 3.1.

As in the rest of this work, we restrict to *balanced* quivers. Indeed, we discuss only the situation in which both the electric and the dual magnetic quivers are balanced. As we saw, this is possible only if there is only one flavour group, equivalently, only one stack of D5 branes, that have all the same linking numbers. These conditions imply that the rank function of the electric and mirror magnetic quivers are ‘triangular’.

Consider then, the (electric) quiver field theory described by a generic rank function studied in Section 3.3.1. We summarise it in eq.(3.4.9) to ease the reading.



$$; \quad \mathcal{R}_e(\eta) = \begin{cases} N\eta & \eta \in [0, S] \\ \frac{SN}{P-S}(P-\eta) & \eta \in [S, P] \end{cases} \quad (3.4.9)$$

Let us summarise some numbers (number of branes, vectors, hypers and dimension of the Higgs branch) characterising the electric description of this quiver (see also figure 3.2).

$$\begin{aligned} N_{NS5}^{(e)} &= P, \quad N_{D5}^{(e)} = \mathcal{R}'_e(0) - \mathcal{R}'_e(P) = \frac{PN}{P-S}, \quad N_{D3}^{(e)} = \int_0^P \mathcal{R}_e d\eta = \frac{NPS}{2}. \quad (3.4.10) \\ n_v^{(e)} &= \sum_{k=1}^S (Nk)^2 + \sum_{k=1}^{P-S-1} \left(\frac{SN}{P-S}(P-S-k) \right)^2 = \frac{N^2PS}{6P-6S}(1+2SP-2S^2), \\ n_h^{(e)} &= \sum_{k=1}^{S-1} N^2k(k+1) + \sum_{k=0}^{P-S-1} \left(\frac{SN}{P-S} \right)^2 (P-S-k)(P-S-k-1) + \frac{SPN^2}{(P-S)} = \\ &= \frac{N^2PS}{3P-3S}(2+SP-2S^2), \\ \dim \mathcal{M}_H^{(e)} &= n_h^{(e)} - n_v^{(e)} = \frac{N^2PS}{2P-2S}. \end{aligned}$$

This should not surprise us, as the holographic central charge (or the Free Energy) should coincide in both descriptions, namely

$$c_{hol}^{(e)} = \frac{\pi}{8} \sum_{k=1}^{\infty} k \left(a_k^{(e)} \right)^2 = \frac{\pi}{8} \sum_{k=1}^{\infty} k \left(a_k^{(m)} \right)^2 = c_{hol}^{(m)}.$$

Notice that, this also implies the equality of $\hat{W}_e(\sigma, \eta)$ and of $\hat{V}_e(\sigma, \eta)$ with their magnetic counterparts. We summarise these findings in eq.(3.4.14).

$$\begin{aligned} N_{NS5}^e &\leftrightarrow N_{D5}^m \\ N_{D5}^e &\leftrightarrow N_{NS5}^m \\ N_{D3}^e &\leftrightarrow \dim \mathcal{M}_H^m \\ \dim \mathcal{M}_H^e &\leftrightarrow N_{D3}^m \\ a_k^e ; c_{hol}^e &\leftrightarrow a_k^m ; c_{hol}^m \end{aligned} \tag{3.4.14}$$

3.4.2 A purely geometric formulation of mirror symmetry

With the restriction of having balanced quivers, both in the electric and the magnetic descriptions, we can formulate mirror symmetry purely in geometrical terms by observing an interesting scaling on the electric rank function. In fact, we scale the coordinate η and the intervals $[a, b]$ according to,

$$\eta \leftrightarrow \frac{N_{NS5}}{N_{D5}} \hat{\eta}, \quad [a, b] \leftrightarrow \left[\frac{N_{D5}}{N_{NS5}} a, \frac{N_{D5}}{N_{NS5}} b \right]. \tag{3.4.15}$$

Analysing this scaling for the electric rank function written in eq.(3.4.9), we find the magnetic rank function in eq.(3.4.11). Similarly, we can check that $a_k^{(e)} \leftrightarrow a_k^{(m)}$.

In other words, we could ‘ignore’ the existence of mirror symmetry, consider the electric rank function and perform the scaling in eq.(3.4.15). We recover the rank function and quiver for the second field theory. The D5 and NS5 branes get exchanged and the dimension of the Higgs branch is calculated by the number of D3 branes of the transformed theory. As a bonus, it is easy to see that both quiver field theories have the same $V(\sigma, \eta)$ and holographic central charge. The scaling in eq.(3.4.15) is simple and could be applied to other systems with similar description.

3.4.3 The scaling for generic rank functions

Let us study an interesting by-product of our picture of mirror symmetry.

Consider a generic rank function and apply the scaling in eq.(3.4.15). This will generically *not* produce the mirror dual. In fact, generically the mirror of a quiver is an unbalanced quiver, which is not described with the formalism we developed in this work. In other

words, for generic balanced quivers with ‘polygonal’ (rather than triangular) rank function, the scaling in eq.(3.4.15) generates another balanced quiver. This corresponds to a new CFT in which the role of NS5 and D5 branes is exchanged. The dimension of the Higgs branch of one theory is *not* calculated by the number of D3 branes in the transformed theory. Interestingly, both CFTs will share the same holographic central charge. Of course, this result might be a peculiarity of the holographic description and fail when $1/N$ corrections are taken into account. Let us consider an example to illustrate this point.

Consider a particular case of the second example of quivers discussed in Section 3.3.2. Choose $M = Q = 1, S = P - 2$. We have the quiver and rank function in eq.(3.4.16).

$$\begin{array}{c}
 \begin{array}{c}
 \square \\
 | \\
 \circ \\
 N
 \end{array}
 \quad
 \begin{array}{c}
 \square \\
 | \\
 \circ \\
 N
 \end{array}
 \quad
 \dots
 \quad
 \begin{array}{c}
 \square \\
 | \\
 \circ \\
 N
 \end{array}
 \\
 \underbrace{\hspace{10em}}_{P-1 \text{ nodes}}
 \end{array}
 ; \quad
 \mathcal{R}(\eta) = \begin{cases}
 N\eta & \eta \in [0, 1] \\
 N & \eta \in [1, P-1] \\
 N(P-\eta) & \eta \in [P-1, P]
 \end{cases}
 \quad (3.4.16)$$

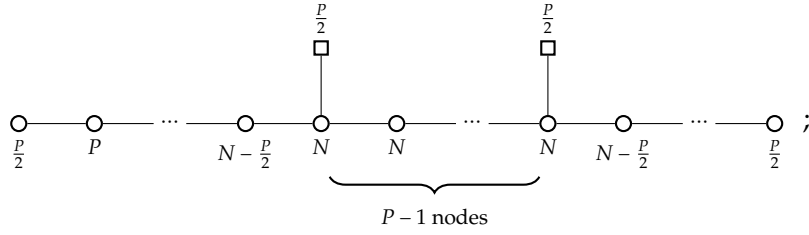
This implies the numbers,

$$\begin{aligned}
 Q_{NS5} &= P, \quad Q_{D5} = 2N, \quad Q_{D3} = N(P-1). & (3.4.17) \\
 n_v &= N^2(P-1), \quad n_h = N^2P, \quad \dim \mathcal{M}_H = n_h - n_v = N^2. \\
 a_k &= \frac{NP}{k^2\pi^2} \left[\sin\left(\frac{k\pi}{P}\right) + \sin\left(\frac{k\pi(P-1)}{P}\right) \right], \\
 c_{hol} &= \frac{N^2P^2}{32\pi^2} \operatorname{Re} \left(7\zeta(3) - 4\operatorname{Li}_3\left(e^{\frac{2\pi i}{P}}\right) + 4\operatorname{Li}_3\left(-e^{\frac{2\pi i}{P}}\right) \right).
 \end{aligned}$$

We perform the rescaling,

$$\eta \rightarrow \frac{P}{2N}\hat{\eta}, \quad [a, b] \rightarrow \left[\frac{2N}{P}a, \frac{2N}{P}b \right].$$

This generates a rank function and quiver depicted in eq.(3.4.18).



$$(3.4.18)$$

$$\hat{\mathcal{R}}(\hat{\eta}) = \begin{cases} \frac{P}{2}\hat{\eta} & \hat{\eta} \in [0, \frac{2N}{P}] \\ N & \hat{\eta} \in [\frac{2N}{P}, \frac{2N}{P}(P-1)] \\ \frac{P}{2}(2N - \hat{\eta}) & \hat{\eta} \in [\frac{2N}{P}(P-1), 2N] \end{cases}$$

In this theory we calculate,

$$\begin{aligned} \hat{Q}_{NS5} &= 2N, \quad \hat{Q}_{D5} = P, \quad \hat{N}_{D3} = \frac{2N^2}{P}(P-1), \\ \hat{n}_v &= 2 \sum_{k=1}^{2N/P-1} \left(N - \frac{kP}{2}\right)^2 + N^2 \left(1 + 2N \left(1 - \frac{2}{P}\right)\right) = \frac{N}{6P}(P^2 + 4N^2(3P-4)), \\ \hat{n}_h &= 2 \sum_{k=0}^{2N/P-2} \left(N - \frac{kP}{2}\right) \left(N - (k+1)\frac{P}{2}\right) + NP = \frac{2N}{3P}(P^2 + 2N^2), \\ \dim \hat{\mathcal{M}}_H &= N^3 \left(\frac{4}{P} - 2\right) + \frac{NP}{2}, \\ \hat{a}_k &= \frac{NP}{k^2\pi^2} \left[\sin\left(\frac{k\pi}{P}\right) + \sin\left(\frac{k\pi(P-1)}{P}\right) \right], \\ \hat{c}_{hol} &= \frac{N^2 P^2}{32\pi^2} \operatorname{Re} \left(7\zeta(3) - 4\operatorname{Li}_3\left(e^{\frac{2\pi i}{P}}\right) + 4\operatorname{Li}_3\left(-e^{\frac{2\pi i}{P}}\right) \right). \end{aligned}$$

Hence, we have two different theories, with the same central charge. In the case $P = 2$ both theories discussed above are mirror pair.

3.5 Summary

Let us start with a brief summary of the contents of this chapter.

In Section 3.1, we present a holographic formulation of $\mathcal{N} = 4$ $d = 3$ SCFTs describing the IR fixed point of balanced linear quivers of gauge group $\prod_{i=1}^{P-1} \mathrm{U}(N_i)$ and flavour group $\prod_{j=1}^{P-1} \mathrm{SU}(F_j)$. The type IIB configuration in eq.(3.1.1) include the presence of NS, D3 and D5 branes. Importantly, it is written in terms of a Potential function $V(\sigma, \eta)$ or equivalently $\hat{W}(\sigma, \eta)$. This function solves a Laplace partial differential equation. This PDE should be supplemented with boundary and initial conditions, hence defining an electrostatic problem.

It is in these initial conditions that the ‘kinematical’ data of the dual CFT is encoded. In the case we focused here, the quivers are balanced and the initial condition can be easily given in terms of a ‘rank function’ $\mathcal{R}(\eta)$. By quantising Page charges, we learn in Section 3.2 that the rank function must be a piecewise continuous and linear function. The values of $\mathcal{R}(\eta)$ at integer values of the coordinate must also be integer, as it is associated with the number of branes in the corresponding Hanany–Witten set-up.

Given a balanced linear quiver, we present a clear procedure to automatically write the dual Type IIB configuration. In this way, this work moves forward the project of giving an *electrostatic* description of all half-BPS $\text{AdS}_D \times S^2$ spaces in dimensions $D = 2, 3, 4, 5, 6, 7$. In some dimensions $D = 4$ (the case of interest in this work) and in $D = 6$, there is a pre-existent formulation in the bibliography, based on a coupled of holomorphic functions [142], [144]. We have clarified the map between our formulation and that of [142] in the original work which this chapter is based on [74].

Also in Section 3.2, we defined a quantity that counts the number of degrees of freedom of the QFT. This quantity is proportional to the Free Energy of the field theory on S^3 . We refer to it as holographic central charge. In Section 3.3, we worked out a set of examples and analysed the behaviour of the holographic central charge of these examples and special limits thereof. We make clear the non-perturbative character of the result, typically involving Polylogarithmic functions of order three in the parameters of the field theory.

In Section 3.4, we pedagogically presented various aspects of the QFTs with emphasis on Mirror symmetry. The way in which our holographic backgrounds display Mirror symmetry is discussed. We presented the mirror mapping between two holographic field theories and display the exchange of NS5 and D5 branes, the exchange of the dimensions of the Higgs and Coulomb branches (represented by the number of D3 branes in the system), the equality of the central charge and background for both descriptions, etc. As a byproduct of this analysis we discuss an operation that given a balanced quiver produces a different balanced one with the same holographic central charge as the original one.

Conclusions

In this thesis, we presented three independent, yet closely related lines of enquiry. In chapter 1, we explored the relationship between string theory and non-supersymmetric QFTs. We explored the world of magnetic quivers and 5d SCFTs in chapter 2. Finally, we presented the holographic duals to 3d $\mathcal{N} = 4$ linear quivers in chapter 3. Here we wish to discuss some potential future directions for research, prompted by these studies. Some of these are currently under investigation by the author.

It would be desirable to come up with a systematic algorithm to determine the magnetic quivers for brane webs which use an orientifold plane, similar to [69]. One might then hope to implement this algorithm into a computer program similar to what was done in [59]. In verifying the dualities between OSp and unitary quivers, it would be interesting to gather more evidence by matching quantities such as the sphere partition function or the superconformal index, similar to what was done in [153]. There is still no satisfactory path integral interpretation of non-simply-laced edges in 3d $\mathcal{N} = 4$ quivers. However, the ubiquity of these theories by now makes such an attempt a well motivated direction for future studies.

The electrostatic description of the holographic duals to 3d $\mathcal{N} = 4$ theories presented in chapter 3 opens new and interesting avenues for research, here is a non-exhaustive list:

- It seems natural to attempt to understand how our formalism can be extended/adapted to *non-balanced* quivers.
- Exploring other observables, for example Wilson loops in different representations and their behaviour under Mirror symmetry.
- It would be interesting to present a holographic description of the QFT with special-unitary (rather than unitary) gauge groups. This may follow the ideas of [154], probably using recent developments in higher form symmetries.
- Developing an analog description for circular quivers, following the work of [155].
- This work furthers the project of finding electrostatic description for holographic duals to linear quivers that flow to SCFTs_d , with $d = 1, 2, 3, 4, 5, 6$. It seems natural to study the relations among moduli spaces of these different SCFTs_d along the lines of [55–57].

- The program of relating half-BPS AdS-solutions and SCFTs needs more work, particularly in the cases of AdS_3 and AdS_2 . The methods developed here suggest new AdS_2 backgrounds that would be nice to study.

Bibliography

- [1] I. Bah, D. Freed, G. W. Moore, N. Nekrasov, S. S. Razamat, and S. Schäfer-Nameki, *Snowmass Whitepaper: Physical Mathematics 2021*, [arXiv:2203.05078](#).
- [2] A. Giveon and D. Kutasov, *Brane dynamics and gauge theory*, *Rev. Mod. Phys.* **71** (1999) 983–1084, [[hep-th/9802067](#)].
- [3] K. A. Intriligator and N. Seiberg, *Mirror symmetry in three-dimensional gauge theories*, *Phys. Lett. B* **387** (1996) 513–519, [[hep-th/9607207](#)].
- [4] A. Hanany and E. Witten, *Type IIB superstrings, BPS monopoles, and three-dimensional gauge dynamics*, *Nucl. Phys.* **B492** (1997) 152–190, [[hep-th/9611230](#)].
- [5] J. M. Maldacena, *The Large N limit of superconformal field theories and supergravity*, *Adv. Theor. Math. Phys.* **2** (1998) 231–252, [[hep-th/9711200](#)].
- [6] Z. Komargodski and N. Seiberg, *A symmetry breaking scenario for QCD₃*, *JHEP* **01** (2018) 109, [[arXiv:1706.08755](#)].
- [7] N. Seiberg, *Five-dimensional SUSY field theories, nontrivial fixed points and string dynamics*, *Phys.Lett.* **B388** (1996) 753–760, [[hep-th/9608111](#)].
- [8] K. A. Intriligator, D. R. Morrison, and N. Seiberg, *Five-dimensional supersymmetric gauge theories and degenerations of Calabi-Yau spaces*, *Nucl.Phys.* **B497** (1997) 56–100, [[hep-th/9702198](#)].
- [9] O. J. Ganor, D. R. Morrison, and N. Seiberg, *Branes, Calabi-Yau spaces, and toroidal compactification of the N=1 six-dimensional E(8) theory*, *Nucl. Phys.* **B487** (1997) 93–127, [[hep-th/9610251](#)].
- [10] A. Brandhuber and Y. Oz, *The D-4 - D-8 brane system and five-dimensional fixed points*, *Phys. Lett. B* **460** (1999) 307–312, [[hep-th/9905148](#)].
- [11] O. Aharony, A. Hanany, and B. Kol, *Webs of (p,q) five-branes, five-dimensional field theories and grid diagrams*, *JHEP* **9801** (1998) 002, [[hep-th/9710116](#)].
- [12] O. Aharony and A. Hanany, *Branes, superpotentials and superconformal fixed points*, *Nucl.Phys.* **B504** (1997) 239–271, [[hep-th/9704170](#)].
- [13] O. Bergman, D. Rodríguez-Gómez, and G. Zafrir, *Discrete θ and the 5d superconformal index*, *JHEP* **1401** (2014) 079, [[arXiv:1310.2150](#)].
- [14] O. Bergman, D. Rodríguez-Gómez, and G. Zafrir, *5-Brane Webs, Symmetry Enhancement, and Duality in 5d Supersymmetric Gauge Theory*, *JHEP* **03** (2014) 112, [[arXiv:1311.4199](#)].
- [15] O. Bergman and G. Zafrir, *Lifting 4d dualities to 5d*, *JHEP* **1504** (2015) 141, [[arXiv:1410.2806](#)].

- [16] O. Bergman and G. Zafrir, *5d fixed points from brane webs and O7-planes*, *JHEP* **12** (2015) 163, [[arXiv:1507.03860](#)].
- [17] G. Zafrir, *Brane webs and O5-planes*, *JHEP* **03** (2016) 109, [[arXiv:1512.08114](#)].
- [18] H. Hayashi, S.-S. Kim, K. Lee, M. Taki, and F. Yagi, *More on 5d descriptions of 6d SCFTs*, *JHEP* **10** (2016) 126, [[arXiv:1512.08239](#)].
- [19] G. Zafrir, *Brane webs, 5d gauge theories and 6d $\mathcal{N} = (1, 0)$ SCFT's*, *JHEP* **12** (2015) 157, [[arXiv:1509.02016](#)].
- [20] H. Hayashi, S.-S. Kim, K. Lee, and F. Yagi, *6d SCFTs, 5d Dualities and Tao Web Diagrams*, *JHEP* **05** (2019) 203, [[arXiv:1509.03300](#)].
- [21] G. Zafrir, *Brane webs in the presence of an O5⁻-plane and 4d class S theories of type D*, *JHEP* **07** (2016) 035, [[arXiv:1602.00130](#)].
- [22] H. Hayashi, S.-S. Kim, K. Lee, and F. Yagi, *Equivalence of several descriptions for 6d SCFT*, *JHEP* **01** (2017) 093, [[arXiv:1607.07786](#)].
- [23] H. Hayashi and G. Zoccarato, *Partition functions of web diagrams with an O7⁻-plane*, *JHEP* **03** (2017) 112, [[arXiv:1609.07381](#)].
- [24] H. Hayashi and K. Ohmori, *5d/6d DE instantons from trivalent gluing of web diagrams*, *JHEP* **06** (2017) 078, [[arXiv:1702.07263](#)].
- [25] H. Hayashi, S.-S. Kim, K. Lee, and F. Yagi, *Discrete theta angle from an O5-plane*, *JHEP* **11** (2017) 041, [[arXiv:1707.07181](#)].
- [26] H. Hayashi, S.-S. Kim, K. Lee, and F. Yagi, *5-brane webs for 5d $\mathcal{N} = 1$ G_2 gauge theories*, *JHEP* **03** (2018) 125, [[arXiv:1801.03916](#)].
- [27] H. Hayashi, S.-S. Kim, K. Lee, and F. Yagi, *Dualities and 5-brane webs for 5d rank 2 SCFTs*, *JHEP* **12** (2018) 016, [[arXiv:1806.10569](#)].
- [28] H. Hayashi, S.-S. Kim, K. Lee, and F. Yagi, *Rank-3 antisymmetric matter on 5-brane webs*, *JHEP* **05** (2019) 133, [[arXiv:1902.04754](#)].
- [29] H.-C. Kim, M. Kim, S.-S. Kim, and K.-H. Lee, *Bootstrapping BPS spectra of 5d/6d field theories*, *JHEP* **04** (2021) 161, [[arXiv:2101.00023](#)].
- [30] H.-C. Kim, S.-S. Kim, and K. Lee, *Gauging \mathbb{Z}_N Discrete Symmetry of 5d SCFTs*, [[arXiv:2112.14550](#)].
- [31] M. R. Douglas, S. H. Katz, and C. Vafa, *Small instantons, Del Pezzo surfaces and type I-prime theory*, *Nucl.Phys.* **B497** (1997) 155–172, [[hep-th/9609071](#)].
- [32] D. R. Morrison and N. Seiberg, *Extremal transitions and five-dimensional supersymmetric field theories*, *Nucl.Phys.* **B483** (1997) 229–247, [[hep-th/9609070](#)].
- [33] P. Jefferson, S. Katz, H.-C. Kim, and C. Vafa, *On Geometric Classification of 5d SCFTs*, *JHEP* **04** (2018) 103, [[arXiv:1801.04036](#)].

- [34] C. Closset, M. Del Zotto, and V. Saxena, *Five-dimensional SCFTs and gauge theory phases: an M-theory/type IIA perspective*, [arXiv:1812.10451](#).
- [35] L. Bhardwaj, *On the classification of 5d SCFTs*, [arXiv:1909.09635](#).
- [36] F. Apruzzi, S. Schafer-Nameki, and Y.-N. Wang, *5d SCFTs from Decoupling and Gluing*, [arXiv:1912.04264](#).
- [37] L. Bhardwaj and G. Zafrir, *Classification of 5d $\mathcal{N} = 1$ gauge theories*, *JHEP* **12** (2020) 099, [[arXiv:2003.04333](#)].
- [38] J. Tian and Y.-N. Wang, *5D and 6D SCFTs from \mathbb{C}^3 orbifolds*, [arXiv:2110.15129](#).
- [39] B. Acharya, N. Lambert, M. Najjar, E. E. Svanes, and J. Tian, *Gauging Discrete Symmetries of T_N -theories in Five Dimensions*, [arXiv:2110.14441](#).
- [40] O. Bergman, D. Rodríguez-Gómez, and C. F. Uhlemann, *Testing AdS_6/CFT_5 in Type IIB with stringy operators*, *JHEP* **08** (2018) 127, [[arXiv:1806.07898](#)].
- [41] M. Fluder and C. F. Uhlemann, *Precision Test of AdS_6/CFT_5 in Type IIB String Theory*, *Phys. Rev. Lett.* **121** (2018), no. 17 171603, [[arXiv:1806.08374](#)].
- [42] J. Kaidi and C. F. Uhlemann, *M-theory curves from warped AdS_6 in Type IIB*, *JHEP* **11** (2018) 175, [[arXiv:1809.10162](#)].
- [43] C. F. Uhlemann, *AdS_6/CFT_5 with $O7$ -planes*, *JHEP* **04** (2020) 113, [[arXiv:1912.09716](#)].
- [44] C. F. Uhlemann, *Exact results for 5d SCFTs of long quiver type*, *JHEP* **11** (2019) 072, [[arXiv:1909.01369](#)].
- [45] A. Legramandi and C. Nunez, *Electrostatic Description of Five-dimensional SCFTs*, [arXiv:2104.11240](#).
- [46] A. Legramandi and C. Nunez, *Holographic description of $SCFT_5$ compactifications*, [arXiv:2109.11554](#).
- [47] J. Gray, A. Hanany, Y.-H. He, V. Jejjala, and N. Mekareeya, *SQCD: A Geometric Apercu*, *JHEP* **05** (2008) 099, [[arXiv:0803.4257](#)].
- [48] A. Hanany and N. Mekareeya, *Counting Gauge Invariant Operators in SQCD with Classical Gauge Groups*, *JHEP* **10** (2008) 012, [[arXiv:0805.3728](#)].
- [49] O. DeWolfe, T. Hauer, A. Iqbal, and B. Zwiebach, *Uncovering the symmetries on $[p, q]$ seven-branes: Beyond the Kodaira classification*, *Adv.Theor.Math.Phys.* **3** (1999) 1785–1833, [[hep-th/9812028](#)].
- [50] O. DeWolfe, T. Hauer, A. Iqbal, and B. Zwiebach, *Uncovering infinite symmetries on $[p, q]$ 7-branes: Kac-Moody algebras and beyond*, *Adv.Theor.Math.Phys.* **3** (1999) 1835–1891, [[hep-th/9812209](#)].
- [51] O. DeWolfe, A. Hanany, A. Iqbal, and E. Katz, *Five-branes, seven-branes and five-dimensional $E(n)$ field theories*, *JHEP* **03** (1999) 006, [[hep-th/9902179](#)].

- [52] H.-C. Kim, S.-S. Kim, and K. Lee, *5-dim Superconformal Index with Enhanced E_n Global Symmetry*, *JHEP* **1210** (2012) 142, [[arXiv:1206.6781](#)].
- [53] F. Apruzzi, C. Lawrie, L. Lin, S. Schäfer-Nameki, and Y.-N. Wang, *Fibers add Flavor, Part I: Classification of 5d SCFTs, Flavor Symmetries and BPS States*, *JHEP* **11** (2019) 068, [[arXiv:1907.05404](#)].
- [54] G. Ferlito, A. Hanany, N. Mekareeya, and G. Zafrir, *3d Coulomb branch and 5d Higgs branch at infinite coupling*, *JHEP* **07** (2018) 061, [[arXiv:1712.06604](#)].
- [55] M. Akhond, F. Carta, S. Dwivedi, H. Hayashi, S.-S. Kim, and F. Yagi, *Five-brane webs, Higgs branches and unitary/orthosymplectic magnetic quivers*, [arXiv:2008.01027](#).
- [56] M. Akhond, F. Carta, S. Dwivedi, H. Hayashi, S.-S. Kim, and F. Yagi, *Factorised 3d $\mathcal{N} = 4$ orthosymplectic quivers*, [arXiv:2101.12235](#).
- [57] M. Akhond and F. Carta, *Magnetic quivers from brane webs with $O7^+$ -planes*, [arXiv:2107.09077](#).
- [58] M. van Beest, A. Bourget, J. Eckhard, and S. Schafer-Nameki, *(5d RG-flow) Trees in the Tropical Rain Forest*, [arXiv:2011.07033](#).
- [59] M. van Beest, A. Bourget, J. Eckhard, and S. Schafer-Nameki, *(Symplectic) Leaves and (5d Higgs) Branches in the Poly(go)nesian Tropical Rain Forest*, [arXiv:2008.05577](#).
- [60] M. van Beest and S. Giacomelli, *Connecting 5d Higgs Branches via Fayet-Iliopoulos Deformations*, [arXiv:2110.02872](#).
- [61] A. Bourget, S. Cabrera, J. F. Grimminger, A. Hanany, and Z. Zhong, *Brane Webs and Magnetic Quivers for SQCD*, *JHEP* **03** (2020) 176, [[arXiv:1909.00667](#)].
- [62] A. Bourget, J. F. Grimminger, A. Hanany, M. Sperling, G. Zafrir, and Z. Zhong, *Magnetic quivers for rank 1 theories*, [arXiv:2006.16994](#).
- [63] A. Bourget, J. F. Grimminger, A. Hanany, M. Sperling, and Z. Zhong, *Magnetic Quivers from Brane Webs with $O5$ Planes*, [arXiv:2004.04082](#).
- [64] A. Bourget, S. Giacomelli, J. F. Grimminger, A. Hanany, M. Sperling, and Z. Zhong, *S-fold magnetic quivers*, [arXiv:2010.05889](#).
- [65] A. Bourget, J. F. Grimminger, A. Hanany, R. Kalveks, M. Sperling, and Z. Zhong, *Magnetic Lattices for Orthosymplectic Quivers*, [arXiv:2007.04667](#).
- [66] A. Bourget, J. F. Grimminger, A. Hanany, R. Kalveks, M. Sperling, and Z. Zhong, *Folding Orthosymplectic Quivers*, [arXiv:2107.00754](#).
- [67] C. Closset, S. Giacomelli, S. Schäfer-Nameki, and Y.-N. Wang, *5d and 4d SCFTs: Canonical Singularities, Trinions and S-Dualities*, [arXiv:2012.12827](#).
- [68] C. Closset, S. Schafer-Nameki, and Y.-N. Wang, *Coulomb and Higgs Branches from Canonical Singularities: Part 0*, [arXiv:2007.15600](#).
- [69] S. Cabrera, A. Hanany, and M. Sperling, *Magnetic quivers, Higgs branches, and 6d $\mathcal{N}=(1,0)$ theories*, *JHEP* **06** (2019) 071, [[arXiv:1904.12293](#)]. [Erratum: *JHEP* **07**, 137 (2019)].

- [70] F. Carta, S. Giacomelli, N. Mekareeya, and A. Mininno, *Conformal Manifolds and 3d Mirrors of Argyres-Douglas theories*, [arXiv:2105.08064](#).
- [71] S. Elitzur, A. Giveon, and D. Kutasov, *Branes and $N=1$ duality in string theory*, *Phys. Lett.* **B400** (1997) 269–274, [[hep-th/9702014](#)].
- [72] A. Giveon and D. Kutasov, *Seiberg Duality in Chern-Simons Theory*, *Nucl. Phys.* **B812** (2009) 1–11, [[arXiv:0808.0360](#)].
- [73] M. Akhond, A. Armoni, and S. Speziali, *Phases of $U(N_c)$ QCD_3 from Type 0 Strings and Seiberg Duality*, *JHEP* **09** (2019) 111, [[arXiv:1908.04324](#)].
- [74] M. Akhond, A. Legramandi, and C. Nunez, *Electrostatic description of 3d $N = 4$ linear quivers*, *JHEP* **11** (2021) 205, [[arXiv:2109.06193](#)].
- [75] O. Aharony, G. Gur-Ari, and R. Yacoby, *$d=3$ Bosonic Vector Models Coupled to Chern-Simons Gauge Theories*, *JHEP* **03** (2012) 037, [[arXiv:1110.4382](#)].
- [76] S. Giombi, S. Minwalla, S. Prakash, S. P. Trivedi, S. R. Wadia, and X. Yin, *Chern-Simons Theory with Vector Fermion Matter*, *Eur. Phys. J.* **C72** (2012) 2112, [[arXiv:1110.4386](#)].
- [77] O. Aharony, *Baryons, monopoles and dualities in Chern-Simons-matter theories*, *JHEP* **02** (2016) 093, [[arXiv:1512.00161](#)].
- [78] P.-S. Hsin and N. Seiberg, *Level/rank Duality and Chern-Simons-Matter Theories*, *JHEP* **09** (2016) 095, [[arXiv:1607.07457](#)].
- [79] A. Karch and D. Tong, *Particle-Vortex Duality from 3d Bosonization*, *Phys. Rev.* **X6** (2016), no. 3 031043, [[arXiv:1606.01893](#)].
- [80] J. Murugan and H. Nastase, *Particle-vortex duality in topological insulators and superconductors*, *JHEP* **05** (2017) 159, [[arXiv:1606.01912](#)].
- [81] T. Appelquist and D. Nash, *Critical Behavior in (2+1)-dimensional QCD*, *Phys. Rev. Lett.* **64** (1990) 721.
- [82] A. Armoni, T. T. Dumitrescu, G. Festuccia, and Z. Komargodski, *Metastable Vacua in Large- N QCD_3* , [arXiv:1905.01797](#).
- [83] A. Armoni and V. Niarchos, *Phases of QCD_3 from Non-SUSY Seiberg Duality and Brane Dynamics*, *Phys. Rev.* **D97** (2018), no. 10 106001, [[arXiv:1711.04832](#)].
- [84] K. Jensen and A. Karch, *Embedding three-dimensional bosonization dualities into string theory*, *JHEP* **12** (2017) 031, [[arXiv:1709.07872](#)].
- [85] R. Argurio, M. Bertolini, F. Bigazzi, A. L. Cotrone, and P. Niro, *QCD domain walls, Chern-Simons theories and holography*, *JHEP* **09** (2018) 090, [[arXiv:1806.08292](#)].
- [86] S. Kachru, M. Mulligan, G. Torroba, and H. Wang, *Nonsupersymmetric dualities from mirror symmetry*, *Phys. Rev. Lett.* **118** (2017), no. 1 011602, [[arXiv:1609.02149](#)].
- [87] G. Gur-Ari and R. Yacoby, *Three Dimensional Bosonization From Supersymmetry*, *JHEP* **11** (2015) 013, [[arXiv:1507.04378](#)].

- [88] A. Armoni, M. Shifman, and G. Veneziano, *Exact results in non-supersymmetric large N orientifold field theories*, *Nucl. Phys.* **B667** (2003) 170–182, [[hep-th/0302163](#)].
- [89] A. Armoni, M. Shifman, and G. Veneziano, *From superYang-Mills theory to QCD: Planar equivalence and its implications*, in *From fields to strings: Circumnavigating theoretical physics. Ian Kogan memorial collection (3 volume set)* (M. Shifman, A. Vainshtein, and J. Wheeler, eds.), pp. 353–444. 2004. [hep-th/0403071](#).
- [90] S. Murthy and J. Troost, *D-branes in non-critical superstrings and duality in $N=1$ gauge theories with flavor*, *JHEP* **10** (2006) 019, [[hep-th/0606203](#)].
- [91] A. Fotopoulos, V. Niarchos, and N. Prezas, *D-branes and SQCD in non-critical superstring theory*, *JHEP* **10** (2005) 081, [[hep-th/0504010](#)].
- [92] D. Israel and V. Niarchos, *Tree-Level Stability Without Spacetime Fermions: Novel Examples in String Theory*, *JHEP* **07** (2007) 065, [[arXiv:0705.2140](#)].
- [93] A. Armoni, D. Israel, G. Moraitis, and V. Niarchos, *Non-Supersymmetric Seiberg Duality, Orientifold QCD and Non-Critical Strings*, *Phys. Rev.* **D77** (2008) 105009, [[arXiv:0801.0762](#)].
- [94] C. Angelantonj and A. Sagnotti, *Open strings*, *Phys. Rept.* **371** (2002) 1–150, [[hep-th/0204089](#)]. [Erratum: *Phys. Rept.* 376, no. 6, 407 (2003)].
- [95] R. Blumenhagen, A. Font, and D. Lust, *Nonsupersymmetric gauge theories from D-branes in type 0 string theory*, *Nucl. Phys.* **B560** (1999) 66–92, [[hep-th/9906101](#)].
- [96] R. Blumenhagen, A. Font, and D. Lust, *Tachyon free orientifolds of type 0B strings in various dimensions*, *Nucl. Phys.* **B558** (1999) 159–177, [[hep-th/9904069](#)].
- [97] A. Sagnotti, *Surprises in open string perturbation theory*, *Nucl. Phys. Proc. Suppl.* **56B** (1997) 332–343, [[hep-th/9702093](#)].
- [98] A. Sagnotti, *Some properties of open string theories*, in *Supersymmetry and unification of fundamental interactions. Proceedings, International Workshop, SUSY 95, Palaiseau, France, May 15-19, 1995*, pp. 473–484, 1995. [hep-th/9509080](#).
- [99] M. Unsal and L. G. Yaffe, *(In)validity of large N orientifold equivalence*, *Phys. Rev.* **D74** (2006) 105019, [[hep-th/0608180](#)].
- [100] J. Polchinski, S. Chaudhuri, and C. V. Johnson, *Notes on D-branes*, [hep-th/9602052](#).
- [101] A. M. Uranga, *Comments on nonsupersymmetric orientifolds at strong coupling*, *JHEP* **02** (2000) 041, [[hep-th/9912145](#)].
- [102] I. R. Klebanov and A. A. Tseytlin, *D-branes and dual gauge theories in type 0 strings*, *Nucl. Phys.* **B546** (1999) 155–181, [[hep-th/9811035](#)].
- [103] N. J. Evans, C. V. Johnson, and A. D. Shapere, *Orientifolds, branes, and duality of 4-D gauge theories*, *Nucl. Phys.* **B505** (1997) 251–271, [[hep-th/9703210](#)].
- [104] A. Armoni and E. Ireson, *Level-rank duality in Chern–Simons theory from a non-supersymmetric brane configuration*, *Phys. Lett.* **B739** (2014) 387–390, [[arXiv:1408.4633](#)].

- [105] C. Córdova, P.-S. Hsin, and N. Seiberg, *Time-Reversal Symmetry, Anomalies, and Dualities in $(2+1)d$* , *SciPost Phys.* **5** (2018), no. 1 006, [[arXiv:1712.08639](#)].
- [106] S. Cremonesi, G. Ferlito, A. Hanany, and N. Mekareeya, *Coulomb Branch and The Moduli Space of Instantons*, *JHEP* **12** (2014) 103, [[arXiv:1408.6835](#)].
- [107] F. Benini, S. Benvenuti, and Y. Tachikawa, *Webs of five-branes and $N=2$ superconformal field theories*, *JHEP* **0909** (2009) 052, [[arXiv:0906.0359](#)].
- [108] F. Benini, Y. Tachikawa, and D. Xie, *Mirrors of 3d Sicilian theories*, *JHEP* **09** (2010) 063, [[arXiv:1007.0992](#)].
- [109] S. Cabrera, A. Hanany, and F. Yagi, *Tropical Geometry and Five Dimensional Higgs Branches at Infinite Coupling*, *JHEP* **01** (2019) 068, [[arXiv:1810.01379](#)].
- [110] S. Cremonesi, A. Hanany, and A. Zaffaroni, *Monopole operators and Hilbert series of Coulomb branches of 3d $\mathcal{N} = 4$ gauge theories*, *JHEP* **01** (2014) 005, [[arXiv:1309.2657](#)].
- [111] B. Feng and A. Hanany, *Mirror symmetry by O_3 planes*, *JHEP* **11** (2000) 033, [[hep-th/0004092](#)].
- [112] S. Benvenuti, B. Feng, A. Hanany, and Y.-H. He, *Counting BPS Operators in Gauge Theories: Quivers, Syzygies and Plethystics*, *JHEP* **11** (2007) 050, [[hep-th/0608050](#)].
- [113] B. Feng, A. Hanany, and Y.-H. He, *Counting gauge invariants: The Plethystic program*, *JHEP* **03** (2007) 090, [[hep-th/0701063](#)].
- [114] A. Hanany and R. Kalveks, *Highest Weight Generating Functions for Hilbert Series*, *JHEP* **10** (2014) 152, [[arXiv:1408.4690](#)].
- [115] O. Chacaltana and J. Distler, *Tinkertoys for the D_N series*, *JHEP* **02** (2013) 110, [[arXiv:1106.5410](#)].
- [116] J. Distler, B. Ergun, and F. Yan, *Product SCFTs in Class-S*, [[arXiv:1711.04727](#)].
- [117] J. Distler and B. Ergun, *Product SCFTs for the E_7 Theory*, [[arXiv:1803.02425](#)].
- [118] B. Ergun, Q. Hao, A. Neitzke, and F. Yan, *Factorized class S theories and surface defects*, [[arXiv:2010.06722](#)].
- [119] A. Sen, *F theory and orientifolds*, *Nucl. Phys. B* **475** (1996) 562–578, [[hep-th/9605150](#)].
- [120] T. Banks, M. R. Douglas, and N. Seiberg, *Probing F theory with branes*, *Phys. Lett. B* **387** (1996) 278–281, [[hep-th/9605199](#)].
- [121] D. Gaiotto and E. Witten, *S-Duality of Boundary Conditions In $N=4$ Super Yang-Mills Theory*, *Adv. Theor. Math. Phys.* **13** (2009), no. 3 721–896, [[arXiv:0807.3720](#)].
- [122] A. Hanany and A. Zajac, *Ungauging Schemes and Coulomb Branches of Non-simply Laced Quiver Theories*, *JHEP* **09** (2020) 193, [[arXiv:2002.05716](#)].
- [123] A. Hanany and M. Sperling, *Coulomb branches for rank 2 gauge groups in 3d $\mathcal{N} = 4$ gauge theories*, *JHEP* **08** (2016) 016, [[arXiv:1605.00010](#)].
- [124] E. Beratto, S. Giacomelli, N. Mekareeya, and M. Sacchi, *3d mirrors of the circle reduction of twisted A_{2N} theories of class S*, *JHEP* **09** (2020) 161, [[arXiv:2007.05019](#)].

- [125] G. Ferlito and A. Hanany, *A tale of two cones: the Higgs Branch of $Sp(n)$ theories with $2n$ flavours*, [arXiv:1609.06724](#).
- [126] A. Hanany and R. Kalveks, *Quiver Theories for Moduli Spaces of Classical Group Nilpotent Orbits*, *JHEP* **06** (2016) 130, [[arXiv:1601.04020](#)].
- [127] J. A. Minahan and D. Nemeschansky, *An $N=2$ superconformal fixed point with $E(6)$ global symmetry*, *Nucl. Phys. B* **482** (1996) 142–152, [[hep-th/9608047](#)].
- [128] J. A. Minahan and D. Nemeschansky, *Superconformal fixed points with $E(n)$ global symmetry*, *Nucl. Phys. B* **489** (1997) 24–46, [[hep-th/9610076](#)].
- [129] S. Cremonesi, G. Ferlito, A. Hanany, and N. Mekareeya, *Instanton Operators and the Higgs Branch at Infinite Coupling*, *JHEP* **04** (2017) 042, [[arXiv:1505.06302](#)].
- [130] A. Hanany and A. Zaffaroni, *Branes and six-dimensional supersymmetric theories*, *Nucl. Phys.* **B529** (1998) 180–206, [[hep-th/9712145](#)].
- [131] S. Cremonesi, A. Hanany, N. Mekareeya, and A. Zaffaroni, *Coulomb branch Hilbert series and Hall-Littlewood polynomials*, *JHEP* **09** (2014) 178, [[arXiv:1403.0585](#)].
- [132] S. Cremonesi, A. Hanany, N. Mekareeya, and A. Zaffaroni, *Coulomb branch Hilbert series and Three Dimensional Sicilian Theories*, *JHEP* **09** (2014) 185, [[arXiv:1403.2384](#)].
- [133] A. Hanany, N. Mekareeya, and S. S. Razamat, *Hilbert Series for Moduli Spaces of Two Instantons*, *JHEP* **01** (2013) 070, [[arXiv:1205.4741](#)].
- [134] Y. Lozano, C. Nunez, A. Ramirez, and S. Speziali, *New AdS_2 backgrounds and $\mathcal{N} = 4$ conformal quantum mechanics*, *JHEP* **03** (2021) 277, [[arXiv:2011.00005](#)].
- [135] Y. Lozano, C. Nunez, and A. Ramirez, *$AdS_2 \times S^2 \times CY_2$ solutions in Type IIB with 8 supersymmetries*, *JHEP* **04** (2021) 110, [[arXiv:2101.04682](#)].
- [136] C. Couzens, C. Lawrie, D. Martelli, S. Schafer-Nameki, and J.-M. Wong, *F-theory and AdS_3/CFT_2* , *JHEP* **08** (2017) 043, [[arXiv:1705.04679](#)].
- [137] Y. Lozano, N. T. Macpherson, C. Nunez, and A. Ramirez, *AdS_3 solutions in massive IIA, defect CFTs and T-duality*, *JHEP* **12** (2019) 013, [[arXiv:1909.11669](#)].
- [138] D. Gaiotto and J. Maldacena, *The Gravity duals of $N=2$ superconformal field theories*, *JHEP* **10** (2012) 189, [[arXiv:0904.4466](#)].
- [139] C. Nunez, D. Roychowdhury, and D. C. Thompson, *Integrability and non-integrability in $\mathcal{N} = 2$ SCFTs and their holographic backgrounds*, *JHEP* **07** (2018) 044, [[arXiv:1804.08621](#)].
- [140] F. Apruzzi, M. Fazzi, D. Rosa, and A. Tomasiello, *All AdS_7 solutions of type II supergravity*, *JHEP* **04** (2014) 064, [[arXiv:1309.2949](#)].
- [141] O. Bergman, M. Fazzi, D. Rodríguez-Gómez, and A. Tomasiello, *Charges and holography in $6d$ $(1,0)$ theories*, *JHEP* **05** (2020) 138, [[arXiv:2002.04036](#)].
- [142] E. D'Hoker, J. Estes, and M. Gutperle, *Exact half-BPS Type IIB interface solutions. II. Flux solutions and multi-Janus*, *JHEP* **06** (2007) 022, [[arXiv:0705.0024](#)].

- [143] L. Coccia and C. F. Uhlemann, *On the planar limit of $3d T_p^\sigma$ [SU(N)]*, *JHEP* **06** (2021) 038, [[arXiv:2011.10050](#)].
- [144] E. D'Hoker, M. Gutperle, A. Karch, and C. F. Uhlemann, *Warped $AdS_6 \times S^2$ in Type IIB supergravity I: Local solutions*, *JHEP* **08** (2016) 046, [[arXiv:1606.01254](#)].
- [145] C. F. Uhlemann, *Wilson loops in 5d long quiver gauge theories*, *JHEP* **09** (2020) 145, [[arXiv:2006.01142](#)].
- [146] A. Hanany and E. Witten, *Type IIB superstrings, BPS monopoles, and three-dimensional gauge dynamics*, *Nucl.Phys.* **B492** (1997) 152–190, [[hep-th/9611230](#)].
- [147] B. Assel, C. Bachas, J. Estes, and J. Gomis, *Holographic Duals of $D=3$ $N=4$ Superconformal Field Theories*, *JHEP* **08** (2011) 087, [[arXiv:1106.4253](#)].
- [148] N. T. Macpherson, C. Núñez, L. A. Pando Zayas, V. G. J. Rodgers, and C. A. Whiting, *Type IIB supergravity solutions with AdS_5 from Abelian and non-Abelian T dualities*, *JHEP* **02** (2015) 040, [[arXiv:1410.2650](#)].
- [149] Y. Bea, J. D. Edelstein, G. Itsios, K. S. Kooner, C. Nunez, D. Schofield, and J. A. Sierra-Garcia, *Compactifications of the Klebanov-Witten CFT and new AdS_3 backgrounds*, *JHEP* **05** (2015) 062, [[arXiv:1503.07527](#)].
- [150] M. V. Raamsdonk and C. Waddell, *Holographic and localization calculations of boundary F for $\mathcal{N} = 4$ SUSY Yang-Mills theory*, *JHEP* **02** (2021) 222, [[arXiv:2010.14520](#)].
- [151] A. Kapustin and M. J. Strassler, *On mirror symmetry in three-dimensional Abelian gauge theories*, *JHEP* **04** (1999) 021, [[hep-th/9902033](#)].
- [152] P. C. Argyres, M. R. Plesser, and N. Seiberg, *The Moduli space of vacua of $N=2$ SUSY QCD and duality in $N=1$ SUSY QCD*, *Nucl. Phys. B* **471** (1996) 159–194, [[hep-th/9603042](#)].
- [153] S. Nawata, M. Sperling, H. E. Wang, and Z. Zhong, *Magnetic quivers and line defects — On a duality between $3d \mathcal{N} = 4$ unitary and orthosymplectic quivers*, *JHEP* **02** (2022) 174, [[arXiv:2111.02831](#)].
- [154] A. Collinucci and R. Valandro, *A string theory realization of special unitary quivers in 3 dimensions*, *JHEP* **11** (2020) 157, [[arXiv:2008.10689](#)].
- [155] B. Assel, C. Bachas, J. Estes, and J. Gomis, *IIB Duals of $D=3$ $N=4$ Circular Quivers*, *JHEP* **12** (2012) 044, [[arXiv:1210.2590](#)].